In vivo Measurement of Bone Aluminum in Alzheimer's Disease and Related Studies

IN VIVO MEASUREMENT OF BONE ALUMINUM IN ALZHEIMER'S DISEASE AND RELATED STUDIES

By HEDIEH K. MOHSENI, M.Sc.

A Thesis

Submitted to the School of Graduate Studies in Partial Fulfilment of the Requirements for the Degree Doctor of Philosophy

DOCTOR OF PHILOSOPHY (2016)

(Medical Physics)

McMaster University, Hamilton, Ontario

TITLE: *In Vivo* Measurement of Bone Aluminum in Alzheimer's Disease and Related Studies

AUTHOR: Hedieh K. Mohseni

SUPERVISOR: Dr. David. R. Chettle

NUMBER OF PAGES: xx, 204

Lay Abstract

Alzheimer's disease is the most common form of dementia. The cause of Alzheimer's disease is unknown, but both genetic and environmental factors are known to be involved. Different elements have been studied for their possible role in this disease. Aluminum and to a lesser extent magnesium have been linked to the etiology of Alzheimer's disease. The current thesis presents the results of a clinical study that utilizes the method of *in vivo* neutron activation analysis to measure aluminum and magnesium in the hand bone of Alzheimer's disease and control subjects. *In vivo* neutron activation analysis is a non-invasive method that uses neutrons to activate elements in the human body and measures the radiation emitted. Different methods of analyzing the resulting data were investigated to find the most suitable analysis approach. The biological half-lives of sodium and chlorine were also measured to investigate their short-term kinetic behaviour and pattern with age.

Abstract

Alzheimer's disease accounts for up to 80% of the cases of dementia making it the most common type of dementia. As of 2015, 46.8 million people are suffering from Alzheimer's disease worldwide with an alarming rate of increase in the onset of the disease. Despite the ongoing research, the true cause of Alzheimer's disease remains unknown. Aluminum is one of the major environmental toxins linked to the etiology of Alzheimer's disease. A pilot clinical study for non-invasive measurement of bone aluminum was performed at the *in vivo* neutron activation analysis facility at McMaster University including 15 Alzheimer's and 15 control subjects. A significant difference in bone aluminum, relative to calcium, was found between the two groups. Multiple methods of analysis were investigated to determine the method with the lowest minimum detection limit. The method of in vivo neutron activation analysis allows for the simultaneous activation of multiple elements. As such, it was possible to measure the magnesium levels, which has been shown to be involved in Alzheimer's disease, in the study subjects. The results of bone measurements did not show a significant association between bone magnesium levels and Alzheimer's disease. Moreover, the short-term kinetic behaviours of sodium and chlorine, both essential for the human body, were studied. The outcome of this study revealed an increase in the biological half-lives of sodium and chlorine with age and a higher variability in Alzheimer's patients compared to control subjects. Finally, bone samples from parenteral nutrition patients were analyzed to determine their

aluminum content for comparison and benchmarking purposes. The present results suggest a possible association between bone aluminum and the presence of Alzheimer's disease. No such association was found for magnesium or the biological half-lives of sodium and chlorine. The technique of in vivo neutron activation analysis was shown to be a promising tool for measuring bone aluminum and magnesium; however, a better detection limit is required to strengthen the current results.

Acknowledgements

It is my pleasure to thank the many people who made this thesis possible.

It would be difficult to overstate my gratitude to my supervisor Dr. David Chettle. Thank you for being the best supervisor and mentor I could ever ask for. Your patience, generosity, motivation, and immense knowledge made my PhD studies an incredible experience.

My deep gratitude extends to Dr. William Prestwich who supported me in more ways that I can express. I greatly appreciated his enthusiasm, great ideas, and constant encouragement.

I would like to thank the rest of my supervisory committee members, Dr. Soo Hyun Byun, Dr. Jovica Atanackovic, and Dr. Nicholas Priest, for their insightful comments and encouragements.

I am grateful to the Medical Physics staff for assisting me in many different ways during my time at McMaster University. I would also like to thank Justin Bennett for keeping the Tandetron accelerator up and running and for assisting with the clinical study and subject measurements, even during his paternity leave.

Last but certainly not least, I would like to thank my family, whose love and support have always been a great source of motivation for me. I would have been lost without them. Big thanks to my cousin Parsian for being my favourite cousin, supporter, and best friend.

Table of Contents

List of Figures

List of Tables

List of abbreviations

AD: Alzheimer's disease

CDR: Clinical Dementia Rating

DD: Deuterium-deuterium

DFX: Disferroxamine

ETAAS: Electro-thermal atomic absorption spectrometry

HDPE: High density polyethylene

ICRP: International commission on radiological protection

IVNAA: *In vivo* neutron activation analysis

IVWM: Inverse-variance weighted mean

MAL: McMaster accelerator laboratory

MDL: Minimum detection limit

PN: Parenteral nutrition

sMMSE: Standardized mini mental state examination

Outline of the thesis

The first chapter in this thesis presents article I, and intends to provide an introduction to aluminum, as it relates to human health. It also delivers an overview of the technique of in vivo neutron activation analysis and its history as it applies to measuring aluminum in human subjects.

Chapter 2 presents article II, in which the development, testing, and comparison of different methods of aluminum data analysis are discussed in detail. Appendix A to the thesis provides additional information pertaining to data analysis. Appendix A also includes the details of optimization of the irradiation parameters.

Chapter 3 presents article III and the results of the in vivo measurement of aluminum in human subjects suffering from Alzheimer's disease, as well as control subjects. The raw data for this study can be found in Appendix B.

Chapter 4 contains article IV where the details of the magnesium measurements in Alzheimer's disease and control subjects are presented and discussed. Additional data pertaining to this study are provided in Appendix C.

Chapter 5 presents article V, in which the short-term kinetic behaviour of sodium and chlorine are presented. Appendix D contains the ancillary tables related to this chapter.

Lastly, chapter 6 provides a summary and conclusions on each of the contributions in the thesis and offers the future directions envisioned for expanding the present work further.

Chapter 1

A History of *In Vivo* Neutron Activation Analysis in Measurement of Aluminum in Human Subjects

Introduction to article I

Aluminum is the most abundant metal in the earth's crust, and due to its ubiquitous nature, has a wide presence in human life. The interest in measuring bone aluminum *in vivo* started in the 1970s with the cases of dialysis encephalopathy, and has since undergone continuous improvement to enable measuring the low levels of bone aluminum. This first chapter describes the history of *in vivo* neutron activation analysis as it applies to measurement of aluminum in bone and its evolution over the years. Aluminum has also been linked to the etiology of Alzheimer's disease. It is important to note, however, that the role of aluminum in Alzheimer's disease has been the subject of continuous debate. There is a substantial body of literature in support of aluminum's association with Alzheimer's disease, and there also exist a non-negligible number of research findings that challenge such association.

The research done in preparing this review article presented in Chapter 1 was done by the author of this thesis under the supervision of Dr. David Chettle.

Contents of Article I

The following article was accepted for publication in the Journal of Alzheimer's Disease (*J Alzheimer's Dis* **50**, 913-926).

A History of *In Vivo* Neutron Activation Analysis in Measurement of Aluminum in Human Subjects

Hedieh K.Mohseni[1], David R. Chettle[1]

[1]Department of Medical Physics and Applied Radiation Sciences, McMaster University, Hamilton, Ontario, Canada

Abstract

Aluminum, as an abundant metal, has gained widespread use in human life, entering the body predominantly as an additive to various foods and drinking water. Other major sources of exposure to aluminum include medical, cosmetic, and occupational routes. As a common environmental toxin, with well-known roles in several medical conditions such as dialysis encephalopathy, aluminum is considered a potential candidate in the causality of Alzheimer's disease. Aluminum mostly accumulates in the bone, which makes bone an indicator of the body burden of aluminum and an ideal organ as a proxy for the brain. Most of the techniques developed for measuring aluminum include bone biopsy, which requires invasive measures, causing inconvenience for the patients. There has been a considerable effort in developing non-invasive approaches, which allow for monitoring aluminum levels for medical and occupational purposes in larger populations. *In vivo* neutron activation analysis, a method based on nuclear activation of isotopes of elements in the body and their subsequent detection,

has proven to be an invaluable tool for this purpose. There are definite challenges in developing *in vivo* non-invasive techniques capable of detecting low levels of aluminum in healthy individuals and aluminum-exposed populations. The following review examines the method of *in vivo* neutron activation analysis in the context of aluminum measurement in humans focusing on different neutron sources, interference from other activation products and the improvements made in minimum detectable limits and patient dose over the past few decades.

Keywords- Aluminum, dementia, Alzheimer's disease, *in vivo* neutron activation analysis, bone, gamma spectroscopy

1. Introduction

Aluminum, being the most abundant metal and the third most common element in the earth's crust, has a significant presence in our environment. Due to aluminum's reactivity, it can only exist in bonded states in nature, most of which have very low water solubility, rendering low availability in surface waters. It can be found in a wide range of plants, drinking water, and food items, both natural and processed. The concentration of aluminum in processed food, however, is much higher because aluminum compounds are used as food additives, resulting in exposures that are more pronounced in industrialized societies. As a non-food, it has found uses in different industries and medical applications such as in antacids, aspirin coating, and vaccines, to name a few[1].

The routes of exposure for aluminum include ingestion, skin uptake, and inhalation, with the first being considered as the most common path of intake for the general public and the last being more significant in occupational settings. Its bioavailability, however, is quite low, as the gastrointestinal tract, the skin, and the lungs limit the absorption of aluminum to about 0.1% [1,2]. Unlike its ubiquitous distribution in the environment, once absorbed, aluminum accumulates mostly in bone, lungs, muscle, liver, and brain, making the bone a favorable organ for measurement. Aluminum is categorized as a non-essential element for the human body and excessive amounts of it can be toxic [3]. Aluminum neurotoxicity was known as early as 1942 through the work of Kopeloff [2,4].

In the 1970s, there was a clear association between excess amounts of aluminum in the body and dialysis encephalopathy [2,5]. Research conducted by various groups using different methods showed elevated aluminum concentrations in bones, sera, and brains of patients with renal failure who were undergoing dialysis therapy [5–8], some of whom had accumulated about 10 times more aluminum than healthy individuals [9]. In these patients, aluminum-contaminated water was used for preparation of the dialysate and aluminum-based phosphate binders were used in the treatment of hyperphosphatemia following dialysis [2,6,10]. In the early publications, a death rate of 35-50% was reported in dialysis centres where large amounts of aluminum were used [2,7,11]. Osteomalacia, characterized by bone pain and fractures, is another medical

condition linked to dialysis. Osteomalacia seems to heal upon aluminum removal [6]. This has led to the investigation of other sources of exposure to aluminum and their possible effects.

Early studies based on animal models, as well as isolated cases of individuals exposed to aluminum, support a role for aluminum in Alzheimer's type dementia [12-14]. Twin studies indicate that the etiology of AD has both genetic and environmental components [15-18]. Because of its high prevalence, the sporadic or late-onset of AD has been largely associated with environmental toxins and exposures, and has made a stronger case for aluminum causality [19]. There is a clear need for further investigation of aluminum in the context of AD through development of accurate and sensitive techniques of measurement and clinical studies.

The link between aluminum and encephalopathy in dialysis patients became a motivation for investigation of aluminum in industrial and occupational exposures. One of the earliest studies, carried out in Sweden, investigated the concentration of aluminum in blood and urine samples collected from welders and aluminum production workers [20]. This showed higher concentrations of aluminum both in urine and blood samples compared to the healthy individuals that were nevertheless lower than the levels found in dialysis encephalopathy patients.

Another area of interest for measuring aluminum concerns long-term parenteral nutrition patients, for both infants and adults, where aluminum contamination of

parenteral solutions poses the risk of aluminum toxicity and bone disease similar to that of dialysis patients [21]. Research findings in infants and adults receiving parenteral nutrition indicated elevated bone aluminum levels [22-24]. Controlling aluminum levels in patients receiving long-term parenteral nutrition and lowering their aluminum burden is of great importance, which requires routine monitoring. A non-invasive approach to aluminum monitoring is an invaluable tool in such cases, as bone biopsies cannot be considered as a method of routine monitoring due to the inconvenience to the patients.

Non-invasive aluminum monitoring could also prove to be very helpful in providing a screening technique for identifying patients with possible Alzheimer's disease at an early stage. There is a clear need for development of methods that allow for accurate, sensitive and reproducible measurement of aluminum *in vivo*. Currently, neutron activation analysis is the only available *in vivo* method for measuring aluminum concentration in human subjects.

With the growing interest in aluminum and its effects in the context of health and safety, different methods have been developed to measure aluminum accurately and with high sensitivity. Most of the studies on aluminum measurement use different methods of atomic absorption spectrometry [14,25,26], mass spectrometry [27,28], histochemical techniques [29], and instrumental neutron activation analysis [30-32]. All of these methods rely on in vitro approaches, and therefore, cannot be used on living humans.

An important consideration in measuring aluminum *in vivo* is determining the site of measurement, which depends strongly on the medical condition being investigated. Dialysis encephalopathy and Alzheimer's disease are both conditions that are associated with elevated brain aluminum levels, subsequently making the brain an ideal site for measurement. *In vivo* measurement of aluminum in the brain of living subjects is not feasible due to the high doses of radiation required to penetrate the skull and the critical nature and radiosensitivity of the brain and its surrounding structures. Also, the measurement would have to be made by directing the neutron beam through the skull, which would generate an aluminum signal which would mask that from brain. As such, other sites need to be considered as a proxy for brain, with biokinetic and tissue deposition behaviour of aluminum, feasibility of measurement, and ethical concerns taken into consideration. Aluminum can be measured in blood, more specifically in plasma, where it binds to transferrin, a protein associated with iron transport [1]. Urine is another medium for monitoring aluminum; however, it better reflects recent exposures and not the aluminum body burden [1]. Carrying about 60% of the aluminum body burden, the skeleton is considered the aluminum depot in the body, followed by the lungs, muscle and liver [1]. The skeletal distribution provides a unique advantage in terms of the flexibility in the choice of measurement site. Additionally, Alzheimer's disease has been associated with a higher risk of bone fractures, rendering the skeleton as an important site for measurement [33,34].

Each of the above mentioned proxy systems present certain advantages, challenges, and limitations. *In vitro* systems such as urine and plasma come with the inherent risk of contamination due to the ubiquitous nature of aluminum in the environment, which begs the question of reliability and reproducibility, especially when low levels of aluminum are involved. Strict measures in sample collection and processing need to be taken in order to avoid contamination if the results are to be reliable. Most of the studies rely on a single sample collection, in order to reduce the inconvenience to the subjects, and therefore, reproducibility is most likely to be achieved through inter-laboratory collaborations. *In vivo* neutron activation measurement requires exposing subjects to ionizing radiation; this poses a limitation on dose and site of measurement. Extremities are considered the most suitable site due to their distance from critical and radiosensitive structures, as well as their higher regulatory dose limit [35]. Hand is a more convenient choice from the point of view of irradiation and shielding design which plays an important role in the experimental setup. The major difference between the hand and the foot is that the hand is mainly comprised of cortical bone, whereas the foot, and especially the calcaneus, is trabecular bone. While aluminum accumulates in both bone types, higher concentrations of aluminum have been measured in trabecular compared to cortical bone [36].

Bone biopsy for the purpose of measuring aluminum in living subjects, being an invasive method, is usually secondary to a surgical procedure. Therefore, the type of bone sample depends on the procedure and is often trabecular bone

[37,38]. Thus, *in vivo* measurement of aluminum in the trabecular bone would allow for inter-laboratory comparison of the results.

Defining typical values for bone aluminum based on the literature is challenging, as a wide range of concentrations measured using various methods have been reported by different researchers. To complicate matters further, based on the method used, the results are reported per gram of wet weight, dry weight, or relative to the calcium content of the bone, with no direct and accurate conversion factor available. Perhaps, the most comprehensive and relatively recent study conducted on measuring aluminum in bone is that of Hellström et al [38]. Bone biopsy samples from 172 subjects suffering from different types of dementia including Alzheimer's disease, as well as a control group were analyzed. Part of their results is shown in Table 1.1.

Table 1.1. Typical aluminum content in different tissues in healthy humans.

Medium	Number of samples	Mean ± SD	Range	Reference
Blood	NA	-	1-3 µg/L	Yegambaram et al. [40]
Urine	NA	23.7 µg/L	-	Yegambaram et al. [40]
Brain	n=16	-	0.1-4.5 µg/g dry weight	Exley et al. [39]
Bone	n= 69	1.06 µg/g dry weight	-	Hellström et al. [38]

Also shown in Table 1.1 are aluminum levels in blood, urine, and brain samples in healthy individuals based on recent studies. There are considerable variations in values reported in the literature and between different subjects, as reflected by the wide range of aluminum content reported. In the case of the brain, varying concentrations of aluminum have been reported for different regions of the brain [12,25,39]. As such, it is important to note that Table 1.1 is meant merely as a guide to provide the readers with estimates of aluminum content and the minimum levels that are likely to be detected in healthy humans.

2. *In vivo* neutron activation analysis

In vivo neutron activation analysis (IVNAA) is a method of measurement and analysis of living humans which can provide invaluable information for advances in medical research and well-being of mankind. The non-destructive nature of this method enables its application to humans. Additionally, it offers simultaneous measurement of several elements. It is based on the detection of characteristic gamma rays emitted during de-excitation of neutron activated nuclei. It is limited, however, by the number of elements which not only can become radioactive when bombarded by neutrons, but also have strong enough gamma emissions that can be detected using the current detection systems. For elements satisfying such criteria, IVNAA can become the method of choice, provided that measurements can be performed with sensitivity and accuracy that is dictated by the current exposure levels of those elements.

The first requirement for IVNAA is the neutron source for activating the elements of interest. Neutrons can be produced using a variety of sources (nuclear reactors, accelerators, and neutron-emitting radioisotopes) and reactions for the purpose of *in vivo* measurements, most of which are discussed in the review article by Chettle and Fremlin [41]. The activation rate, R, for a given element in a medium bombarded by neutrons is shown in the equation below:

$$R = \int_0^\infty N\varphi(E)\sigma(E)\,dE$$

Where σ(E) is the absorption cross-section (probability of interaction), φ(E) is the neutron fluence, and N is the number density which depends on the isotope and its content in the medium. The neutron capture cross-section also depends on the isotope and varies considerably with neutron energy. The energy spectrum of the neutron source, therefore, is of great importance and should be considered when investigating interfering reactions such as that of aluminum and phosphorus. Neutron fluence is the only source-dependent variable which can be controlled depending on the choice and availability of sources. The choice of neutron source affects both the energy spectrum and the fluence of neutrons.

Aluminum is one of the elements satisfying the criteria for IVNAA, by means of the nuclear reaction in which stable ^{27}Al absorbs a neutron, forming radioactive ^{28}Al. The relatively short half-life of this decay makes it a suitable radioisotope for *in vivo* measurements as the detection time can be kept reasonably short. The

relevance of a short half-life is that it allows for multiple of half-lives of the radioisotope to be acquired within a reasonable detection time, resulting in a more accurate analysis with smaller statistical uncertainty without requiring the participants to remain motionless for an extended period of time.

Table 1.2. Major elements with significant thermal neutron cross-section in the bone and their reactions. (* Phosphorus has a cross-section of 0.172 b for 14 MeV neutrons).

Element	Abundance (%)	Nuclear Reaction	Thermal Neutron Capture Cross-section (Barn)	Gamma Energy (MeV)	Half-life
Aluminum	100	$^{27}Al(n,\gamma)\ ^{28}Al$	0.23	1.78	2.24 min
Calcium	0.187	$^{48}Ca(n,\gamma)\ ^{49}Ca$	1.1	3.08	8.72 min
Sodium	100	$^{23}Na(n,\gamma)\ ^{24}Na$	0.53	1.37, 2.75	15.02 h
Magnesium	11.01	$^{26}Mg(n,\gamma)\ ^{27}Mg$	0.037	0.84, 1.01	9.46 min
Chlorine	24.23	$^{37}Cl(n,\gamma)\ ^{38}Cl$	0.43	1.64 , 2.17	37.3 min
Phosphorus*	100	$^{31}P(n,\alpha)\ ^{28}Al$	-	1.78	2.24 min

When irradiating a biological medium, in addition to the element of interest, other elements with significant neutron activation cross-sections will become activated. While this provides the advantage of measuring multiple elements simultaneously, some of the activation products may interfere with the radioisotope of interest. For the case of bone as the *in vivo* activation medium, the stable elements, activation reactions and cross sections are listed in Table 1.2. Phosphorus, chlorine and to a lesser extent sodium, are the major interfering

reactions which affect the detection of aluminum in different ways. Phosphorus in particular presents a major challenge as $^{31}P(n,\alpha)^{28}Al$ reaction shares the same activation product as aluminum i.e. ^{28}Al. Several issues must be considered in addressing the phosphorus interference. For the $^{31}P(n,\alpha)^{28}Al$ reaction to take place, neutrons must have the minimum required energy dictated by the rest mass differences of the particles involved in the reaction giving a threshold energy of 2.01 MeV. Moreover, the probability of the alpha particle escaping the nucleus, also known as the Coulomb barrier, at 6.22 MeV for $^{31}P(n,\alpha)^{28}Al$, further inhibits the reaction. The total effect is such that there are no existing data showing a significant reaction rate for neutron energies below 3 MeV as shown in the excitation function (neutron absorption cross-section against neutron energy) in Figure 1.1. It should be noted that P/Al activation ratio increases with increasing neutron energy and decreases with increasing sample size. The latter is due to the slowing down and moderation of neutrons in the body. The larger the amount of irradiated tissue, the more significant the moderation of neutrons will be. The phosphorus content in the bone and soft tissue is considerably higher than aluminum. According to ICRP 65, the reference man has 780 g and 0.06 g of phosphorus and aluminum, respectively [42]. Given the amount of phosphorous versus aluminum in the body, it is important preferably to eliminate the probability of reaction or devise other ways of accounting for its effect. $^{31}P(n,\alpha)^{28}Al$ has a threshold of 2.01 MeV and as can be seen in the Figure 1.1, there is no cross-section for this reaction for neutron energies below the

threshold. This is important, as it provides a means for eliminating the interference, if neutrons of 2 MeV and above can be removed from the beam.

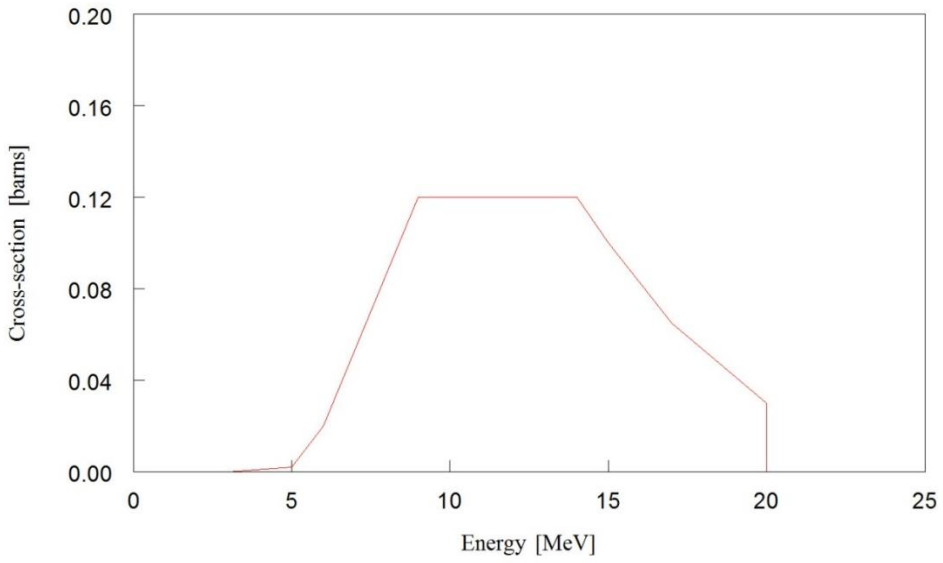

Figure 1.1. $^{31}P(n,\alpha)^{28}Al$ excitation function (Taken from ENDF/B-VII Incident-neutron data [43]).

Another challenge when irradiating *in vivo* is the exposure of the subjects to ionizing radiation and the consequent dose. Precise measurement of the dose delivered to an individual is a complicated task in that both the dose from neutrons and the gamma dose from the neutron source or the target need to be taken into account.

The first attempt at using IVNAA goes back to 1964 and the work of Anderson et al. who measured Ca, Na, and Cl in two healthy individuals using 14 MeV neutrons [44]. They reported that while their Ca results agreed with the value reported for the ICRP's (1959) "reference man", the values for Cl and Na may

have been overestimated. Their work was further expanded for other elements by Boddy et al. and other groups [45-48], but it wasn't until 1980 that IVNAA was used for measurement of aluminum.

2.1. East Kilbride group (14 MeV neutron generator)

IVNAA has been used to measure whole body aluminum [49]. The system was previously developed and evaluated for measuring calcium, phosphorus, sodium, and nitrogen [46,50]. Williams and the East Kilbridge group's aim was to measure aluminum in subjects with chronic renal failure and healthy individuals. Their study cohort consisted of 38 subjects divided into three groups; subjects undergoing regular dialysis with and without dialysis encephalopathy and a control group not undergoing dialysis.

The criteria for dialysis encephalopathy included but were not limited to serum aluminum levels higher than 350µg/l. Their irradiation setup consisted of two 14 MeV neutron generator tubes placed above and below the patient. A whole body counter made up of two 29 cm dia × 10 cm NaI(Tl) detectors was then used to detect the activity. The total dose delivered was 10 mSv at the body surface. As mentioned, the major drawback of using high energy neutrons in IVNAA is that the fast neutrons in the beam activate phosphorus which is a highly abundant element in the human body. However, measurements done on anthropomorphic phantoms revealed that 1 g of aluminum had the same signal as 8 g of phosphorus.

Irradiating the whole body provides significant moderation, thus partially thermalizing neutrons and giving rise to a low P/Al ratio. The remaining proportion of fast neutrons has a large enough contribution to phosphorus activation that aluminum can only be measured indirectly when 14 MeV neutrons are employed. The indirect measurement of aluminum then relies on the assumed more or less constant ratio of bone phosphorus to calcium (P/Ca) in healthy humans. Bone in adults contains almost the entire body burden of calcium and about 80% of phosphorus, in a ratio of 0.46 ± 0.01 [51]. The remaining 20% is considered as non-bone phosphorus, in which any change is attributable to aluminum activation.

To calculate the non-bone phosphorus, the measured calcium multiplied by the P/Ca ratio (0.46) is subtracted from the total measured phosphorus. In order to account for variations in body size, the results are normalized to weight. Fluid retention and lean body mass are accounted for by normalizing to total body nitrogen and potassium, respectively.

One concern when using the standard P/Ca is to apply the ratio in healthy humans to cases of renal failure which commonly have bone disease and calcium depletion that in turn affects the P/Ca ratio. The error associated with such variations is reported as the ratio of measured to predicted calcium. The results showed significantly higher non-bone phosphorus in all subjects with chronic renal failure compared to the controls, while the serum phosphorus

remained slightly above normal in the case of the former, which eliminated the possibility of increased phosphorus. There is also an insignificant increase in the non-bone phosphorus in subjects suffering from dialysis encephalopathy as compared to other dialysis patients.

Williams' work set the first building block for *in vivo* measurement of aluminum and gave the first estimate of the upper limit for whole body aluminum of about 3 g. One advantage of the system was patient set-up. Having the subjects in the supine position provides comfort during measurement, in particular for measurements as long as 40 minutes. The other advantage of their system was its cost effectiveness. Neutron generators are a much cheaper alternative to using a reactor or a cyclotron, while offering relatively simpler operation with minimal warm up time [46].

While offering advantages in cost and operation, these 14 MeV neutron generators are not considered as a suitable source of neutrons due to the interference from phosphorus caused by the high energy neutrons and also their low neutron yield. Determining the aluminum content solely based on the non-bone phosphorus in the body may lead to an underestimation due to the fact that bone is the main depot for aluminum. Therefore, the contribution from the phosphorus in the skeleton cannot be ignored. Additionally, while the ratio of phosphorus to calcium in the bone is known to be constant in healthy individuals, it may be subject to considerable variation in the elderly, especially those

suffering from bone ailments. The last, however, was accounted for by observing the ratio of measured to expected calcium in the subjects.

2.2. Brookhaven group (Research reactor)

Ellis et al. improved the methodology for measuring aluminum in several ways [52]. Instead of using a neutron generator, they used a medical research reactor, which offered a thermal-epithermal neutron beam. The advantage of using a reactor beam is that it offers a higher neutron flux and, therefore, more activation and better detection. The beam used at Brookhaven had a thermal flux of about 10^7 $n.cm^{-2}.sec^{-1}$. Using this beam allowed for activation of aluminum, though the presence of a minor component of fast neutrons in the beam still activated phosphorus. Moreover, they limited the radiation exposure to the subject's hand which reduced the dose to the patient while giving a reasonable estimate of aluminum burden in the body. The beam area was shielded down to about 10 cm × 20 cm to accommodate a human hand. Following an irradiation time of 2 minutes and 2 minutes of delay for transferring to the counting facility, the activity in subjects' hand was measured for 200 seconds. The detection system was another area of improvement where it used 4 NaI(Tl) detectors (4" × 4" × 16") instead of two detectors in a quasi-4π geometry placed inside lead shielding. The minimum detection limit of the system was found to be 0.4 mg of aluminum based on phantoms containing relevant amounts of sodium, calcium and chloride compared to that of the "reference man".

This study involved two separate groups of participants. The first group underwent total body neutron activation, and their whole body aluminum content was calculated based on total phosphorus and the fixed phosphorus to calcium ratio in the skeleton. The second group consisted of 10 subjects with total body measurements for calcium and phosphorus and partial body measurement for hand aluminum. Serum aluminum measurements were performed before and after administration of Disferroxamine (DFX), which is an aluminum binder. These subjects had no clinical indication of aluminum-related diseases. Results of the hand irradiation were reported as the ratio of aluminum to calcium (Al/Ca) to account for variations in hand size. The aim of the total body measurement for this group was to provide an estimate of the total body calcium in order to convert from hand aluminum to total body aluminum. The serum Al ranges before and after DFX were 19 - 98 μg/L and 32 - 450 μg/L, respectively. The Al/Ca range for this group was 0.02 - 0.76 mg Al/g Ca, with a ratio of 0.04 or less considered within the normal range. For the same group, the total body Al ranged from undetectable to 2683 mg with a mean of 1350 mg skeletal Al burden range was 12 - 280 mg with a mean value of 162 mg. The mean total body and skeletal burden aluminum found in this group were higher than the reference man values [42] by factors of 8 and 20, respectively. The results of total body measurements done on 178 males showed a higher aluminum level based on total phosphorus for renal failure patients undergoing dialysis compared to the group suffering from renal disease but not on dialysis. They concluded that baseline and post-DFX

serum aluminum levels did not correlate with total body aluminum, even though serum aluminum measurement is a common clinical method of estimating aluminum burden in the body. There was also no significant correlation between the total body aluminum and skeletal aluminum burden or Al/Ca ratio in the hand. They did, however, find a significant correlation between post-DFX serum aluminum and Al/Ca ratio in the hand. It's important to note that phosphorus contamination in the hand measurement was estimated to be equivalent to 0.7 mg of aluminum. For the total body irradiation, the anthropomorphic phantom study showed that 1 g of aluminum had the same signal as 68.3 g of phosphorus, due to the significant moderation of neutrons both in the shielding and within the body.

2.3. Birmingham group (accelerator)

Green and Chettle examined the feasibility of using an accelerator as a more available means of producing neutrons as compared to a reactor-based system, without a major compromise in the neutron flux [53]. They used the Dynamitron accelerator available at the University of Birmingham's School of Physics and Space Research; a 3 MV machine that used a tritium target and its $^{3}H(p,n)^{3}He$ reaction to produce neutrons. The use of an accelerator offered the possibility of varying the incident proton energy and hence provided a neutron energy spectrum that enabled them to optimise neutron energy and, therefore, the dose.

The technique of microdosimetry allows for a detailed investigation of dose distribution in the irradiation cavity for various energies. It also has the advantage of providing information about the quality of radiation, also known as radiation weighting factor. Radiation weighting factor is a parameter that is used to convert the absorbed dose measured by radiation detection devices to equivalent dose. Equivalent dose is a quantity that is described to provide a common scale for biological damages of all types of ionizing radiation. This is because the extent of damage done by ionizing radiation can vary significantly with the type of radiation.

Two groups of phantoms with varying amounts of aluminum up to 100 mg or 130 mg were made with one group containing tissue-relevant concentrations of Na and Cl. The irradiation and counting protocol consisted of a 30 second irradiation time followed by transfer and counting times of 30 and 300 seconds, respectively. The detection system chosen was an assembly of four NaI(Tl) 51mm dia×152mm L detectors. Microdosimetry results showed that the optimum proton energy could be less than the lowest measured energy of 1.1 MeV. However, using lower energies was not practical due to cross-section restrictions of the target, causing a drastic drop in neutron fluence for energies less than 1.2 MeV. For this reason, all but one experiment (Ep= 1.05 MeV) were performed at the energy of 1.2 MeV. As expected, the NaI(Tl) detector assembly provided a better efficiency, and therefore, higher number of counts compared to germanium detectors.

The minimum detectable limit (MDL) achieved for 1.05 MeV and 1.2 MeV, were 2.0 mg and 1.2 mg, respectively. Comparing their MDL results with other published *in vivo* aluminum measurements, the authors concluded that using an accelerator with tritium target was a feasible method of measuring aluminum *in vivo* with suggested future work on improving the sensitivity of the system including detector upgrades, dose delivery and energy optimizations, and data analysis.

In a later study, Green et al. made improvements on dose measurement and also performed experiments comparing the phantom set made at Birmingham University to that from Swansea group [54]. The Swansea phantoms were saline bags with physiologically relevant concentrations of Ca, Na, Cl, and P with varying amounts of Al (0 - 30 mg), whereas the Birmingham phantoms were smaller bottles of $AlCl_3$ with aluminum ranging up to 130 mg. The detection system was changed to two NaI (Tl) detectors of different sizes, and the analysis was improved by employing a non-linear least-squares method. Two irradiation protocols of 60 s and 30 s corresponding to high and low dose delivery were used, followed by a 30 s transfer time and 300 s of counting time. The calibration lines generated from each set of phantoms revealed a difference in the slopes which was attributed to the fact that the flexible containment of Swansea phantoms allowed for a closer positioning with respect to the detectors. Additionally, the measurements done on Swansea phantoms indicated that the interference from phosphorus was insignificant. The response of 1 g of

phosphorus was equivalent to less than 0.1 g of aluminum and, therefore, was not considered as a concern for the irradiation protocol used.

2.4. Swansea group (^{252}Cf neutron source)

In an attempt to make the technique of IVNAA more available, Wyatt et al. developed a system using ^{252}Cf as the neutron source [55]. The main advantage in using ^{252}Cf is that it's a readily available radionuclide that can be used as a source of neutrons, whereas reactors or accelerators are not widely available for clinical applications. The major disadvantages of ^{252}Cf are the low thermal neutron yield and also the recurring issue of interference from the P reaction with fast neutrons. ^{252}Cf has a neutron energy range of up to 10 MeV with an average energy of 2.2 MeV. Phantom measurements indicated that the interference from 7 g of P was equal to 1 g of Al. The mean neutron energy of ^{252}Cf is lower than the 14 MeV neutron generator, thus reducing phosphorus activation in comparison. However, partial-body irradiation of the hand means a smaller sample size and consequently, weaker moderation. In order to enhance the activation in favor of aluminum, the beam was moderated using water which, while increasing the ratio of thermal to fast neutrons, reduced the thermal neutron flux. Water has moderating properties similar to that of the tissue, which provided the additional advantage of eliminating the need for tissue thickness correction. The detection system consisted of two NaI (Tl) detectors in a shielded enclosure with an opening for inserting the hand. System calibration using tissue equivalent

phantoms with varying concentrations of aluminum was performed which verified the analysis technique.

Seven patients with a mean age of 54.4 years and range of 43 - 70 years were recruited for the clinical study, all of whom were suffering from end-stage renal failure and were either already on dialysis treatment or about to receive it. In an attempt to compensate for the low neutron yield, a cyclic technique was used. Four cycles of irradiation and counting of each 300 seconds were used, with a transfer time of 30 seconds between irradiation and counting. This technique improved the activation of aluminum by a factor of 2.5 compared to a single irradiation previously used by the same group and resulted in a dose equivalent of 36 mSv to the hand and an estimated total body dose equivalent of less than 0.2 mSv.

Wyatt et al. used the P/Ca ratios obtained by Ellis et al. [52] to account for the activation of phosphorus in the hand. Iliac bone samples from the same patients were analyzed for aluminum and calcium content using electrothermal atomic absorption spectrometry for comparison purposes. The range of aluminum found in the iliac bone samples was 47 - 108 μg Al/g dry weight or 353 - 1121 μg Al/g Ca. The results of the IVNAA were analyzed using library least squares fitting, based on the counts per gram for each of the elements in the tissue-equivalent phantoms, and were reported as the Al/ Ca ratio. The phantom results showed close agreement with the actual amounts of aluminum in each phantom. Al/Ca

ratio in the hand ranged from - 42 to 518 μg Al/g Ca. The authors attributed the higher Al/Ca ratio in biopsy samples, compared to IVNAA of the hand, to the variations in the type of the bone measured. Iliac bone is trabecular, while hand is mostly cortical bone. The former has been shown to accumulate more aluminum but less calcium than the latter [36,56]. IVNAA hand aluminum levels were in good agreement with the results obtained by Ellis et al [52]. The MDL achieved was 180 μg Al/g Ca or approximately 2.2 mg of aluminum in the hand which is higher than the amount found in the hand of the reference man by a factor of 7 [42]. Such detection limit renders the system unsuitable for measuring aluminum in the normal population. However, it can be used successfully in patients suffering from renal failure as their bone aluminum levels can reach up to 50 times the amount found in healthy individuals [7].

2.5. McMaster group (McMaster research reactor and KN accelerator)

Palerme et al. [57] investigated the feasibility of using different neutron sources available at McMaster University with the goal of establishing a facility for measuring aluminum in bone using IVNAA. These sources included a nuclear reactor and a KN accelerator. Two of the reactor beams were investigated; one with a degraded fission spectrum, but no thermalization of neutrons. The other has silicon and sapphire crystal filtration which removes fast neutrons from the beam, hence reducing the probability of phosphorus activation.

The ratio of fast to thermal neutron flux was taken as indicative of the extent of aluminum production from silicon and phosphorus and samples of all three elements in powder form were measured. The KN accelerator used a lithium target with proton energy of 2 MeV, eliminating the activation of silicon and phosphorus due to the insufficient energy of the resulting neutron spectrum. The unfiltered reactor beam showed a clear contribution from silicon and phosphorus while the filtered beam had a 3.5% ratio of fast to thermal fluence. While the accelerator provided the best results in terms of interference-free activation of aluminum, practical difficulties forced the experiments to be carried out using the filtered beam of the reactor.

Resin-based hand phantoms with the geometry of a clenched fist were constructed and irradiated for 3 minutes, and the data were subsequently acquired using two 200 mm dia × 50 mm thick NaI(Tl) detectors (120 mm of separation) after a transfer time of 45 seconds. Data analysis consisted of fitting two Gaussians to the chlorine and aluminum peaks and a single Gaussian to the calcium peak. Results were reported as the ratio of aluminum to calcium. The minimum detectable limit was calculated to be 1.5 mg of Al or 0.1 mg Al/g Ca. The neutron flux of 4×10^7 $n.cm^{-2}.s^{-1}$ resulted in a dose of 4 mSv to the phantoms. While this work improved the detection limit of aluminum by about 70%, presence of high energy neutrons in the beam and the subsequent interference from phosphorous remained a problem; a problem that could be solved using the accelerator available on site.

Comsa et al. [58] mainly focused on improving the MDL through data acquisition and analysis techniques at the already existing neutron activation analysis facility at McMaster University. They employed the method of spectral decomposition in order to take advantage of the total number of counts in the spectra, as opposed to the traditional photo-peak analysis. Single-element phantoms containing elements with significant thermal neutron cross-sections were constructed and irradiated to make up a library of spectra.

An algorithm was written to sum the contributions from each element in the fitted spectrum. Additionally, in order to improve the detection of aluminum, an electronic coincidence rejection system was developed to diminish the effect of Cl and Na in the spectra.

Al emits a single gamma, whereas both Cl and Na emit gamma rays in a cascade. By rejecting the events that are detected in both detectors within the resolving time, the effects of both Na and Cl are greatly reduced. This is particularly important in the case of Cl, one of the peaks of which (1.64 MeV) is in the vicinity of the Al peak (1.78 MeV), as this method partially removes the overlapping of Al and Cl peaks in favor of Al. These modifications reduced the MDL to 0.7 mg of Al while keeping the equivalent dose at 20 mSv. It was shown that using the spectral decomposition technique improved the MDL by a factor of 1.7 when compared to the traditional method of least squares fitting. While an

improvement to the previous work done, the MDL of 0.7 mg was still above the levels expected in the hand of a healthy individual.

Figure 1.2. Irradiation cavity of the Tandetron accelerator at McMaster University showing a subject positioned for irradiation.

Further improvements on the accelerator-based NAA system at McMaster paved the way for the pilot *in vivo* studies. One area of improvement included the development of a 4π detection system consisting of 8 NaI(Tl) detectors, the details of which are reported elsewhere [59,60]. The new detection system together with the previous analysis upgrades i.e. spectral decomposition, led to an estimated reduced MDL of 0.24 mg Al [61]. Furthermore, the Van de Graff

accelerator used in the previous studies was replaced with a high-current Tandetron accelerator which made shorter irradiation times possible. The newly designed and constructed irradiation cavity, shown in Figure 1.2, was another area of improvement expected to improve the MDL by a factor of 1.2 - 1.25 [61].

2.6. McMaster group (Tandetron accelerator)

Davis et al. [62] and Aslam et al. [63] performed pilot *in vivo* studies measuring aluminum in the hand of healthy and occupationally exposed individuals using the upgraded NAA system. A phantom study was performed prior to the *in vivo* study. Phantoms were made based on the cortical bone composition of ICRP 23 Reference Man and consisted of Ca, Na, Cl, Mg, and varying amounts of Al in a cylindrical container [42]. The phantoms were irradiated for 3 min, followed by a transfer time of 105 s, and were counted for 10 min. The equivalent and effective doses were determined to be 17.6 mSv (using a quality factor of 13 for neutrons) and 14.4 μSv, respectively.

The pilot study consisted of 20 male volunteers residing in southern Ontario with no history of exposure to aluminum for medical or occupational purposes with a mean age of 51.8 ± 13.1. The second group consisted of 8 subjects with self-reported occupational exposure to aluminum and a mean age of 56.6 ± 5.4. The irradiation cavity was designed to irradiate the fingers and palm of the subject and an adjustable water sleeve was fitted around the arm to protect the subject

from unnecessary exposure. The same irradiation protocol was used for the phantoms. Results were reported as Al/Ca ratio.

The MDL values determined were 0.29 mg Al or 19.5 µg Al/g Ca for phantoms which is at the low end of the range of 20 - 27 µg Al/g Ca expected in the hand of healthy human. The MDL for the human hand was determined to be 28.1 µg Al/g Ca while the range of aluminum concentration in the hand of healthy subjects varied between - 9.6 ± 11.6 µg Al/g Ca and 60.3 ± 10.4 µg Al/g Ca with a mean value of 27.1 ± 16.1 µg Al/g Ca. The negative concentration was reported as undetectable. For the occupationally exposed, aluminum concentrations ranged from 34.2 ± 19.8 µg Al/g Ca to 44.6 ± 18.5 µg Al/g Ca, with a mean value of 41.2 ± 4.5 µg Al/g Ca. The difference between the two mean values was found to be significant at the 5% level.

The results obtained by Davis et al. [62] were in agreement with the aluminum levels in healthy individuals measured *in vivo* or *in vitro* by other groups. However, most of the measurements were very close to the detection limit of the technique which indicated that while their technique was capable of successfully measuring the aluminum concentration in subjects undergoing dialysis, or those exposed to high levels of aluminum, it was not as reliable in measuring healthy persons and control subjects. Further envisaged enhancements included reducing the irradiation and transfer time to improve the detection limit of the system.

Figure 1.3. The shielded 4π detector assembly at McMaster University.

There were two major improvements made to the system reported by Aslam et al [63]. The first was the use of a high current accelerator, which allowed for reducing the irradiation time in order to increase activation and to minimize decay during irradiation, while maintaining the dose as low as possible. The current was increased from 100 μA to 400 μA and subsequently, the irradiation time was decreased to 45 s from the original 180 s. The second area of improvement involved the detection system shown in Figure 1.3. The previous studies and also the first part of this study was done using an array of 8 NaI(Tl) detectors, two of which had a poor resolution which led to larger uncertainties in the measurements. These two detectors were replaced and an additional smaller detector was added to bring the solid angle even closer to 4π.

The phantom studies performed on the improved system also benefitted from a shorter transfer time of only 45 seconds. The importance of having a shorter

transfer time lies in the fact that due to the 135 second half-life of aluminum, longer transfer times mean decay of the radionuclide during transfer which is undesirable from a detection standpoint. The total effect of increasing the current and reducing the irradiation and transfer times reduced the detection limit to 8.32 μg Al/g Ca from the previously determined 19.5 μg Al/g Ca, making the system capable of measuring much lower concentrations of aluminum likely to be found in unexposed individuals under current exposure levels.

3. Future Directions

The most recent improvements on the analysis technique and phantom measurements performed by Matysiak et al. at McMaster University were presented at the 10th Keele Meeting on Aluminum, held in Winchester, England in 2013. The main areas of improvement were: (1) using the technique of digital anticoincidence counting to reduce the interference from the chlorine peak by a factor of 4 [59], (2) using a half-life analysis, and (3) using low concentration phantoms which better resembled the aluminum levels found in human subjects.

Accelerator-based neutron beams offer many advantages by providing high fluence rates while eliminating or reducing the effect of interfering nuclear reactions. However, their limited availability in clinical settings, due to size and cost considerations, renders them impractical when large clinical studies or routine patient monitoring is of interest. Recently, Liu et al. [64,65] investigated the feasibility of using a deuterium-deuterium (DD) neutron generator as a

portable system for the *in vivo* measurement of manganese. The DD neutron source provides neutrons with the energy of about 2.45 MeV. Such a system can be very promising for IVNAA of aluminum, because of its technical characteristics, as well as cost and portability. Compared to a full scale accelerator-based system, the portable DD neutron source can be purchased at a fraction of the cost of the standard-sized system without the need for a large space. The DD system has a high neutron yield compared to the ^{252}Cf neutron source previously used by Wyatt et al [55].

The neutron energy generated by the deuterium-deuterium fusion is also much lower than the 14 MeV neutrons used by Williams et al. [49] with the deuterium-tritium fusion reaction as the neutron source. While the 2.45 MeV neutrons generated by the DD system are above the energy threshold for the ^{31}P(n,α) ^{28}Al reaction, considering the Coulomb barrier of 6.22 MeV for the reaction the probability of the activation of ^{31}P would be low. The exact details of this activation reaction are currently being investigated at McMaster University. Given the above mentioned advantages, the DD neutron generator has considerable potential for the measurement of aluminum.

Another area which requires further investigation is the inter-laboratory comparison of aluminum measurements. While IVNAA results are reported as the Al/Ca ratio, most of the chemical analysis techniques report the results in terms of mass ratio of aluminum to fresh, dry, ash, or wet bone. Parsons et al. [9]

measured the ratio of ash/dry weight and dry/wet weight for control and renal failure, and dialysis samples; but to date, there are no validated conversion methods for comparing the results of different laboratories. The current method involves crude estimation of the amount of calcium in dry or wet bones which may not lead to accurate results. Inter-laboratory collaborations in measuring the same samples with different methods and comparing the results can provide invaluable information about the aluminum body burden in different medical and occupational scenarios.

4. Conclusions

Due to the evidence for Al involvement in multiple medical conditions such as Alzheimer's disease, as well as occupational hazards, more research needs to be done in the field of *in vivo* measurement of aluminum. More specifically, there is a need for clinical studies to test the new techniques and challenge their detection limits in clinical settings. For an IVNAA technique to be successful under the circumstances of a clinical study, certain technical criteria must be met. First and foremost, is the choice of a neutron source. An ideal neutron source has a high thermal neutron flux and zero or negligible high-energy neutrons to avoid the activation of ^{31}P. This will maximize the activation of aluminum, while keeping the patient's exposure to ionizing radiation as low as possible. While ^{252}Cf enjoys the benefit of being more readily available, the current low levels of aluminum limit the choices to sources that offer a high flux of neutrons, such as

thermalized reactor beams and accelerator beams, where the incident energy can be controlled. The choice of the site of measurement has important implications, both in terms of convenience and radiation safety. Bone is the ideal site for measurement of aluminum as most of the aluminum burden of the body is stored in the bone. The question of whether or not bone is a suitable proxy for brain needs to be addressed through post-mortem analysis of both brain and bone samples of Alzheimer's disease and control subjects, though this is outside the scope of *in vivo* aluminum measurement.

Ellis et al. is the only group comparing IVNAA with an alternative proxy system by reporting serum aluminum levels in renal failure patients as well bone aluminum [52]. Serum aluminum levels in healthy individuals are believed to be in the range of 1-3 μg/L [40]. The baseline serum aluminum levels found in patients with renal failure in Ellis' study were significantly raised compared to the healthy individuals; a result that was observed by Harrington et al. [66]. However, there was no correlation between baseline serum aluminum and the total body and skeletal aluminum levels. There was however, a significant correlation between the skeletal burden of aluminum and serum aluminum after administration of DFX. The reason for the lack of correlation in baseline values might be the fact that serum is considered as the transport system for aluminum and, therefore, may not accurately reflect long-term exposures and aluminum body burden. In general, serum and urine are better indicators of recent aluminum exposures [1].

Early IVNAA studies used the method of total body irradiation exposing the entire body to neutrons and hence delivering unnecessary dose to sensitive organs. The human hand has been the site of choice by many researchers for a variety of reasons. Human hand bone accounts for 1.5% of the skeleton. In general, extremities are not particularly radiosensitive [35] which makes the hand a suitable site for irradiation. The effective dose is also low due to the relatively small tissue weighting factors of skin and bone. Moreover, the hand is also a convenient site in terms of instrumentation and constructing the radiation cavity in such way that would protect the rest of the body from the harmful effects of radiation. The calcaneus bone in the foot is a less convenient choice which may be favoured as trabecular bone has been shown to have a higher aluminum content compared to the cortical bone in the hand [36]. There is still need for further optimization and improvement in the field of IVNAA to make routine monitoring of bone aluminum possible.

Table 1.3 lists the progress of IVNAA studies in terms of MDL and the dose delivered to the subjects. As can be seen, even though the reactor provided a better neutron flux and lower MDL in the work of Ellis et al. in 1988 [52], the progress made over the next years on accelerator setup in terms of irradiation and detection geometries and analysis methods helped it to achieve even better detection limits and a lower dose to the subjects.

Table 1.3. Performance of different methods of IVNAA.

Study	Neutron source	MDL		Dose	
		Al (mg)	μgAl/gCa	Equivalent (mSv)	Effective (μSv)
Williams- 1981	14 MeV neutron Generator	-	-	-	-
Ellis- 1988	Reactor	0.4	-	20	26
Green- 1992	Accelerator- 1.05MeV	2.0	-	50	65
	Accelerator- 1.2MeV	1.2	-	50	65
Green- 1992	Accelerator- 1.2MeV	3.2	-	13	17
Wyatt	Accelerator- 1.2MeV	1.3	-	46	60
Palerme- 1993	Reactor	1.5	-	4	-
Pejovic- Milic- 1998	Accelerator	2.5	-	12	16
Comsa- 2004	Accelerator	0.7	-	20	26
Davis- 2008	Accelerator	0.29	19.48	17.6	14.4
Aslam- 2009	Accelerator	0.12	8.32	17.6	14.4

Table 1.4 summarizes the results of the clinical studies performed with IVNAA. While the continuous improvements in the detection limit over the years and its successful application in measuring bone aluminum in dialysis subjects is quite encouraging, a successful IVNAA system must be capable of detecting aluminum levels found in healthy subjects. Assuming the 1.06 μg/g dry weight listed in Table 1.1 is the mean bone aluminum content of healthy individuals, a crude conversion factor of 4 can be adopted between the dry weight and calcium content of the bone. This is based on the ratio of the percentage of the inorganic component of the bone crystal which makes up the dry weight of the bone and

the calcium content. Currently, the lowest MDL reported in the literature is 8.32 µg Al/g Ca, reported by Aslam et al. [63]. An approximate aluminum content of 4.24 µg Al/g Ca can be adopted for healthy individuals using the above conversion factor, which is lower than the current MDL by a factor of two. This is also indicated by the wide range of aluminum in healthy subjects as reported by Davis et al. [62] and shown in Table 4. These results further strengthen the need for achieving yet lower detection limits and conducting extensive clinical studies.

Table 1.4. Results of clinical studies using IVNAA.

					Al range	
Study	Number of subjects	Medical condition	Serum Al (µg/l)	Mean hand Al (µg Al/g Ca)	Hand µg Al/g Ca	Total body Al (mg)
Williams	48	Renal failure with and without DE	-	-	-	2200 - 3300
Ellis	10, 185	Renal failure	19-98	209	20 - 760	764-2683
Wyatt	7	Renal failure	-	-	-42 - 518	N/A
Davis	20	Control	-	27.1	-9.6 - 60.3	N/A
Aslam	8	Al welders	-	41.2	34.2 - 44.6	N/A
ICRP	-	-	-	-	20	21

References

[1] Yokel RA (2013) Aluminum, In *Encyclopedia of human nutrition*, Waltham: MA, Academic Press. **1**, pp.57–63.

[2] Alfrey AC (1983) Aluminum. *Adv. Clin. Chem.* **23**, 69–91.

[3] Valkovic V (1980) Is aluminum essential for life. *Orig. Life* **10**, 301–305.

[4] Kopeloff LM, Kopeloff EB (1942) Recurrent convulsive seizures in animals produced by immunologic and chemical means. *Am. J. Psychiatry* **98**, 881–902.

[5] Parkinson IS, Ward MK, Kerr DNS (1981) Dialysis encephalopathy, bone disease and anaemia: the aluminium intoxication syndrome during regular haemodialysis. *J. Clin. Pathol.* **34**, 1285–1294.

[6] Ellis HA, McCarthy JH, Herrington J (1979) Bone aluminium in haemodialysed patients and in rats injected with aluminium chloride: relationship to impaired bone mineralisation. *J. Clin. Pathol.* **32**, 832–44.

[7] Alfrey AC, Hegg A, Craswell P (1980) Metabolism and toxicity of aluminum in Renal Failure. *Am. J. Clin. Nutr. J. Clin. Nutr.* **33**, 1509–1516.

[8] Dunea G, Mahurkar SD, Mamdani B, Smith EC (1978) Role of aluminum in dialysis dementia. *Ann. Intern. Med.* **88**, 502–504.

[9] Parsons V DC, Goode C, Ogg C, Siddiqui J (1971) Aluminium in bone from patients with renal failure. *Br. Med. J.* **4**, 273–275.

[10] Cartier F, Allain P, Gary J, Chatel M, Menault F, Pecker S (1978) Progressive myoclonic encephalopathy in dialysis patients- role of water used for hemodialysis. *Nouv. Press. MEDICALE* **7**, 97–102.

[11] Arieff AI, Cooper JD, Armstrong D, Lazarowitz VC (1979) Dementia , renal failure , and brain aluminum. *Ann. Intern. Med. Med.* **90**, 741–747.

[12] Crapper DR, Krishnan SS, Dalton AJ (1973) Brain Aluminum Distribution in Alzheimer's Disease and Experxmental Neurofibrillary Degeneration. *Sci. New Ser.* **180**, 511–513.

[13] Exley C, Vickers T (2014) Elevated brain aluminium and early onset Alzheimer's disease in an individual occupationally exposed to aluminium: a case report. *J. Med. Case Rep.* **8**, 41. doi: 10.1186/1752-1947-8-41

[14] Andrasi E, Pali N, Molnar Z, Kosel S (2005) Brain aluminum, magnesium and phosphorus contents of control and Alzheimer-diseased patients. *J. Alzheimers. Dis.* **7**, 273–84.

[15] Nee LE, Eldridge ER, Sunderland T, Thomas CB, Katz D, Thompson KE, Weingartner H, Weiss H, Julian C, Cohen R (1987) Dementia of the Alzheimer's type- Clinical and family study of 22 twin pairs. *Neurology* **37**, 359–363.

[16] Räihä I, Kaprio J, Koskenvuo M, Rajala T, Sourander L (1996) Alzheimer's disease in Finnish twins. *Lancet* **347**, 573–578.

[17] Räihä I, Kaprio J, Koskenvuo M, Rajala T, Sourander L (1998) Environmental differences in twin pairs discordant for Alzheimer's disease. *J. Neurol. Neurosurg. Psychiatry* **65**, 785–787.

[18] Pedersen NL, Gatz M, Berg S, Johansson B (2004) How heritable is Alzheimer's disease late in life? Findings from Swedish twins. *Ann. Neurol.* **55**, 180–5. doi: 10.1002/ana.10999.

[19] Walton JR (2014) Chronic aluminum intake causes Alzheimer's disease: applying Sir Austin Bradford Hill's causality criteria. *J. Alzheimers. Dis.* **40**, 765–838. doi: 10.3233/JAD-132204 .

[20] Sjogren B, Lundberg I, Lidums V (1983) Aluminium in the blood and urine of industrially exposed workers. *Br. J. Ind. Med.* **40**, 301–304.

[21] Klein GL, Targoff CM, Ament ME, Sherrard DJ, Bluestone R, Young JH, Norman AW, Coburn JW (1980) Bone-disease associated with total parenteral nutrition. *Lancet* **2**, 1041–1044.

[22] Sedman AB, Klein GL, Merritt RJ, Miller NL, Weber KO, Gill WL, Anand H, Alfrey AC (1985) Evidence of aluminum loading in infants receiving intravenous therapy. *N. Engl. J. Med.* **312**, 1337–43. doi: 10.1056/NEJM198505233122101.

[23] Kruger PC, Parsons PJ, Galusha AL, Morrissette M, Recker RR, Howard LJ (2013) Excessive aluminum accumulation in the bones of patients on long-term parenteral nutrition: postmortem analysis by electrothermal atomic absorption spectrometry. *JPEN. J Parenter Enteral Nut.* **38**, 728-735.

[24] Fewtrell MS, Bishop NJ, Edmonds CJ, Isaacs EB LA (2009) Aluminum exposure from parenteral nutrition in preterm infants: bone health at 15-year follow-up. *Pediatrics* **124**, 1372–9.

[25] House E, Esiri M, Forster G, Ince PG, Exley C (2012) Aluminum, iron, and copper in human tissues donated to the medical research council's cognitive function and ageing study. *Metallomics*. **4**, 56-65.

[26] Elinder C, Ahrengart L, Lidums V, Pettersson E, Sjogren B (1991) Evidence of aluminium accumulation in aluminium welders. *Br. J. Ind. Med.* **48**, 735–738.

[27] Hellström H, Lindh U, Mjöberg B (2000) Measurement accuracy of aluminium content in bone. *Ups. J. Med. Sci.* **105**, 67–71.

[28] Gonzalez-Domiguez R, Garcia-Barrera T, Gomez-Ariza JL (2014) Characterization of metal profiles in serum during the progression of Alzheimer's disease, *Metallomics*, **6**, 292-300.

[29] Denton J, Freemont AJ, Ball J (1984) Detection and distribution of aluminium in bone. *J. Clin. Pathol.* **37**, 136–42.

[30] Bogdanovich E, Krishnan SS, Pei Y, Hercz G, Lui SM, Hancock R, Harrison JE, Bone A (1992) Non-destructive bone aluminum assay by neutron activation analysis. *J. Radioanal. Nucl. Chem.* **164**, 293–302.

[31] Blotcky AJ, Rack EP, Recker RR, Leffler JA, Teitelbaum S (1978) Trace aluminum determination and sampling problems of archeological bone employing destructive neutron activation analysis. *J. Radioanal. Chem.* **43**, 381–388.

[32] Sharif AAM, Ghafourian H, Ahmadiniar A, Waqif HS, Saber-Tehrani M, Ghods H (2004) Determination of aluminum levels in serum and red blood cells from long-term haemodialysis patients using instrumental neutron activation analysis. *J. Radioanal. Nucl. Chem.* **262**, 473–477.

[33] Hussain A, Barer D (1995) Fracture risk in patients with Alzheimer's disease. *J Am Geriatr Soc*. **43**, 454.

[34] Sato Y, Kanoko T, Satoh K, Iwamoto J (2004) Risk factors for hip fracture among elderly patients with Alzheimer's disease. *J Neurol Sci*. **2**, 107-12.

[35] ICRP (1991) *Annals of the International Commission on Radiation Protection*, *Publication 60*. Pergamon, Oxford.

[36] Lefebvre A, Horlait S, Chappuis P, Moynot A, Masselot JP, Gueris J, de Vernejoul MC (1988) Cortital vs trabecular bone aluminum in dialyzed patients. *Am J Kidney Dis*. **12**, 220-6.

[37] O'Mahony D, Denton J, Templar J, O'Hara M, Day JP, Murphy S, Walsh JB, Coakley D (1995) Bone aluminum content in Alzheimer's disease. *Dementia*, **6**, 69-72.

[38] Hellström H, Mjoberg B, Mallmin H, Michaelsson K (2005) The aluminum content of bone increases with age, but is not higher in hip fracture cases with or without dementia compared to controls. *Osteoporos Int*, **16**, 1982-1988.

[39] Exley C, House ER (2011) Aluminum in human brain. *Monatsh Chem*, **142**, 357-363.

[40] Yegambaram M, Manivannan B, Beach TG, Halden RU (2015) Role of environmental contaminants in the etiology of Alzheimer's disease: A review. *Curr Alzheimer's Res*, **12**, 116-46.

[41] Chettle DR, Fremlin JH, (1984) Techniques of in vivo neutron activation analysis. *Phys Med Biol*, **29**, 1011-43.

[42] ICRP (1974) *Report of the task group on reference man*, *Publication 23*. Pergamon, Oxford.

[43] ENDF/B-VII Incident-neutron data, https://t2.lanl.gov/nis/data/endf/endfvii-n.html, Accessed on October 2, 2015.

[44] Anderson J, Osborn SB, Tomlinson RW, Newton D, Rundo J, Salmon L, Smith JW (1964) Neutron activation analysis in man in vivo: A new technique in medical investigation. *Lancet* **2**, 1201–1205.

[45] Boddy K, Holloway I, Elliot A (1973) A Simple facility for total body in vivo activation analysis. *Int. J. Appl. Radiat. Isot.* **24**, 428–430.

[46] Williams ED, Boddy K, Harvey I, Haywood JK (1978) Calibration and evaluation of a system for total body in vivo activation analysis using 14 MeV neutrons. *Phys. Med. Biol.* **23**, 405–415.

[47] Spinks TJ, Bewley DK, Joplin GF, Ranicar ASO (1976) Neutron-activation measurement of metabolic activity of sodium in the human hand. *J. Nucl. Med.* **17**, 724–729.

[48] Spinks TJ, Bewley DK, Paolillo M, Vlotides J, Joplin GF, Ranicar ASO (1980) Metabolic activity of sodium , measured by neutron activation , in the hands of patients suffering from bone diseases: concise communication. *J. Nucl. Med.* **21**, 41–46.

[49] Williams ED, Elliott HL, Boddy K, HaywoodD JK, Henderson IS, Harvey I, Kennedy AC (1980) Whole-body aluminum in chronic renal failure and dialysis encephalopathy. *Clin. Nephrol.* **14**, 198–200.

[50] Nelp WB, Denney JD, Murano R, Hinn GM, Williams JL, Rudd TG, Palmer HE (1978) A two-way scanning method for total body in vivo neutron activation analysis. *Phys. Med. Biol.* **23**, 865–875.

[51] Nelp WB, Denney JD, Murano R, Hinn GM, Williams JL, Rudd TG, Palmer HE (1972) Absolute measurement of total body calcium (bone mass) in vivo. *J. Lab. Clin. Med.* **79**, 430–8.

[52] Ellis KJ, Kelleher S, Savory J, Wills M (1988) In vivo monitoring of skeletal aluminum burden in patients with renal failure. *J. Radioanal. Nucl. Chem.* **124**, 85–95.

[53] Green S, Chettle DR (1992) A feasibility study of the in vivo measurement of aluminum in peripheral bone. *Phys. Med. Biol.* **31**, 2287–2296.

[54] Green S, Bradley DA, Mountford PJ, Morgan WD, Chettle DR, Weaver DR (1993) Characteristics of an accelerator based system for in-vivo aluminum measurement in peripheral bone. *Basic Life Sci.* 289–293.

[55] Wyatt RM, Ryde SJ, Morgan WD, McNeil EA, Hainsworth IR, Williams AJ (1993) The development of a technique to measure bone aluminium content using neutron activation analysis. *Physiol. Meas.* **14**, 327–35.

[56] Alfrey AC, LeGendre GR, Kaehny WD (1976) The dialysis encephalopathy syndrome. Possible aluminum intoxication. *N. Engl. J. Med.* **294**, 184–8. doi: 10.1056/NEJM197601222940402.

[57] Palerme S, Chettle DR, Kennett TJ, Prestwich WV, Webber CE (1993) Pilot-studies for in-vivo bone aluminum measurement. *Basic Life Sci.* 303–306.

[58] Comsa DC, Prestwich WV, McNeill FE, Byun SH (2004) Application of spectral decomposition analysis to in vivo quantification of aluminum by neutron activation analysis. *Appl. Radiat. Isot.* **61**, 1353–60. doi: 10.1016/j.apradiso.2004.03.062

[59] Byun SH, Prestwich WV, Chin K, Mcneill FE, Chettle DR (2006) 4-pi NaI(Tl) detector array for in vivo neutron activation analysis. *IEEE Trans. Nucl. Sci.* **53**, 2944–2947. doi: 10.1109/TNS.2006.880115.

[60] Byun SH, Pejović-Milić a, McMaster S, Matysiak W, Liu Z, Watters LM, Prestwich W V, McNeill FE, Chettle DR (2007) Dosimetric characterization of the irradiation cavity for accelerator-based in vivo neutron activation analysis. *Phys. Med. Biol.* **52**, 1693–1703. doi: 10.1088/0031-9155/52/6/010.

[61] Pejović-Milić A, Byun SH, Comsa DC, McNeill FE, Prestwich WV, Chettle DR (2005) In vivo measurement of bone aluminium: recent developments. *J. Inorg. Biochem.* **99**, 1899–903. doi: 10.1016/j.jinorgbio.2005.06.010.

[62] Davis K, Pejović-Milić A, Chettle DR (2008) In vivo measurement of bone aluminum in population living in southern Ontario, Canada. *Med. Phys.* **35**, 5115. doi: 10.1118/1.2996177.

[63] Aslam, Davis K, Pejović-Milić A, Chettle DR (2009) Noninvasive measurement of aluminium in human bone: preliminary human study and improved system performance. *J. Inorg. Biochem.* **103**, 1585–90. doi: 10.1016/j.jinorgbio.2009.07.021.

[64] Liu Y, Koltick D, Byrne P, Wang H, Zheng W, Nie LH (2013) Development of a transportable neutron activation analysis system to quantify manganese in bone in vivo: feasibility and methodology. *Physiol. Meas.* **34**, 1593–609. doi: 10.1088/0967-3334/34/12/1593.

[65] Liu Y, Byrne P, Wang H, Koltick D, Zheng W, Nie LH (2014) A compact DD neutron generator-based NAA system to quantify manganese (Mn) in bone in vivo. *Physiol. Meas.* **35**, 1899–911. doi: 10.1088/0967-3334/35/9/1899.

[66] Harrington CR, Wischik CM, McArthur FK, Taylor GA, Edwardson JA, Candy JM (1994) Alzheimer's-disease-type changes in tau protein processing:association with aluminum accumulation in brains of renal dialysis patients. *Lancet*, **343**, 993-97.

[67] Pejovic-Milic A, McNeill FE, Prestwich WV, Waker AJ, Chettle DR (1998) Development of an accelerator based determination of Al burden in peripheral bone by Neutron Activation Analysis. *Appl. Radiat. Isot.* **49**, 717–719.

Chapter 2

Optimization of Data Analysis for the *In vivo* Neutron Activation Analysis of Aluminum in Bone

Introduction to Article II

Article II, presented in this chapter, describes in detail, the methods of data analysis developed and tested in order to investigate the best approach in extracting the aluminum counts from the gamma spectra and achieving the lowest minimum detection limit based on phantom studies. This is an important step, as the aluminum content of the human hand bone is small compared to the other elements with significant neutron capture cross-sections. Additionally, the aluminum peak is overlapped by the adjacent chlorine peak, making its detection more challenging.

The experimental work and analyses presented in the following article was performed by the author of this thesis under the supervision of Dr. David Chettle, and with guidance of Dr. Witold Matysiak, Dr. Bill Prestwich, Dr. Soo Hyun Byun, Dr. Nicholas Priest, and Dr. Jovica Atanackovic.

Contents of Article II

The following article has been submitted for publication in the journal of Applied Radiation and Isotopes (manuscript ID: ARI-D-16-00137).

Optimization of Data Analysis for the *In Vivo* Neutron Activation Analysis of Aluminum in Bone

H. Katalmohseni[1], W. Matysiak[2], D.R. Chettle[1], S.H. Byun[1], N. Priest[3], J. Atanackovic[4], W.V. Prestwich[1]

[1]Medical Physics & Applied Radiation Sciences, McMaster University, Hamilton, Canada
[2]University of Florida Proton Therapy Institute, Jacksonville, FL, USA
[3]Canadian Nuclear Laboratories, Chalk River Laboratories, Ontario, Canada
[4]Ontario Power Generation, Whitby, Ontario, Canada

Abstract

An existing system at McMaster University has been used for the *in vivo* measurement of aluminum in the human bone. Precise and detailed analysis approaches are necessary to determine the aluminum concentration because of the low levels of aluminum found in the bone and the challenges associated with its detection. Phantoms resembling the composition of the human hand with varying concentrations of aluminum were made for testing the system prior to the application to human studies. A spectral decomposition model and a region-based model involving the inverse-variance weighted mean and a time-dependant analysis were explored to analyse the results and determine the model with the best performance and lowest minimum detection limit. The results

showed that the spectral decomposition and the region-based model with the inverse variance weighted mean both provided the better results compared to the other methods tested. The spectral decomposition method resulted in a marginally lower detection limit (5 μg Al/g Ca) compared to the inverse-variance weighted mean (5.2 μg Al/g Ca), rendering both equally applicable to human measurements.

Keywords- *in vivo* neutron activation, aluminum, bone, data analysis, gamma spectroscopy, spectral decomposition, region-based analysis

1. Introduction

Aluminum (Al), as the most common metal in the earth's crust, plays an important role in our everyday lives. It is non-essential for the human body with known neurotoxicity in high concentrations [1]. Exposure to Al has been studied in the context of environmental, medical, and occupational exposures. In most of these cases routine monitoring is favourable, which calls for safe and non-invasive measurement techniques. Because of aluminum's ubiquitous nature, in vitro measurement of Al such as urine and serum measurements can be challenging due to the high risk of contamination. The skeleton is considered as the Al depot, storing about 60% of Al body burden [2], and as such, a suitable medium for measuring Al. The human body retains only about 0.1% of its total Al intake, and therefore, measuring Al content even in the bone can be challenging. The most

common method of measuring the bone Al content requires bone biopsy, an invasive method that cannot be used for routine and repeated measurements.

In vivo neutron activation analysis (IVNAA) has been considered as method of choice for decades for the total body measurement of elements such as calcium, sodium, and phosphorous [3-6]. IVNAA was first used in measuring Al in 1980 [7]. It has since gone under continuous improvement to increase its performance, sensitivity and detection limit [7-12].The system developed at McMaster has been used to measure multiple elements in human bones [11-16]. Many hardware and software upgrades have been made to allow for optimization for different measurements. These have been reported in detail in the literature [12, 17-19]. In order for a measurement technique to be suitable for application in humans, it needs to be sensitive enough to detect the levels of Al found in healthy individuals. This can be achieved in part by hardware upgrades and also improving the data analysis approaches. The current work focuses on the development of methods for spectral analysis of Al data with the goal of extracting the maximum amount of information with minimum uncertainty. The performance of each method is investigated in terms of the minimum detection limit and a comparison of the results is made to determine the best method for application to human measurements.

2. Methods

IVNAA is based on the activation of isotopes of elements with significant cross-sections for thermal neutron capture within the tissue, which in turn relies on the neutron energy. For the energy range of neutrons generated by the accelerator and the hand bone as the medium, the major isotopes are ^{48}Ca, ^{37}Cl, and ^{23}Na. ^{27}Al, the only stable isotope of aluminum, has a thermal neutron cross-section of 0.23 b. The resultant ^{28}Al radioisotope is unstable and decays via β emission and a 1.78 MeV gamma ray to stable ^{28}Si. Extracting the Al counts in the spectra is a challenging task due to the low concentrations of Al found in the biological tissues and the complications arising from spectral interferences with other radioisotopes.

For the high efficiency NaI(Tl) detector system used, the 1.78 MeV gamma-ray of Al is overlapped by the adjacent 1.64 MeV gamma-ray of ^{38}Cl. Cl is physiologically more abundant and ^{37}Cl has a neutron capture cross-section of 0.43 b which is higher than that of Al. As a result, the 1.64 MeV peak of ^{38}Cl dominates the Al peak at 1.78 MeV. The resolution of the NaI(Tl) detector is not high enough to resolve the 1.64 MeV and 1.78 MeV peaks completely. However, the 1.64 MeV gamma-ray is always emitted in cascade with the 2.17 MeV gamma-ray of ^{38}Cl. ^{24}Na is another radioisotope that emits two gamma-rays in cascade. Using anticoincidence counting reduces the number of counts associated with events that take place in coincidence, which is the case for ^{38}Cl.

While ^{24}Na is not in the close vicinity to the 1.78 MeV peak of Al, the anticoincidence mode helps to reduce the continuum due to ^{24}Na's 2.75 MeV peak.

2.1. System

The measurements were performed at the IVNAA facility at the McMaster Accelerator Laboratory (MAL). The IVNAA facility has been discussed in details in the literature by our group [11-18]. Briefly, the Tandetron accelerator used for generating neutrons is a 1.25 MV high-current tandem machine producing neutrons using a thick lithium target through the ^{7}Li(p,n)^{7}Be reaction. The target, together with the irradiation cavity is confined in a shielded box shown in Figure 2.1, which was designed and developed at McMaster University [18].

Figure 2.1. Irradiation cavity of the Tandetron accelerator at McMaster University.

The detection system shown in Figure 2.2 consists of 9 NaI(Tl) scintillation detectors arranged in a 4π geometry with an opening for inserting the sample [17]. The detectors are fitted with different photomultiplier tubes (PMT) and have different energy resolutions.

The digital processing system (DSP), also developed in-house, acquires and compiles the data from the 9 detectors. The DSP system is designed such that it can collect data in coincidence and anticoincidence modes, in addition to single detector responses [17].

Figure 2.2. The shielded 4π detector assembly at McMaster University.

2.2. Phantoms

In order to evaluate the performance of the system and the data analysis methods, hand phantoms were made based on the composition of the human hand, comprising both the cortical bone and soft tissue as published in ICRP 23 [20]. Only elements with large neutron capture cross-sections were included in the phantoms. These are Ca, Na, Cl and Al with reactions $^{48}Ca(n,\gamma)^{49}Ca$, $^{23}Na(n,\gamma)^{24}Na$, $^{37}Cl(n,\gamma)^{38}Cl$, and $^{27}Al(n,\gamma)^{28}Al$, respectively. The phantoms were made in triplicates of high purity compounds in an aqueous base containing 14.9 g of Ca, 1.3 g of Na, and 1.2 g of Cl. Varying concentrations of aluminum were added to the phantoms including zero, 250 µg, 500 µg, 750 µg, 1000 µg, 2000 µg, and 5000 µg, corresponding to zero, 16.8, 33.6, 50.3, 67.1, 134.2, and 335.6 µg Al/g Ca. The phantoms were contained in low density polyethylene (LDPE) Nalgene™ bottles to avoid Al contamination. However, since further measurements revealed that traces of Al were present in the LDPE bottles, it was decided to transfer the contents of the bottles to un-irradiated bottles immediately after irradiation to remove the possibility of detecting Al counts originating from the bottles.

2.3. Measurements and data collection

The phantoms were irradiated at a proton energy of 2.3 MeV and proton current of 400 µA for 45 sec. The irradiation protocol was optimized to maximize the activation of Al while reducing the decay during irradiation. Moreover, at the proton energy of approximately 2.3 MeV, the maximum energy of the produced

neutrons is 0.55 MeV, which prevents the activation of Phosphorus (P) through the interfering $^{31}P(n,\alpha)^{28}Al$ reaction with the neutron energy threshold of 2.01 MeV. It is noted that P is an abundant element in the biological samples, and therefore, could be a source of significant interference with Al.

Spectral data were acquired in 10 cycles of 60 sec to allow for the decay of multiple half-lives of Al. Moreover, saving the data in one-minute intervals allows for following the exponential decay of the radionuclides of interest, i.e. Al and Ca. Figure 2.3 shows the spectrum acquired from the first cycle of the 33.6 µg Al/g Ca phantom.

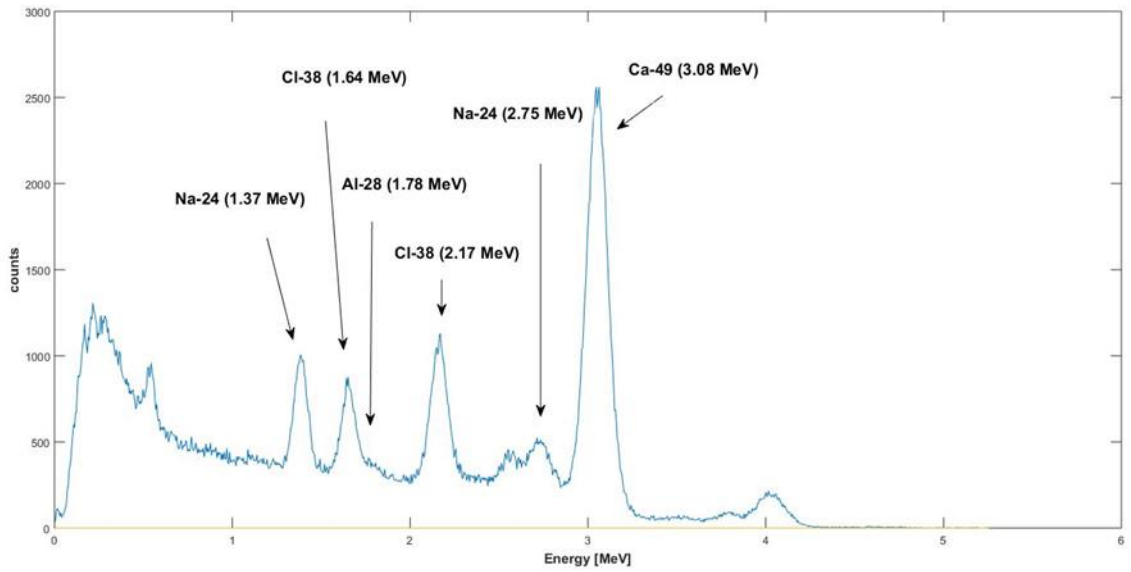

Figure 2.3. Gamma-ray spectrum of a 33.6 µg Al/g Ca phantom.

2.4. Analysis

The analysis of gamma spectra was performed using two different approaches. The first and most commonly used method was the region-based analysis, in which only energy regions containing the peaks of interest were analysed. The second method was a library-based method of spectral decomposition which makes use of the entire spectrum. Each of the methods described herein were applied to each of the 10 cycles of data, unless otherwise stated. The results were reported as the ratio of Al to Ca (μg/g) to eliminate the variations due to changes in the neutron fluence and also positioning of the phantom in the irradiation cavity.

As mentioned above, the detection system consists of 9 NaI(Tl) detectors. The gain of the detectors, defined as the ratio of energy to channel number, is subject to variation from one measurement to the next. Potential reasons for this behaviour are non-linearity in different components of the pulse processing electronics and the variations in the ambient temperature. The gain variations and the consequent gain misalignment in the 9 detectors are manifested in the resulting spectra in the form of shifted peak positions and peak width changes. In addition to the gain variations among the 9 detectors, non-linearity in the gain of each individual detector within a single measurement can further complicate the analysis. In order for the data from all detectors to be compiled for analysis, the gains of all detectors were aligned prior to each measurement. This was

achieved by using a calibration source, which in this case was ^{60}Co. ^{60}Co de-excites through the cascade emission of two gamma-rays with energies of 1.17 MeV and 1.33 MeV. The higher energy peak is typically used for calibration as it is closer to the peaks of interest and the input voltage of each detector was adjusted to match the 1.33 MeV peak position for all the 9 detectors.

2.4.1. Region-based analysis

In this approach, the analysis was limited to two regions containing the Al and Ca peaks in the approximate energy ranges of 1.5 – 1.9 MeV and 2.8 – 3.3 MeV, respectively. The non-linear least squares approach was employed using the Levenberg-Marquardt method to find the best fit to the data. The isolated Ca peak in the 2.8 – 3.3 MeV region was fitted with one Gaussian and a linear function with both the peak position and width as free parameters, shown in Equation 1. The problem of gain instability was alleviated by allowing the peak positions to float by assigning a fit parameter, as opposed to a fixed peak position.

$$y = a_0 + a_1 x + \frac{a_2}{\sqrt{2\pi a_3}} \exp\left(-\frac{(x-a_4)^2}{2a_3^2}\right) \qquad \text{Equation (1)}$$

Where a_2 is the peak integral count, a_3 is the peak width, and a_4 is the peak centroid.

The 1.5 - 1.9 MeV range was fitted with two Gaussian functions to accommodate both Al and Cl peaks, as well as a linear function to account for the continuum in

the spectra as shown in Equation 2. The Al peak position was fixed to the positions of both Cl and Ca peaks and the widths of both peaks were fixed proportional to $E^{1/2}$, where E is the gamma-ray energy.

$$y = a_0 + a_1 x + \frac{a_2}{\sqrt{2\pi\sigma_{Cl}}} \exp\left(-\frac{(x-a_3)^2}{2\sigma_{Cl}^2}\right) + \frac{a_4}{\sqrt{2\pi\sigma_{Al}}} \exp\left(-\frac{(x-C_{Al})^2}{2\sigma_{Al}^2}\right) \qquad \text{Equation (2)}$$

Where σ_{Al} and σ_{Cl} are the widths of Al and Cl peaks, respectively, a_3 is the centroid of the chlorine peak, and C_{Al} is the centroid of the Al peak derived from the following equation:

$$C_{Al} = C_{Ca} - \left(\frac{C_{Ca}-a_3}{E_{Ca}-E_{Cl}}\right)(E_{Ca} - E_{Al}) \qquad \text{Equation (3)}$$

Where C_{Ca} is the centroid of the Ca peak and E_{Ca} and E_{Cl} are the gamma energies of the ^{49}Ca and ^{38}Cl, respectively. Equation 3 is derived by fitting a linear function to the centroids and energies of Ca and Cl peaks in order to fix the position of Al peak and reduce the number of parameters.

As previously mentioned, the data acquisition was performed in 10 one minute cycles, allowing for different approaches to analysis. The preliminary method developed for data analysis was to analyze the first 3 cycles as one block of data by summing the counts from each one minute acquisition in order to take advantage of the highest number of Al counts with the lowest relative counting

uncertainty. This approach is also justified in view of the half-life comparison between Al and Cl. In 10 minutes, the activity of Al decreases by 95.5% whereas Cl decreases by only 17%. In three minutes, however, the Al and Cl decay by 60% and 5%, respectively. This balances the ratio of the activities of Al to Cl in favor of Al in the first 3 minutes, compared to 10 minutes, thus justifying the approach. Following the analysis, corrections for physical decay during transfer and counting cycles were made to arrive at the number of radioactive nuclei at the end of the 45 sec irradiation time.

While using the first three minutes offers the advantage of omitting the data with large uncertainties, it suffers from an overall loss of counts. Analyzing the 10 cycles provides more counts, and therefore, information. It also allows for half-life fitting of the radioisotopes of interest. Following the cyclic analysis, two approaches are available for the estimation of the number of radioactive nuclei at the end of the irradiation. The time-dependent analysis method involves fitting a two-parameter function including an exponential function with a fixed half-life corresponding to the radioisotope of interest and a constant. It is noted that each cycle is corrected for the physical decay during that cycle as well as the transfer time and delay in the cycle start time. The alternative method in analysing the cycles uses the inverse-variance weighted mean of the physical half-life corrected peak areas in each cycle. The inverse-variance weighted method allows for taking advantage of information in every cycle, while giving less weight to the data with high uncertainty. In all cases the analyses were done for each

set of three phantoms and a calibration line was constructed in order to determine the MDL for each method. The MDL was defined as twice the uncertainty in the zero concentration phantom divided by the slope of the calibration line.

2.4.2. Spectral decomposition

In contrast to the region-based analysis, the spectral decomposition takes advantage of a larger part of the spectra aiming to provide more information with stronger statistics. Furthermore, this approach avoids introducing approximate mathematical functions to represent the data by using the shape of the spectra in the library to match the unknown spectra. Spectral decomposition employed a library of standard spectra acquired from single-element phantoms containing Na (1.3 g), Cl (1.2 g), Ca (14.9 g), and Al (5000 g). The algorithm was based on linear least squares fitting whereby the unknown sample was reconstructed based on linear contributions from each of the background-subtracted library standards summed with varying intensities or weights. The square of the differences between the unknown spectra and the fitted spectra was minimized until the least-squares difference between the two spectra was reached.

The problem of gain variation is much more evident in spectral decomposition, where the effect is observed through the relatively high chi-squared (χ^2) values. An algorithm was developed in order to align the gains and to improve the goodness of the fitting algorithm. The gains of the library standards and the

sample were determined for the 1.37 MeV peak of ^{24}Na, 1.64 MeV peak of ^{38}Cl, and 3.08 MeV peak of ^{49}Ca. Initially, the slope of the linear fit of the Na, Cl, and Ca gains was taken as the gain of the spectrum, but upon the observation of gain non-linearity within the each spectrum, alternative approaches such as the mean of the gains, Ca gain, Al gain were explored. The gain of Ca was taken as the representing gain for the entire spectrum, as it provided the best fit with smallest χ^2 values. The gain of the library standard Ca phantom was taken to represent the gain of the library standards. It is noted that all library standard phantoms were measured on the same day to reduce the effect of neutron fluence variations. Moreover, accurate calibration was performed prior to each measurement to ensure minimal and uniform gain shift. The ratio of the library standard gain to the sample gain, R, was taken to determine the need for gain alignment and the extent of it. No alignment was performed when $0.999 < R$ and $R > 1.001$, as this translated into a gain shift of 0.1% or less, corresponding to less than one channel shift in 1000 channels. For $R \geq 1.001$, the gain of the sample was shifted in one channel or 0.1% increments to match the gain of the library and for $R \leq 0.999$; the gain of the library standards was shifted in the same manner to match the sample gain. Following the gain alignment, the weighted linear least squares fitting was performed and the contributions from each of the library standard phantoms and their uncertainties were extracted.

The MDL in the spectral decomposition was determined by taking twice the mean of the uncertainties in the zero phantoms.

Additionally, a single 500 µg Al (33.6 µg Al/g Ca) phantom was measured 17 different times in order to test the reproducibility of the measurements.

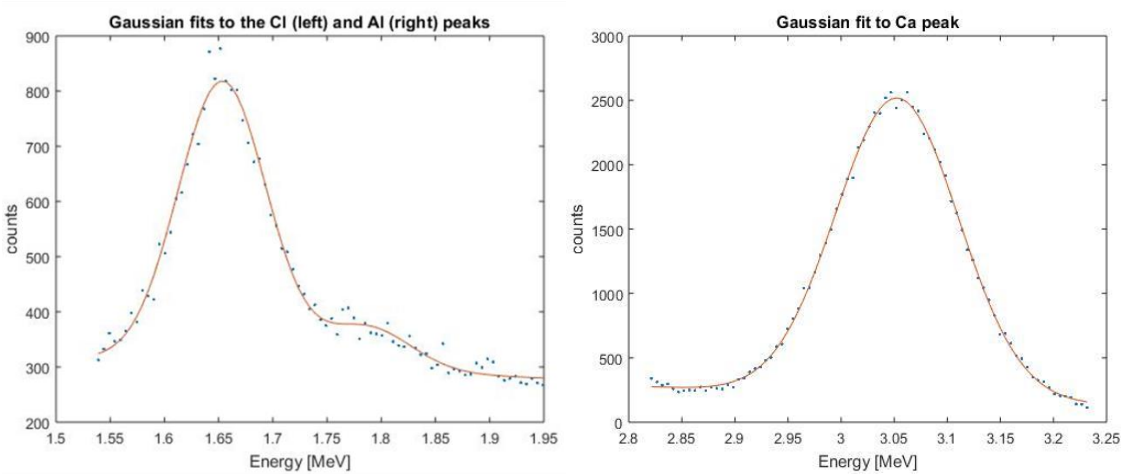

Figure 2.4. Gaussian fits to (a) Al and Cl peaks, and (b) Ca peak of a 33.6 µg Al/g Ca phantom.

3. Results

Figures 2.4 -a and -b show the data and Gaussian fits of a 500 µg Al (33.6 µg Al/g Ca) phantom for the regions of the spectrum containing Al and Cl peaks (Figure 2.4-a), and Ca peak (Figure 2.4-b).

Figures 2.5-a and –b show the exponential fits to the Al and Ca data used for the time-dependent analysis of the spectra fitted in Figure 2.4, respectively. The spectrum and the spectral decomposition fitting for which no gain shift was required by the program, together with the residual and for each data point in the spectrum are shown in Figure 2.6.

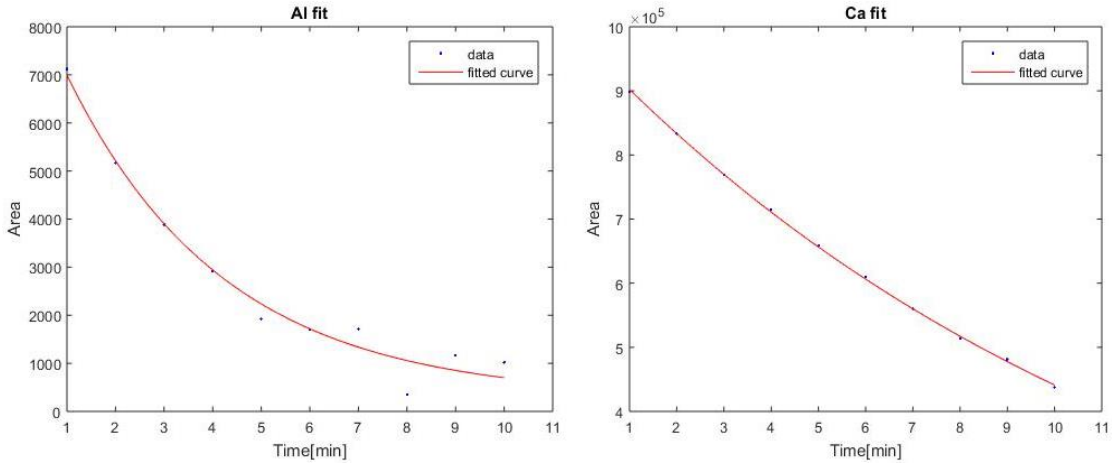

Figure 2.5. Exponential fitting of (a) Al counts, and (b) Ca counts for time-dependent analysis of a 33.6 µg Al/g Ca phantom.

Table 1 shows the results of the methods of data analysis. These results are reported as the means of Al/Ca ratios and their associated uncertainties, together with the standard deviations (SD) for each set of phantoms. Also included in Table 1 are the MDLs for different methods of analysis.

The result of 17 measurements of the same phantom containing 500 µg Al or 33.6 µg Al/g Ca was 38.5 ± 8.4 µg Al/g Ca.

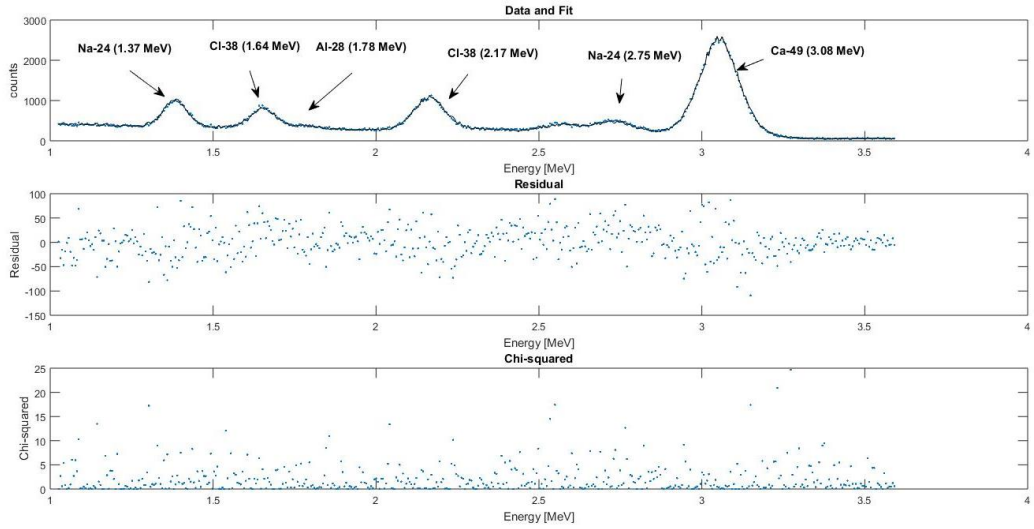

Figure 2.6. Spectral decomposition fitting to the gamma spectrum of a 33.6 µg Al/g Ca phantom (top), together with the residuals (middle) and χ^2 for each data point.

4. Discussion

Different analyses can be compared based on the measurement accuracy for each concentration, which represents the mean estimate of each set of three phantoms, as well as the mean uncertainty and MDL values. Additionally, the standard deviation provides a measure of reproducibility, although there were only 3 measurements for each concentration.

Table 2.1. The results of phantom measurements for various modeling and analysis methods and their corresponding MDLs. All units are in µg Al/g Ca.

	Spectral decomposition			Gaussian-IVWM			Gaussian-Time-dependent			Gaussian-3 min summation		
Phantom concentration	Mean	SD	Mean uncertainty	Mean	SD	Mean uncertainty	Mean	SD	Mean uncertainty	Mean	SD	Mean uncertainty
0.0	3.54	3.11	2.41	5.07	1.62	2.58	0.00	0.00	3.90	2.96	0.68	3.19
16.8	20.27	3.25	2.43	23.33	1.93	2.59	19.70	2.03	3.54	23.37	2.29	3.37
33.6	32.19	5.48	2.54	36.69	3.10	2.51	34.92	4.89	3.13	37.33	4.21	3.37
50.3	50.48	7.04	2.44	55.98	4.41	2.59	51.09	2.74	3.18	62.20	8.75	3.31
67.1	65.61	5.22	2.47	70.42	1.15	2.64	66.00	0.40	3.65	70.39	1.22	3.29
134.2	141.10	13.05	2.57	146.77	10.89	2.82	143.22	12.66	5.81	149.88	18.60	3.69
335.6	328.26	3.83	2.80	339.73	3.02	3.29	336.09	7.43	7.39	356.86	5.17	5.07
MDL	5.0			5.2			7.8			6.4		

The 2.24 min half-life of aluminum and the fact that the Al peak is dominated by the Cl peak with the longer half-life of 37.8 min means that as the counting cycles progress, the Al counts diminish and are more dominated by the Cl counts and the counts in the underlying continuum, in turn giving rise to higher uncertainties in the measurements. For the region-based model, the estimated concentrations of the phantoms by the time-dependent and 3 min methods reveal that the former estimates are closer to the expected concentrations, and therefore, have a higher accuracy compared to the latter. This however comes at the price of higher uncertainty in the time-dependent analysis. Accuracy, precision, and uncertainty are improved when the IVWM method is employed compared to the 3 min analysis. The fact that the inverse-variance weighted mean and time-dependent analyses outperform the 3 min method indicate that there is still significant useful information in the later cycles, despite the increasing statistical uncertainties. Comparing the IVWM and time-dependent analysis reveals an improvement in favor of the IVWM, reflected in the lower mean uncertainty. This is expected, as inverse-variance weighting assigns smaller weights to observations with higher uncertainties, thus reducing the impact of the uncertainty in Al counts in the final cycles, while taking advantage of the Al counts available in those cycles. As a result, the IVWM provides the most favorable results amongst the region-based methods.

For the spectral decomposition least squares analysis, implementing the gain shift algorithm improved the performance of the analysis, on average by a factor

of 1.8 and to a maximum of 4.8, based on the calculated reduced χ^2. While this is a significant improvement, the gain shift algorithm is based on some necessary assumptions that may not hold for each measurement. While taking the ratio of Al to Ca of the spectrum eliminates the variations due to the neutron fluence, it is important to note that each of the library spectra is subject to neutron variations that cannot be accounted for. Moreover, as mentioned previously, the gain shift algorithm assumes gain linearity throughout the spectrum, which has been shown, through analysis, not to hold for all spectra. Additionally, the algorithm does not support minor i.e. less than 0.1% shifts. Consequently, while spectral decomposition takes advantage of a wider range of counts in the spectrum, compared to the region-based model, and should, therefore, result in lower analysis uncertainty; the results of the phantom measurements indicate only a marginal improvement. On average, IVWM led to smaller standard deviations and lower mean uncertainties in lower concentrations, which are more relevant to human measurements, whereas spectral decomposition provided more accurate estimates of the concentration compared to the expected values.

Comparing the MDLs for different analysis methods reveals that the values for the spectral decomposition and IVWM are very close to each other, with the spectral decomposition yielding a slightly lower MDL. The fact that the MDLs are close is reassuring, as it indicates that the two fitting models lead to the same conclusion.

The region-based model has been previously utilized by our group for analysing Al using the same detection system [12]. The current results show an improvement by a factor of 1.7 compared to the best MDL achieved by Aslam et al. [12]. This can be attributed to several factors including different irradiation and counting protocols, as well as the quality of the phantoms used.

Comsa et al. explored using the spectral decomposition method in analysing Al and observed a 1.7 fold improvement over the Gaussian fitting [19]. While the current results support a marginal advantage for spectral decomposition analysis, this improvement is not significant compared to results obtained by Comsa et al. This is mostly due to the fact that Comsa et al. used different irradiation and counting systems. More specifically, the detection system employed in their study included only two NaI(Tl) detectors, compared to the 9 detector array in the current study. They observed no significant gain instability in their two detector setup which reduces the uncertainty in the analysis. The two detector setup is less likely to suffer from effects of gain instability compared to the 9 detector array used in this study. Furthermore, the reduced MDL of the current setup and analysis renders it more sensitive to various sources of uncertainty.

The reproducibility of the results of any measurement or analysis is an important prerequisite in the application of the method, in particular when human measurements are involved. The means of the measurements agree with the expected concentrations within uncertainties, which is reassuring of the long term

performance of the irradiation and detection systems given that these measurements were made over a period of 18 months.

5. Conclusions

This work presents different methods and the results of analysing the gamma-ray spectra following neutron activation analysis for Al measurements performed *in vivo*. The mean uncertainties of spectral decomposition and IVWM analyses were very close to each other and both were lower than the time-dependent analysis and the 3 minute summation. The MDLs of the different methods also supported similar performance for spectral decomposition and IVWM with a marginal advantage for the spectral decomposition method. The measurements were shown to have acceptable reproducibility over an extended period time. Although the methods of analysis discussed in the present study were developed for Al data analysis, they can be applied to other measurements involving gamma spectroscopy, especially where weaker peaks are to be analyzed or significant interferences and overlapping peaks exist.

Acknowledgements

The authors would like to extend their gratitude to Justin Bennett, the accelerator operator at the MAL for assisting in conducting experiments and patient irradiation. They also thank Dr. Farshad Mostafaei for his assistance in patient data collection and Michael Inskip for valuable advice and access to his laboratory. This work was made available through the funding provided by the

Canadian Nuclear Laboratories (CNL) and Natural Sciences and Engineering Research Council of Canada (NSERC).

References

[1] Valkovic V (1980) Is aluminum essential for life. Orig. Life 10, 301–305.

[2] Yokel RA (2013) Aluminum, In Encyclopedia of human nutrition, Waltham: MA, Academic Press. 1, pp.57–63.

[3] Spinks TJ, Bewley DK, Joplin GF, Ranicar ASO (1976) Neutron-activation measurement of metabolic activity of sodium in the human hand. J. Nucl. Med. 17, 724–729.

[4] Spinks TJ, Bewley DK, Paolillo M, Vlotides J, Joplin GF, Ranicar ASO (1980) Metabolic activity of sodium , measured by neutron activation , in the hands of patients suffering from bone diseases: concise communication. J. Nucl. Med. 21, 41–46.

[5] Nelp WB, Denney JD, Murano R, Hinn GM, Williams JL, Rudd TG, Palmer HE (1972) Absolute measurement of total body calcium (bone mass) in vivo. J. Lab. Clin. Med. 79, 430–8.

[6] Anderson J, Osborn SB, Tomlinson RW, Newton D, Rundo J, Salmon L, Smith JW (1964) Neutron activation analysis in man in vivo: A new technique in medical investigation. *Lancet* **2**, 1201–1205.[7] Williams ED, Elliott HL, Boddy K, HaywoodD JK, Henderson IS, Harvey I, Kennedy AC (1980) Whole-body aluminum in chronic renal failure and dialysis encephalopathy. Clin. Nephrol. 14, 198–200.

[8] Ellis KJ, Kelleher S, Savory J, Wills M (1988) In vivo monitoring of skeletal aluminum burden in patients with renal failure. J. Radioanal. Nucl. Chem. 124, 85–95.

[9] Green S, Chettle DR (1992) A feasibility study of the *in vivo* measurement of aluminum in peripheral bone. *Phys Med Biol* **31**, 2287–2296.

[10] Wyatt RM, Ryde SJ, Morgan WD, McNeil EA, Hainsworth IR, Williams AJ (1993) The development of a technique to measure bone aluminium content using neutron activation analysis. *Physiol Meas* **14**, 327–35.

[11] Pejović-Milić A, Byun SH, Comsa DC, McNeill FE, Prestwich WV, Chettle DR (2005) *In vivo* measurement of bone aluminium: recent developments. *J. Inorg. Biochem.* **99**, 1899–903.

[12] Aslam, Davis K, Pejović-Milić A, Chettle DR (2009) Noninvasive measurement of aluminium in human bone: preliminary human study and improved system performance. *J Inorg Biochem* **103**, 1585–90.

[13] Davis K, Pejović-Milić A, Chettle DR (2008) *In vivo* measurement of bone aluminum in population living in southern Ontario, Canada. *Med Phys* **35**, 5115.

[14] Aslam, Pejovic-milic A, McNeill FE, Byun SH, Prestwich WV, Chettle DR (2008) In vivo assessment of magnesium status in human body using

accelerator-based neutron activation measurement of hands: A pilot study. *Med Phys* **35**, 608-616.

[15] Aslam, Pejović-Milić A, Chettle DR, McNeill FE (2008) Quantification of manganese in human hand bones: A feasibility study. *Phys Med Biol* **53**, 4081-4092.

[16] Mostafaei F, McNeill FE, Chettle DR, Wainman BC, Pidruczny AE, Prestwich WV (2015) Measurements of fluorine in contemporary urban Canadians: A comparison of the levels found in human bone using *in vivo* and *ex vivo* neutron activation analysis. *Physiol Meas* **36**, 465-487.

[17] Byun SH, Prestwich WV, Chin K, McNeill FE, Chettle DR (2006) 4-pi NaI(Tl) detector array for *in vivo* neutron activation analysis. *IEEE Trans Nucl Sci* **53**, 2944–2947.

[18] Pejović-Milić A, Arnold ML, McNeill FE, Chettle DR (2000) Monte Carlo design study for in vivo bone aluminum measurement using a low energy accelerator beam. *Appl Radiat Isot* **53**, 657-664.

[19] Comsa DC, Prestwich WV, McNeill FE, Byun SH (2004) Application of spectral decomposition analysis to in vivo quantification of aluminum by neutron activation analysis. Appl. Radiat. Isot. 61, 1353–60. doi: 10.1016/j.apradiso.2004.03.062

[20] ICRP (1974) *Report of the task group on reference man*, Publication 23. Pergamon, Oxford.

Chapter 3

A pilot study measuring aluminum in bone in Alzheimer's and control subjects using *in vivo* neutron activation analysis

Introduction to Article III

Article III presents the clinical study involving the IVNAA bone aluminum measurements, aiming to investigate the possible difference in bone aluminum concentration in Alzheimer's disease and control groups and study the feasibility of measuring aluminum in bone as proxy for the brain. The study was performed on 15 Alzheimer's disease subjects and 15 control subjects recruited from the Hamilton, Ontario area.

The experimental work and analyses presented in the following article were performed by the author of this thesis under the supervision of Dr. David Chettle, and with guidance of Dr. Bill Prestwich, Dr. David Cowan, Dr. Soo Hyun Byun, Dr. Jovica Atanackovic, Dr. Witold Matysiak, Dr. Nicholas Priest, and Dr. Ana Pejović Milić.

Contents of Article III

The following article has been accepted for publication in the Journal of Alzheimer's Disease.

A Pilot Study Measuring Aluminum in Bone in Alzheimer's and Control Subjects Using *In Vivo* Neutron Activation Analysis

H. K. Mohseni[1], D. Cowan[2], D.R. Chettle[1], A. Pejović Milić[3], N. Priest[4], W. Matysiak[5], J. Atanackovic[6], S.H. Byun[1], W.V. Prestwich[1]

[1]Medical Physics & Applied Radiation Sciences, McMaster University, Hamilton, Canada
[2]Department of Medicine, McMaster University, Hamilton, Canada
[3]Department of Physics, Ryerson University, Toronto, Canada
[4]Canadian Nuclear Laboratories, Chalk River Laboratories, Ontario, Canada
[5]University of Florida Proton Therapy Institute, Jacksonville, FL, USA
[6]Ontario Power Generation, Whitby, Ontario, Canada

Abstract

Aluminum, being the most abundant metal in the earth's crust, is widely distributed in the environment, and is routinely taken up by the human body through ingestion and inhalation. Aluminum is not considered an essential element and it can be toxic in high concentrations. Most of the body burden of aluminum is stored in the bones. Aluminum has been postulated to be involved in the causality of Alzheimer's disease. A system for non-invasive measurement of bone aluminum using the *in vivo* neutron activation analysis technique has been developed and previously reported in the literature by our group. The results are

reported as ratio of Al to Ca in order to eliminate the variations in beam parameters and geometry as well as the physical variations among the subjects such as size of the hand and bone structure.

This pilot study included 30 subjects, 15 diagnosed with Alzheimer's disease in mild and moderate stages and 15 control subjects, all of whom were 60 years of age or over. The mean value of aluminum for the control group was 2.7 ± 8.2 μg Al/g Ca (inverse-variance weighted mean 3.5 ± 0.9 μg Al/g Ca) and for the Alzheimer's disease subjects was 12.5 ± 13.1 μg Al/g Ca (inverse-variance weighted mean 7.6 ± 0.6 μg Al/g Ca). The difference between the mean of the Alzheimer's group and the mean of the control group was 9.8 ± 15.9 μg Al/g Ca, with a p-value of 0.02. An age-dependent linear increase in bone aluminum concentration was observed for all subjects. The difference in serum aluminum levels between the two groups did not reach significance.

Keywords- Neutron activation analysis, *in vivo*, Aluminum, Alzheimer's disease, bone, gamma spectroscopy

1. Introduction

Alzheimer's disease (AD) is the most common form of dementia accounting for up to 80% of dementia cases [1]. AD starts with a clinically-dormant phase followed by progressive loss of memory and cognitive functions [2]. According to World Alzheimer's Report, as of 2015, an estimated 46.8 million people worldwide are suffering from dementia with an alarming projection of about 131.5

million by 2050 [3]. This translates into about 40 million cases of AD in 2015. Given the sharp increase in the projected number of AD cases in the coming years [3] and its significant impact on the society, developing methods for understanding the cause and monitoring of symptoms of AD are of great importance.

Many studies have been conducted in an effort to identify the underlying causes of AD. Although genetic, lifestyle, and environmental components are known to be associated with the development of AD, the true cause remains unknown [4-8].

Aluminum (Al) seems to be one of the most likely candidates among the environmental toxicants, partly due to its ubiquitous nature [9]. The contribution of Al to AD has been strengthened through multiple independent observations involving, among other factors, animal models, brain signaling pathways, environmental exposures, and Al-chelating pharmaceutical treatments of AD symptoms [10]. Al is the most abundant metal and the third most abundant element in the earth's crust with widespread applications in industrialized societies, examples of which include food, medical, drinking water, cosmetic, and construction industries [11]. Moreover, Al has been classified as a neurotoxin [12, 13]. Diminished cognitive functions in rats have been observed following chronic exposure to Al [14]. Elevated levels of Al have been detected in neurofibrillary tangle-bearing neurons in experimental animals as well as post-mortem analysis

of human AD brains [15-18]. Measuring Al has been of interest during the past few decades with the focus of the early work in the 1970s and 1980s being on dialysis encephalopathy due to the Al contamination in the water used for preparation of dialysate [19-21]. In subsequent years, with the growing need and interest to investigate Al with respect to occupational exposures [16, 22] and medical conditions such as parenteral nutrition [23-25] led to the development of various *in vitro* techniques such as atomic absorption and emission spectrometry [17, 26] and neutron activation analysis involving sample processing (NAA) [27, 28], all of which were destructive methods or required sample processing.

Measuring and monitoring Al in the context of AD is a complex task as the organ of interest for measuring Al in AD is the brain. Penetrating the brain for the purpose of *in vivo* measurement of Al requires high doses of radiation as the brain is protected by the skull, rendering the method impractical, given the possibility of an Al signal being generated in the skull, masking that of the brain. At the current state of technological advancement, measurement of Al in the brain can only be performed post-mortem. Blood, urine, cerebrospinal fluid, and bone have been investigated *in vitro* as possible proxies for the brain, with elevated levels of Al in these organs observed and reported in the literature [29]. Serum measurement is the most common method of monitoring Al in clinical practice and can be used in conjunction with other measurements. *In vitro* methods of measuring Al suffer from the high risk of contamination, due to abundance of Al. Furthermore, urine is considered as a better measure of acute

exposure to Al [11]. About 60% of the body burden of Al is stored in the bone, rendering the skeleton the Al depot of the body [11]. Bone Al measures are considered to be less susceptible to short-term exposures and better reflect longer term aggregate exposure. Conventional bone Al measurement, however, requires the invasive sample collection procedure of bone biopsy which inhibits subject participation.

In vivo neutron activation analysis (IVNAA) is a method of measuring various elements in the human body using low doses of ionizing radiation. As a non-invasive method, it can be used for monitoring Al levels in humans and screening patients at the early stages of the disease. Furthermore, it does not require sample preparation, which significantly reduces the risk of contamination. IVNAA has been in use for medical and occupational purposes for several decades. The first *in vivo* measurement of Al was performed in 1980 by Williams et al. [30]. IVNAA of Al has since been used by various research groups and has undergone major improvements to increase its sensitivity to match the current low levels of Al detected in humans [31-36]. A comprehensive review of the history of *in vivo* Al measurement has been recently published in the journal of Alzheimer's Disease, which can provide further details about IVNAA methodology [37].

The present work is the first clinical study involving the *in vivo* measurement of Al in bone in AD patients and control. The goal is to i) investigate whether or not differences in levels of bone Al are found in subjects with AD vs normal controls,

ii) determine the viability of measuring bone Al using IVNAA as a possible proxy for monitoring the Al levels in AD subjects, especially in the early stages of the disease, and iii) determine the capacity of the available IVNAA facility for measuring current Al levels in the bone.

2. Materials and Methods

2.1. IVNAA setup

The measurements were performed at the IVNAA facility at the McMaster Accelerator Laboratory (MAL). This facility with a Tandetron accelerator (HVEC) and a 4π detection system has been developed for the purpose of measuring trace elements in the human hand. It has been previously utilized to perform human measurements of Al in healthy and occupationally exposed individuals [35, 36], as well as other elements such as manganese and fluorine [38, 39].The details of the irradiation and detection system have been discussed in previous publications [36, 40, 41]. The Tandetron is a 1.25 MV high-current tandem accelerator capable of accelerating protons to the energies of up to 2.5 MeV. Neutrons are produced through the $^{7}Li(p,n)^{7}Be$ reaction when high-energy protons impinge on the thick ^{7}Li target enclosed in the irradiation cavity. The irradiation cavity is designed to maximize the thermal neutron field and, therefore, activation of the target while reducing the radiation dose outside the cavity to below the regulatory dose limits. The former is achieved through using polyethylene as the moderating material to thermalize the neutrons further and

graphite reflectors to reflect the stray neutrons back into the irradiation cavity. The latter is accomplished by adding shielding and lead filters to absorb the neutrons and the gamma rays produced in the target and other unwanted radiation. Following thermalization, neutrons are incident on the sample for a specific period of time allowing for the neutron activation to occur. This is achieved inside a specially designed irradiation cavity that is large enough to accommodate the human hand [41]. The detector assembly consists of 9 NaI(Tl) scintillation detectors arranged in a 4π geometry with an opening for inserting the sample [40]. The digital processing system (DSP) then acquires and compiles the data from the detectors. The DSP system is designed such that it can collect data in coincidence and anticoincidence modes, in addition to single detector responses. This is an important feature in measuring Al, as anticoincidence significantly reduces the spectral interference of the adjacent chlorine peak located only 0.14 MeV away from the Al peak (Figure 3.1).

Upon bombardment with thermal neutrons, ^{27}Al nuclei in the sample absorb neutrons through the reaction ^{27}Al(n, γ)^{28}Al and the radioisotope ^{28}Al is produced with a thermal neutron cross-section of 0.23 barn. The unstable ^{28}Al decays to ^{28}Si with a half-life of 2.25 minutes and a 1.78 MeV gamma ray is emitted with an emission probability of 100%.

The choice of proton energy determines the maximum energy of the neutrons which not only has important implications in the context of radiation dose to the

subject, but also greatly affects the activation of different elements in the biological sample. While multi-element activation can provide a unique opportunity in terms of investigating multiple elements, it can also be a cause for undesirable interferences. In the case of Al, the interference from phosphorus and silicon, naturally present in the bone, are of great importance as they share the same activation product as ^{27}Al. Phosphorus and silicon have cross-sections for fast neutron activation through the reactions ^{31}P(n,α)^{28}Al and ^{28}Si(n,p)^{28}Al. According to ICRP 23 report on the reference man [39], the human body contains 780 g and 18 g of phosphorus and silicon, respectively. At the proton energy of 2.3 MeV, the maximum neutron energy is 0.55 MeV which is far below the activation thresholds of 2.01 MeV for the ^{31}P(n,α)^{28}Al and 4.00 MeV for the ^{28}Si(n,p)^{28}Al reactions, respectively. Therefore, these elements are not activated and their interference with ^{28}Al is eliminated by the production of neutrons with energies well below the threshold energies.

2.2. Hand phantom measurements

Hand phantoms were made to test the system, generate the calibration line and find the minimum detectable limit (MDL) of the system. Most of the bone in the hand is cortical. The phantoms were made in triplicates and according to the composition of human hand comprising both the cortical bone and soft tissue as published in ICRP 23 [42], including only those elements with significant neutron activation cross-sections and abundances, namely Ca, Na, Cl and Al with reactions ^{48}Ca(n, γ)^{49}Ca, ^{23}Na(n, γ)^{24}Na, ^{37}Cl(n, γ)^{38}Cl and ^{27}Al(n, γ)^{28}Al,

respectively. Each phantom contained 14.9 g Ca, 1.19 g Cl, and 1.25 g Na. Al was added in triplicates, varying concentrations corresponding to zero, 16.8, 33.6, 50.3, 67.1, 134.2, and 335.6 µg Al/g Ca. It is noted, as mentioned above, that while phosphorus and silicon are both present in the skeleton and have cross-sections for fast neutron activation, they are not included in the phantom composition since there is no probability for their activation given the neutron beam energy.

As mentioned previously, one important consideration when measuring Al is contamination. Al has a wide presence in the environment and is found in trace amounts in many materials. Therefore, it is critical to remove all sources of Al contamination in the phantoms if the results are to be accurate and reproducible. The original high density polyethylene (HDPE) Nalgene^{TM} bottles used for preparing the phantoms were found to have significant amounts of Al. Further measurements on the supposedly aluminum-free low density polyethylene (LDPE) bottles revealed that there were still trace amounts of Al present. In order to remove the possibility of activating the aluminum in the bottles, the contents of the phantoms were transferred to un-irradiated bottles immediately after irradiation and prior to detection. Moreover, all the chemicals used in the production of the phantoms were chosen from high purity chemical compounds (Sigma Aldrich) to avoid Al contamination and reduce uncertainty in the phantom measurements and calibration line.

Phantoms or subjects were exposed to thermal neutrons for 45 seconds with the proton energy of 2.3 MeV and the proton current of 400 μA following which they were transferred to the detection system located at some distance from the irradiation facility in order to avoid activating the detector crystals. The mean transfer time for the phantoms was 30 seconds. Once in the detector, the gamma spectra were collected for 10 cycles of 60 seconds. The total time of 10 min was chosen to allow for multiple half-lives of Al to be detected while minimizing inconvenience to the subjects. The effective dose to the subjects was 0.21 mSv, based on the recent dose simulations and measurements [43], which is in the same order of magnitude as a chest x-ray (0.1 mSv) [44].

In addition to the phantoms, the available National Institute of Standards and Technology's (NIST) standard reference material 1400 which consists of bone ash with certified Ca content was measured in the same way as the calibration standards and subjects for the purpose of validating the measurements. The measured NIST standard weighed 23.1 ± 0.1 g and contained 38.18% ± 0.13% of Ca and 530 μg/g of Al. Although the concentration of Al in the sample is not certified, it still provided reassurance of the performance of the system used in this work.

2.3. Clinical study

This *in vivo* study was approved by the research ethics boards of McMaster and Ryerson Universities in southern Ontario. After providing written informed

consent, 15 AD (7 females and 8 males) and 15 control (9 females and 6 males) subjects were recruited for the study from the Hamilton, Ontario area by the collaborating geriatrician. Where it was felt that AD subjects were incapable of providing consent, consent was obtained from their legal proxies. AD subjects were diagnosed according to DSM IV criteria, and were in the mild to moderate stages based upon Clinical Dementia Rating Scale (CDR) and the Standardized Mini Mental State Examination (sMMSE) [45] shown in Tables 3.1 and 3.2, respectively. The control group had no history of AD or other types of dementia. The mean age of the participants was 77.6 with a range of 63 - 89 years. The mean ages for AD and control groups were 80.2 and 75, respectively. The irradiation and counting protocols were the same as phantoms. All subjects received a brief orientation before and upon arrival at the facility. Each subject was seated in a wheelchair for convenience. Using a wheelchair also facilitates safer and faster transfer between the irradiation and counting rooms. Subjects were fitted with a water sleeve which was filled with water once the subject's arm was correctly positioned in the irradiation cavity. Hydrogen, and therefore, water is an effective moderator for neutrons, thus providing additional reduction in the dose. It is important to fill the sleeve with water in such way that there is no or negligible gap between the irradiation cavity wall and subject's arm so to avoid unnecessary radiation exposure to the rest of the body and the accompanying caretaker. Both the subject and caretaker were fitted with electronic dosimeters to measure their neutron and gamma doses actively. Following the 45 sec

irradiation and the removal of the water sleeve, the subject was wheeled to the detection room by the caretaker, where the irradiated hand was positioned in the detection system for counting. The median transfer time for the subjects was 33 sec with a range of 21 - 69 sec. The subjects were instructed to remove all items of jewelry, as well as nail polish from the hand being irradiated to avoid potential contamination, although the latter has been shown not to contain Al [46]. The hand irradiation did not produce any skin irritation, temperature change and/or discomfort to the subjects.

In addition to bone Al measurements, serum Al was measured in the subjects prior to IVNAA of the bone. However, 4 of the study subjects refused to participate in the blood sample collection (2 AD subjects and 2 controls). For these individuals only bone Al measurements were performed.

Table 3.1. CDR scores of AD subjects.

Score	Stage	Number of subjects
CDR-0	Normal	0
CDR-0.5	Questionable	0
CDR-1	Mild	4
CDR-2	Moderate	11
CDR-3	Severe	0
Total		15

2.4. Data Analysis

Data analysis was limited to the relevant regions in the spectra which included Al and Ca peaks at energy ranges of 1.5 - 1.9 MeV, and 2.75 - 3.2 MeV, respectively. Mathematical models using the Marquardt algorithm involving non-linear least squares fitting were used to find the areas under Al (1.78 MeV) and Ca (3.08 MeV) peaks. Analysing the Al peak area is particularly challenging due to the presence of the more biologically abundant Cl at 1.64 MeV adjacent to Al peak. For Al the mathematical model involved two Gaussian functions plus a linear background to account for both Al and Cl peaks. The Ca peak is well separated, and therefore, was fitted with one Gaussian and a linear background. The spectra were analysed for each of the 10 cycles and the inverse-variance-weighted mean of all cycles was taken as the Al area. Corrections were made to account for radioactive decay during transfer and data acquisition as well as the inherent delay in the electronics.

Table 3.2. MMSE scores of AD subjects recruited for this study (*one subject was categorized as aphasic with no MMSE score).

Score	Stage	Number of subjects
26 - 30	Normal	1
20 - 25	Mild	5
10 - 19	Moderate	8
0 - 9	Severe	0
Total		14*

The activation, and therefore, content of radioisotopes found using the current method of IVNAA depend on the neutron fluence which may vary among different measurements due to variations in neutron production within the target. Additionally, variations in the size and shape of each individual's hand, possible movement of subject, and positioning within the irradiation cavity introduce further complexities. These variations can be accounted for by normalizing the Al content to Ca which provides an index of Al levels per unit bone mass.

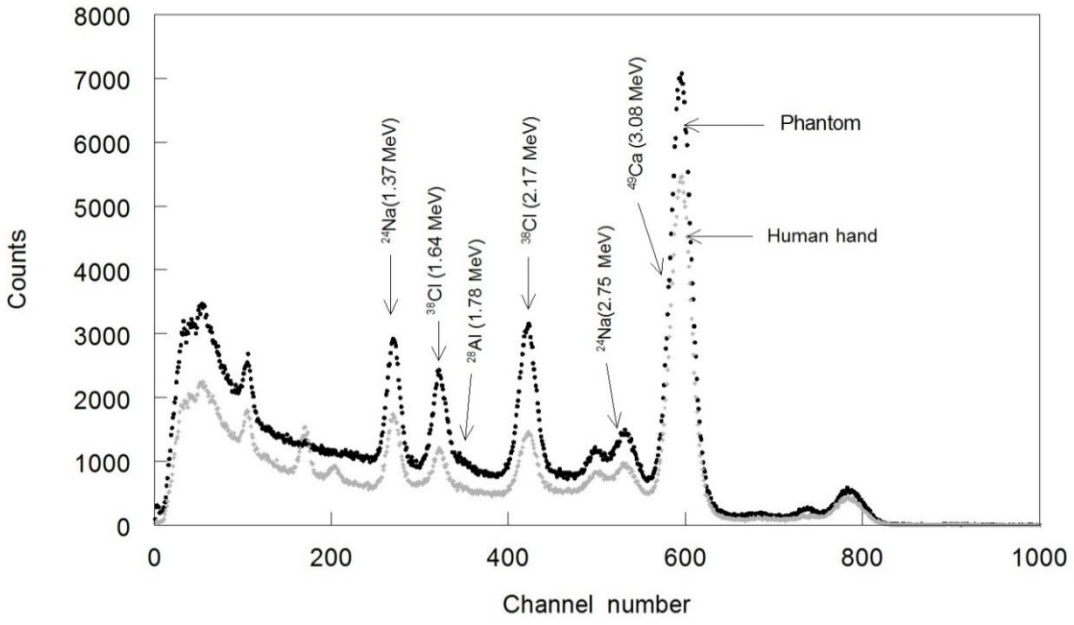

Figure 3.1. Gamma spectra of a phantom (black marks) and an AD subject's hand (gray marks) acquired using the same irradiation and counting conditions, highlighting the agreement between the phantom and human hand.

3. Results

Spectra of a phantom and an AD subject are shown in Figure 3.1, which demonstrates that the composition of the phantom mimics well the major and relevant neutron-activated radionuclides found in the hand.

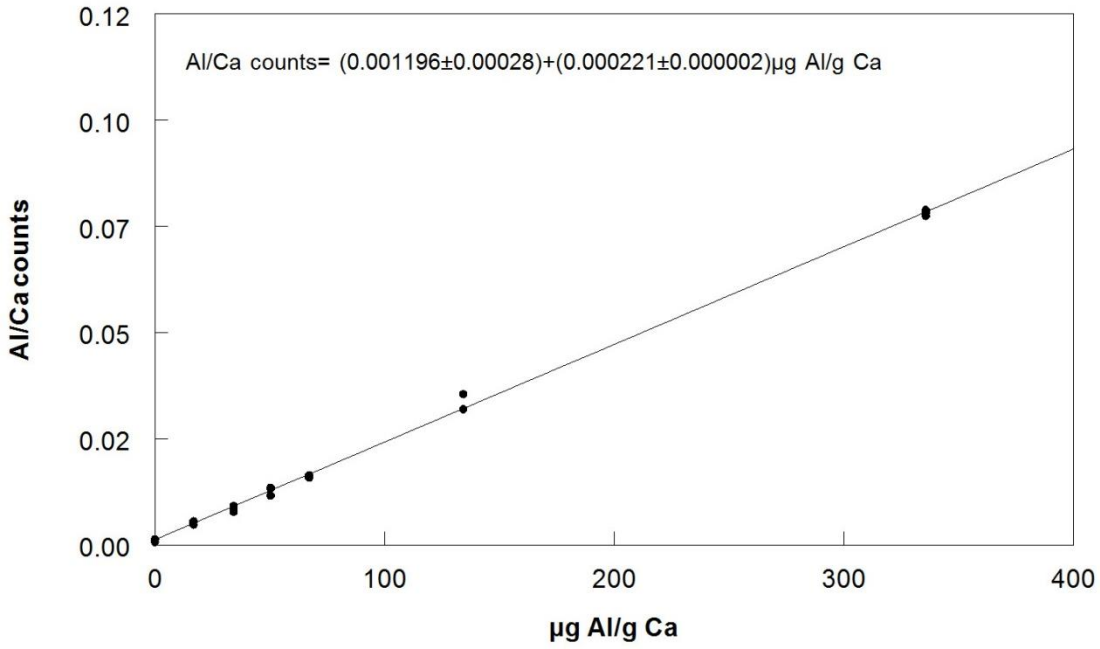

Figure 3.2. Calibration line obtained by irradiating and counting hand phantoms with varying concentrations of Al and constant Ca concentration, resulting in an MDL of 5.2 µg Al/g Ca or 76.9 µg Al (r = 0.999).

Figure 3.2 illustrates the calibration line generated based on phantom measurements. The MDL is defined as twice the uncertainty of the zero concentration phantom divided by the slope of the calibration line. The achieved MDL in phantoms was 5.2 µg Al/g Ca or 76.9 µg of Al. The MDL can also be

defined based on the *in vivo* measurements as twice the median of the uncertainty in all measurements which was 7.2 µg Al/g Ca.

The NIST 1400 sample was measured on 3 separate occasions, the results of which are provided in Table 3.3. The mean of the 3 measurements was 1372.5 ± 65.3 µg Al/g Ca, which agrees with the NIST 1400 Al/Ca ratio of 1388.0 µg Al/g Ca (uncertified) within the error margin of the measurements.

Table 3.3. NIST 1400 bone ash measurements (Al is uncertified and Ca is certified). *SD is standard deviation

Measurement	µg Al/g Ca	Uncertainty
1	1393.4	9.2
2	1424.8	7.9
3	1299.3	8.9
mean	1372.5	65.3 (SD)*
NIST 1400 (uncertified)	1388.0	4.7

Figure 3.3-a and -b show the Al/Ca ratio in hand for control and AD subjects, respectively. The error bars represent the uncertainty of one sigma (68% confidence level). The range of concentrations for control subjects varied from -21.9 ± 7.6 to 15.0 ± 4.7 µg Al/g Ca with a mean of 2.7 ± 8.2 µg Al/g Ca (inverse-variance weighted mean 3.5 ± 0.9 µg Al/g Ca). For the AD subjects the mean

concentration was 12.5 ± 13.1 μg Al/g Ca (inverse-variance weighted mean 7.6 ± 0.6 μg Al/g Ca) with a range of -3.9 ± 2.4 to 37.4 ± 5.3 μg Al/g Ca. The difference in the Al/Ca ratio between AD and control subjects was 9.8 ± 15.9 μg Al/g Ca (inverse-variance weighted mean difference 4.0 ± 0.1 μg Al/g Ca), found to be significant at the 95% confidence level p-value of 0.02 based on the student's t-test, suggesting higher bone Al content in the AD subjects (The 6 highest Al/Ca values were observed in the hand bone of AD subjects).

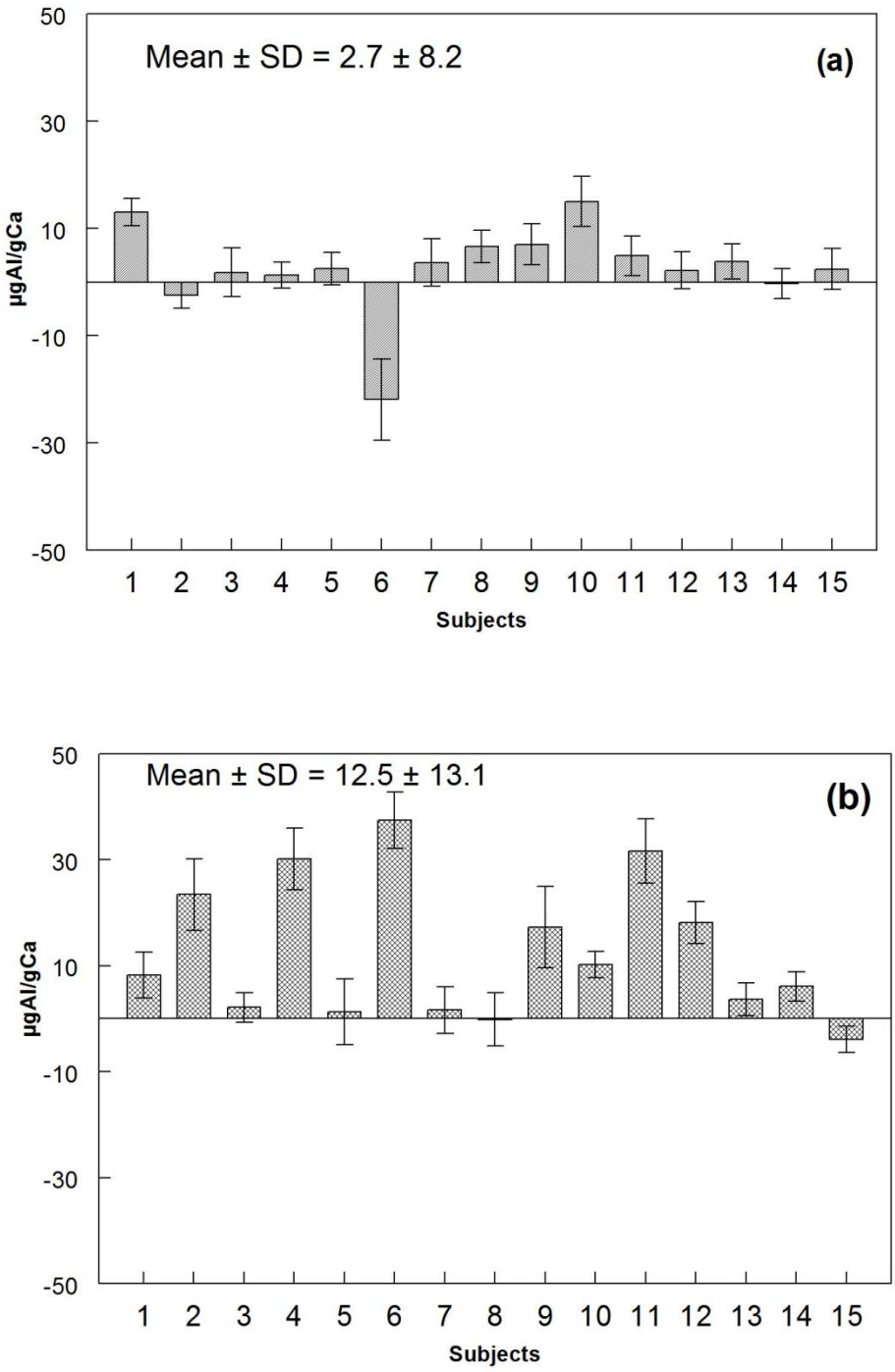

Figure 3.3. Aluminum concentration in (a) control subjects and (b) AD subjects expressed in µg Al/g Ca.

The relationship between age and Al content of the bone for all subjects measured in this study is shown in Figure 3.4. A linear increase in the Al/Ca ratio was observed with increasing age which was significant with $p<0.005$.The linear function provided the best fit with $r = 0.515$. A linear relationship also best described both AD and control groups.

No correlation between CDR ($p = 0.24$) or MMSE rating ($p = 0.15$) and Al/Ca ratio in the AD subjects was observed.

The mean serum Al concentrations in control and AD subjects were 190.2 ± 123.5 nmol/L and 198.9 ± 111.8 nmol/L, respectively, which did not reach significance with a t-test p-value of 0.86.

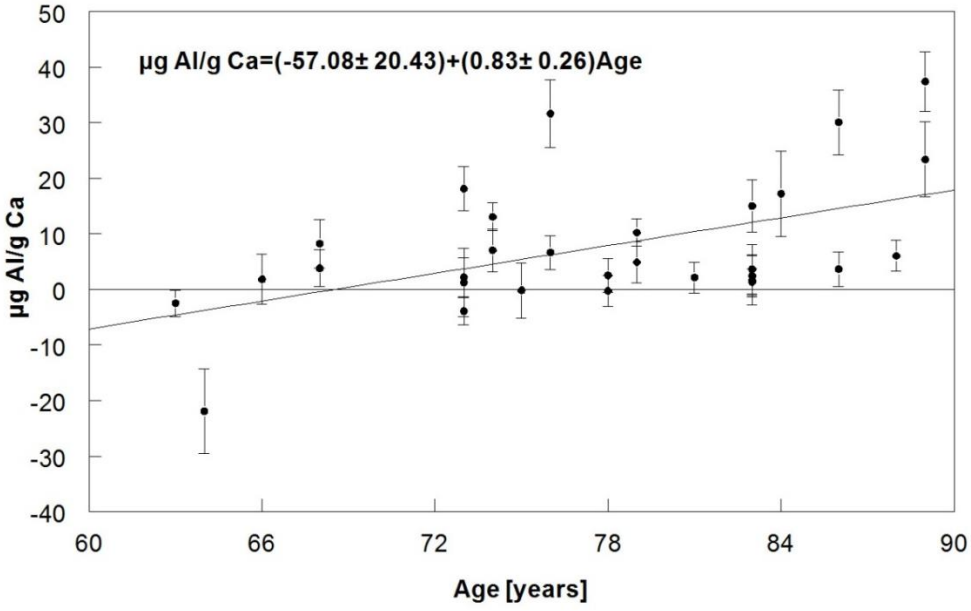

Figure 3.4. Aluminum concentration of all subjects as a function of age, expressed in µg Al/g Ca ($r = 0.555$).

4. Discussion

The spectra shown in Figure 3.1 demonstrate the close agreement between the radioisotopes found in human subjects and that of ICRP's reference man mimicked in the phantoms. There is a difference, however, in the total number of counts in the two spectra. This is due to the differences in hand size and positioning of the subjects compared to the phantoms, as well as the variations in the total number of neutrons emitted.

MDL values of 5.2 μg Al/g Ca for phantoms and 7.2 μg Al/g Ca for *in vivo* hand measurements achieved in this study are major improvements to the previously reported figures in the literature by our group [36]. Phantom and *in vivo* MDLs were reduced by factors of 1.61 and 1.66, respectively, from the previously reported values of 8.32 μg Al/g Ca and 12 μg Al/g Ca [36]. This improvement can be attributed to higher proton energy used in the current study, higher quality phantoms and improved analysis.

Al content of human bone has been previously measured [24, 35, 47]. However, the results of measurements have been reported in different ways, depending on the technique applied and method of normalization. Normalization is usually done in relation to dry weight, wet weight, or calcium content of the bone without a direct means of converting between methods, which in turn leads to discrepancies between the reported values. Comparison of the results is thus limited either to studies that use the same method of normalization or to using

crude conversion factors between different methods. One such conversion factor is that of dry weight (dw) to calcium, calculated on the basis of the ratio of the inorganic component of the bone crystal, representing the dry weight, and the calcium content, yielding a conversion factor of approximately 4. Davis et al. [35] measured Al/Ca ratio in the hand bone of healthy adults living in southern Ontario using IVNAA. However, due to the relatively high MDL of the study (phantom MDL was 19.5 ± 1.5 μg Al/g Ca and *in vivo* MDL was 28.0 μg Al/g Ca), no direct comparison of bone Al concentrations can be drawn between their results and the control subjects in the present work. Bone Al content of 1.06 μg/g dw in healthy controls reported by Hellström et al. [47] agrees with the 2.7 ± 8.2 μg Al/g Ca found in this work, once the conversion factor of 4 is applied. Kruger et al. measured the Al content of bone samples from 7 parenteral nutrition patients and 18 control subjects [24]. They found an average Al content of 32.0 ± 18.7 μg/g dw and 2.6 ± 1.8 μg/g dw in the parenteral nutrition and control subjects, respectively. The bone Al content of the control group in Kruger's study agrees with the results of the present work within the margin of uncertainty, although the mean value in Kruger's study is higher.

The Al/Ca ratio can be treated as the index of elevated Al per unit mass of bone. For the number of participants and the MDL of the current experimental setup, the results indicate a significant difference in Al/Ca in the hand bone between the control and AD group at 95% confidence level, suggesting a possible association between accumulation of Al in bone and the presence of AD. Additionally, bone

Al results signify that the skeleton can potentially be used as a proxy system for the brain; however, more research is required to investigate this outcome further. Furthermore, IVNAA has proven a promising tool for such measurements and also monitoring the Al levels in the bone. It is noted, however, that the present results should be treated with caution for several reasons. Firstly, these findings are based on the relatively small sample size of 30 subjects. Secondly, despite the major improvements in the MDL, most of the *in vivo* measurements are close to or below the *in vivo* detection limit. As such, for these subjects no individual interpretation of Al/Ca ratio can be drawn and the results would be reported as "not detectable" in a clinical setup. Lastly, higher Al/Ca ratios than those reported here have been observed in occupationally exposed, but otherwise healthy individuals [36]. Thus, the likely conclusion based on the present findings would be that Al could be considered as a contributing factor in the causality of Alzheimer's disease; however, more work is required to further investigate its role.

The current findings challenge those reported by Hellström et al. [47] where no significant difference in the Al content of bone was observed following *in vitro* measurement of iliac bone in AD and control subjects.

The increase in the Al/Ca ratio with age in the study subjects is in agreement with the work of Hellström et al. [47]. They also reported an age-dependent increase in bone Al concentration which followed an exponential function. The linear

relationship found in the current study, and therefore the discrepancy in the functions governing the increase, may be due to smaller size of this study and the restricted age range of these subjects, compared to the work of Hellström et al [47]. It is a known fact that human bone loses calcium and other minerals with age as the bone mass decreases. However, the extent to which bone Al is lost relative to Ca is not known and may be a factor in the increase in the Al/Ca ratio with age. The extensive whole body Ca IVNAA measurements conducted by Ellis [48] showed a decline in total body calcium in both male and female subjects with age. This decline however, was not significant within the margins of error for each of the 5-year age groups relevant to the ages studied in the present work.

Serum Al is usually considered as an indication of acute exposures, whereas bone Al better reflects the Al body burden, which may explain the lack of significant difference in serum Al between control and AD groups. Furthermore, blood measurement of Al is subject to a high risk of contamination as Al is ubiquitous and special measures need to be taken to remove Al contamination from the laboratory environment. It is noted that serum Al measurements were performed at a hospital laboratory in Hamilton, ON, and not a research lab with Al-contamination measures in place. Therefore, the possibility of contamination cannot be ruled out. Additionally, 4 out of 30 subjects refused to participate in blood sample collection, which somewhat reduces the statistical significance of the serum Al results.

One limitation in the current clinical study is that it does not include subjects with severe cases of AD. All AD subjects recruited for this study were categorized as mild and moderate, based on CDR and MMSE categories. This was mainly due to the challenges involved in recruiting subjects in advanced stages of the disease in the community, and the distress that measurement in the Tandetron Accelerator may have caused them. If possible, measuring bone Al in severe cases might shed more light on the pattern of Al accumulation through different stages of AD.

5. Conclusions

This work presents, for the first time, the results of *in vivo* measurements of Al in the hand bone of patients suffering from Alzheimer's disease and control subjects. A significant difference with a p-value of 0.02 was observed in the Al/Ca ratio between the two groups. This finding was not inconsistent with the hypothesis of an association between raised levels of Al in the body and the risk of AD. However, these findings must be interpreted with caution. There was a small number of subjects involved in the study, n = 15 in each group. The levels of Al found in the AD remained within the range of values for normal subjects in a much larger study of biopsy samples [47]. There is evidence of higher levels of Al in bone in people with occupational exposure to Al and in people on long term parenteral nutrition; and there is not strong evidence for an association between occupational exposure to Al or parenteral nutrition and the risk of AD. Larger studies are required to complement the current results further, hopefully with the

inclusion of subjects with advanced AD. The majority of measurements reported here are close to or lower than the MDL of the system, warranting further investigation into possible ways of improving the sensitivity of *in vivo* bone Al measurements. The increasing trend in Al/Ca ratio with age observed in this study is consistent with other findings reported in the literature.

Acknowledgements

The authors would like to extend their gratitude to Justin Bennett, the accelerator operator at the MAL for assisting in conducting experiments and patient irradiation. They also thank Dr. Farshad Mostafaei for his assistance in patient data collection and Michael Inskip for valuable advice and access to his laboratory. This work was made available through the funding provided by the Canadian Nuclear Laboratories (CNL) and Natural Sciences and Engineering Research Council of Canada (NSERC).

References

[1] Alzheimer's Association (2015) 2015 Alzheimer's disease facts and figures. *Alzheimers Dement*. **11**, 332-84.

[2] Amieva H, Le Goff M, Millet X, Orgogozo JM, Peres K, Barberger-Gateau P, Jacqmin-Gadda H, Dartiques JF (2008) Prodromal Alzheimer's disease: successive emergence of clinical symptoms. *Annals Neurol* **64**, 492-498.

[3] Prince M, Wimo A, Guerchet M, Ali G, Wu Y, Prina M (2015) World Alzheimer Report, http://www.alz.co.uk/research/world-report-2015, Accessed 8 December 2015.

[4] Nee LE, Eldridge ER, Sunderland T, Thomas CB, Katz D, Thompson KE, Weingartner H, Weiss H, Julian C, Cohen R (1987) Dementia of the Alzheimer's type- Clinical and family study of 22 twin pairs. *Neurology* **37**, 359–363.

[5] Räihä I, Kaprio J, Koskenvuo M, Rajala T, Sourander L (1996) Alzheimer's disease in Finnish twins. *Lancet* **347**, 573–578.

[6] Räihä I, Kaprio J, Koskenvuo M, Rajala T, Sourander L (1998) Environmental differences in twin pairs discordant for Alzheimer's disease. *J. Neurol. Neurosurg. Psychiatry* **65**, 785–787.

[7] Bekris LM, Yu CE, Bird TD, Tsuang DW (2010) Genetics of Alzheimer disease. *J Geriatr Psychiatry Neurol* **23**, 213-27.

[8] Xu W, Tan L, Wang HF, Jiang T, Tan MS, Tan L, Zhao QF, Li JQ, Wang J, Yu JT (2015) Meta-analysis of modifiable risk factors for Alzheimer's disease. *J Neurol Neurosurg Psychiatry* **86**, 1299-306.

[9] Walton JR (2014) Chronic aluminum intake causes Alzheimer's disease: applying Sir Austin Bradford Hill's causality criteria. *J Alzheimers Dis* **40**, 765–838.

[10] Bhattacharjee S, Zhao Y, Hill JM, Percy ME, Lukiw WJ (2014) Aluminum and its potential contribution to Alzheimer's disease. *Front Aging Neurosci*, doi: 10.3389/fnagi.

[11] Yokel RA (2013) Aluminum, In Encyclopedia of human nutrition, Waltham: MA, Academic Press **1**, 57–63.

[12] Simonsen L, Johnsen H, Lund SP, Matikainen E, Midtgard U, Wennberg A (1994) Methodological approach to the evaluation of neurotoxicology data and the classification of neurotoxic chemicals. *Scand J Work Environ Health* **20**, 1-12.

[13] Kopeloff LM, Kopeloff EB (1942) Recurrent convulsive seizures in animals produced by immunologic and chemical means. *Am. J. Psychiatry* **98**, 881–902.

[14] Walton JR (2012) Cognitive deterioration and associated pathology induced by chronic low-level aluminum ingestion in a translational rat

model provides an explanation of Alzheimer's disease, tests for susceptibility and avenues for treatment. *Int J Alzheimers Dis* **2012**, 1-17.

[15] Crapper DR, Krishnan SS, Dalton AJ (1973) Brain Aleminum Distribution in Alzheimer's Disease and Experxmental Neurofibrillary Degeneration. *Sci New Ser* **180**, 511–513.

[16] Exley C, Vickers T (2014) Elevated brain aluminium and early onset Alzheimer's disease in an individual occupationally exposed to aluminium: a case report. *J. Med Case Rep* **8**, 41.

[17] Andrasi E, Pali N, Molnar Z, Kosel S (2005) Brain aluminum, magnesium and phosphorus contents of control and Alzheimer-diseased patients. J. Alzheimers. Dis. 7, 273–84.

[18] Walton JR (2006) Aluminum in hippocampal neurons from humans with Alzheimer's disease. *Neurotoxicology* **27** 285-394.

[19] Ellis HA, McCarthy JH, Herrington J (1979) Bone aluminium in haemodialysed patients and in rats injected with aluminium chloride: relationship to impaired bone mineralisation. *J. Clin. Pathol* **32**, 832–44.

[20] Alfrey AC, Hegg A, Craswell P (1980) Metabolism and toxicity of aluminum in Renal Failure. *Am J Clin Nutr* **33**, 1509–1516.

[21] Parsons V, Davies C, Goode C, Ogg C, Siddiqui J (1971) Aluminium in bone from patients with renal failure. *Br Med J* **4**, 273–275.

[22] Elinder C, Ahrengart L, Lidums V, Pettersson E, Sjogren B (1991) Evidence of aluminium accumulation in aluminium welders. *Br J Ind Med* **48**, 735–738.

[23] Klein GL, Targoff CM, Ament ME, Sherrard DJ, Bluestone R, Young JH, Norman AW, Coburn JW (1980) Bone-disease associated with total parenteral nutrition. *Lancet* **2**, 1041–1044.

[24] Kruger PC, Parsons PJ, Galusha AL, Morrissette M, Recker RR, Howard LJ (2013) Excessive aluminum accumulation in the bones of patients on long-term parenteral nutrition: postmortem analysis by electrothermal atomic absorption spectrometry. *JPEN J Parenter Enteral Nutr* **38**, 728-735.

[25] Fewtrell MS, Bishop NJ, Edmonds CJ, Isaacs EB LA (2009) Aluminum exposure from parenteral nutrition in preterm infants: bone health at 15-year follow-up. *Pediatrics* **124**, 1372–9.

[26] House E, Esiri M, Forster G, Ince PG, Exley C (2012) Aluminum, iron, and copper in human tissues donated to the medical research council's cognitive function and ageing study. *Metallomics*. **4**, 56-65.

[27] Bogdanovich E, Krishnan SS, Pei Y, Hercz G, Lui SM, Hancock R, Harrison JE, Bone A (1992) Non-destructive bone aluminum assay by neutron activation analysis. *J Radioanal Nucl Che*m **164**, 293–302.

[28] Sharif AAM, Ghafourian H, Ahmadiniar A, Waqif HS, Saber-Tehrani M, Ghods H (2004) Determination of aluminum levels in serum and red blood cells from long-term haemodialysis patients using instrumental neutron activation analysis. *J Radioanal Nucl Chem* **262**, 473–477.

[29] Virk SA, Eslick GD (2015) Aluminum levels in brain, serum, and cerebrospinal fluid are higher in Alzheimer's disease cases than in controls: a series of meta-analyses. *J Alzheimers Dis* **47**, 629-38.

[30] Williams ED, Elliott HL, Boddy K, HaywoodD JK, Henderson IS, Harvey I, Kennedy AC (1980) Whole-body aluminum in chronic renal failure and dialysis encephalopathy. *Clin Nephrol* **14**, 198–200.

[31] Ellis KJ, Kelleher S, Savory J, Wills M (1988) *In vivo* monitoring of skeletal aluminum burden in patients with renal failure. *J Radioanal Nucl Chem* **124**, 85–95.

[32] Green S, Chettle DR (1992) A feasibility study of the *in vivo* measurement of aluminum in peripheral bone. *Phys Med Biol* **31**, 2287–2296.

[33] Wyatt RM, Ryde SJ, Morgan WD, McNeil EA, Hainsworth IR, Williams AJ (1993) The development of a technique to measure bone aluminium content using neutron activation analysis. *Physiol Meas* **14**, 327–35.

[34] Pejović-Milić A, Byun SH, Comsa DC, McNeill FE, Prestwich WV, Chettle DR (2005) *In vivo* measurement of bone aluminium: recent developments. *J. Inorg. Biochem.* **99**, 1899–903.

[35] Davis K, Pejović-Milić A, Chettle DR (2008) *In vivo* measurement of bone aluminum in population living in southern Ontario, Canada. *Med Phys* **35**, 5115.

[36] Aslam, Davis K, Pejović-Milić A, Chettle DR (2009) Noninvasive measurement of aluminium in human bone: preliminary human study and improved system performance. *J Inorg Biochem* **103**, 1585–90.

[37] Mohseni HK , Chettle DR (2016) A History of *In Vivo* Neutron Activation Analysis in Measurement of Aluminum in Human Subjects. *J Alzheimers Dis* **50**, 913-26. doi: 10.3233/JAD-150595.

[38] Aslam, Pejović-Milić A, Chettle DR, McNeill FE (2008) Quantification of manganese in human hand bones: A feasibility study. *Phys Med Biol* **53**, 4081-4092.

[39] Mostafaei F, McNeill FE, Chettle DR, Wainman BC, Pidruczny AE, Prestwich WV (2015) Measurements of fluorine in contemporary urban Canadians: A comparison of the levels found in human bone using *in vivo* and *ex vivo* neutron activation analysis. *Physiol Meas* **36**, 465-487.

[40] Byun SH, Prestwich WV, Chin K, McNeill FE, Chettle DR (2006) 4-pi NaI(Tl) detector array for *in vivo* neutron activation analysis. *IEEE Trans Nucl Sci* **53**, 2944–2947.

[41] Pejović-Milić A, Arnold ML, McNeill FE, Chettle DR (2000) Monte Carlo design study for in vivo bone aluminum measurement using a low energy accelerator beam. *Appl Radiat Isot* **53**, 657-664.

[42] ICRP (1974) *Report of the task group on reference man*, Publication 23. Pergamon, Oxford.

[43] Darvish-Molla S, Prestwich WV, Byun SH (2015) Comprehensive radiation dose measurements and Monte Carlo simulation for the ^{7}Li(p,n) accelerator neutron field. *Radiat Prot Dosimetry*, doi:10.1093/rpd/ncv428.

[44] NCRP (2009) Ionizing Radiation Exposure of the Population of the United States, Report No. 160.

[45] Molloy DW, Alemayehu E, Roberts R (1991) Reliability of a Standardized Mini-Mental State Examination compared with the traditional Mini-Mental State Examination. *Am J Psychiatry* **148**, 102-5.

[46] Favaro PC, Bode P, De Nadai Fernandes EA (2005) Trace elements in nail polish as a source of contamination when used in epidemiological studies. *J Radioanal Nucl Chem* **264**, 61-65.

[47] Hellström H, Mjoberg B, Mallmin H, Michaelsson K (2005) The aluminum content of bone increases with age, but is not higher in hip fracture cases with or without dementia compared to controls. *Osteoporos Int* **16**, 1982-1988.

[48] Ellis KJ (1990) Reference man and woman more fully characterized. Variations on the basis of body size, age, sex, and race. *Biol Trace Elem Res* **26-27**, 385-400.

Chapter 4

Non-invasive Measurement of Magnesium in Bone in Alzheimer's Disease and Control Subjects

Introduction to Article IV

The fourth article presents the IVNAA study of magnesium in Alzheimer's disease and control subjects. This study was performed as a spinoff of the in vivo aluminum measurements presented in the previous chapter. Magnesium is one the elements with a suggested association with Alzheimer's disease, with elevated levels reported in the serum, hair and brain tissues of Alzheimer's patients. The present study aims to investigate the possible differences in bone magnesium concentrations between Alzheimer's and control groups.

The experimental work and analyses presented in the following article were performed by the author of this thesis under the supervision of Dr. David Chettle, and with guidance of Dr. Bill Prestwich, Dr. David Cowan, Dr. Soo Hyun Byun, Dr. Nicholas Priest, Dr. Jovica Atanackovic, and Dr. Witold Matysiak.

Contents of Article IV

The following article has been submitted for publication in Physiological Measurement.

Non-invasive Measurement of Magnesium in Bone in Alzheimer's Disease and Control Subjects

H. K. Mohseni[1], D. Cowan[2], D.R. Chettle[1], N. Priest[3], W. Matysiak[4], J. Atanackovic[5], S.H. Byun[1], W.V. Prestwich[1]

[1]Medical Physics & Applied Radiation Sciences, McMaster University, Hamilton, Canada
[2]Department of Medicine, McMaster University, Hamilton, Canada
[3]Canadian Nuclear Laboratories, Chalk River Laboratories, Ontario, Canada
[4]University of Florida Proton Therapy Institute, Jacksonville, FL, USA
[5]Ontario Power Generation, Whitby, Ontario, Canada

Abstract

Magnesium (Mg) is an essential element for the human body with roles in many enzymatic processes. A role for Mg has been suggested in the etiology of Alzheimer's disease (AD). Although blood only contains 0.3% of body Mg, serum analysis is generally used to determine body Mg status in the absence of *in vivo* measurement techniques for Mg in the brain. Skeleton acts as Mg depot, storing 50 - 60% of total body Mg. The *in vivo* neutron activation analysis (IVNAA) system at McMaster University has been used to measure Mg in the hand bone of subjects with AD, as well as reference subjects non-invasively. The phantom-based minimum detectable limit (MDL) of the system was 0.23 mg Mg/g Ca. 15 AD subjects (8 males, 7 females) with mild and moderate CDR and MMSE

scores and 15 controls (7 males, 8 females) were included in the study. The results are reported as the normalized ratio of Mg to Calcium. No significant difference was observed between the two groups ($p = 0.63$) with mean Mg concentration for AD subjects and controls being 13.3 ± 1.1 and 12.8 ± 1.4 mg Mg/g Ca, respectively. There were no correlations found between the Mg/Ca ratios and the age of the subjects. These results indicate that IVNAA has a high sensitivity for measuring Mg in the bone. While bone can be considered as a preferred site for monitoring Mg, it may not be an appropriate proxy for brain in the context of Mg content analysis.

Keywords- *In vivo* measurement, Neutron activation analysis, magnesium, Alzheimer's disease, bone

1. Introduction

Magnesium (Mg) is the eighth most abundant element in the earth's crust [1] and the fourth most common metal in the human body. Mg is considered essential for the human body, having important roles in many enzymatic processes. Mg is also involved in neurotransmission, muscle contraction, and structural composition of the skeleton [1, 2]. The average human body contains about 24 g of Mg [1]. About 50 - 60% of body burden of Mg is stored in bone, a third of which is considered to be exchangeable, available for maintaining physiological processes in the body [1]. Its content in the skeleton is known to decrease with age [1]. Humans need to consume Mg on a daily basis, the exact amount

required varies depending on different recommendations and based on gender and health status [1]. Changes in Mg in the body are linked to a number of health conditions.

Mg has also been linked to the etiology of Alzheimer's disease (AD). Of the estimated 46.8 million cases of dementias as of 2015, Alzheimer's disease is the most common type, accounting for about 85% of the cases [3, 4]. Many attempts have been made over the past few decades to determine the causes or contributing factors to AD. The hypothesis of Mg's involvement in AD was first brought forward by Glick [5]. Upon statistical analysis of the results of the study done by Perl et al. [6] on the increased amount of aluminum in AD brains, Glick found a decrease in the neuronal Mg deposits in the brains of AD patients. Glick's hypothesis proposed alterations in serum albumin leading to a defective transport system that shows a higher affinity for aluminum instead of Mg [5]. This would cause aluminum to compete with Mg for binding sites in the brain, subsequently resulting in simultaneous increase in aluminum content and decrease in Mg content in the brain [5, 7]. Later studies measuring Mg content of the brain confirmed significantly lower Mg in the brain and in particular hippocampus of the AD subjects compared to healthy controls [8]. Mg in hair has also been shown to be significantly lower in in patients with AD. Hair is considered as an indicator of tissue content of Mg which could possibly reflect long-term storage of Mg [9]. Serum measurement is the most common method of assessing Mg status in the body, despite the fact that serum contains only 0.3%

of the Mg in the body [1]. Serum Mg levels in AD subjects have been shown not only to be different than controls, but also vary depending on the severity of the disease [10, 11].

It should be noted that Mg depletion is different from Mg deficiency. The former arises from a disruption in the metabolism of Mg, while the latter is related to insufficient intake of Mg [7]. It is Mg depletion that has been linked to the causality of AD. However, some research findings indicate a protective role in dementias rendered by the dietary supplementation of Mg, both in humans and animal models [12-14].

Bone is considered as the storage unit for many essential and non-essential elements in the human body. 50 - 60% of the total body Mg is stored in the skeleton. There is a lack of investigation of the Mg content in the bone in relation to human health in general and AD specifically.

In vivo neutron activation analysis (IVNAA) is a non-invasive method developed and utilized over the past few decades to measure the body burden of several major, minor, and trace elements. It has been previously used to measure Mg in healthy individuals [2] and in rats [15]. Neutron activation analysis has also been used *in vitro* to analyse the Mg content of the skeleton [16, 17]. The present work investigates the feasibility of *in vivo* Mg in the hand bone as a substitute for brain measurements, as well as the possible difference in the skeletal content of Mg between AD subjects and healthy individuals. Given the high concentration of Mg

in the skeleton, bone measurement may be a reliable indicator of Mg status in the body and its possible depletion in the context of various medical conditions.

2. Materials and Methods

2.1. IVNAA of hand

This study was done as a substudy of a separate investigation measuring aluminum in AD and control subjects. The irradiation and counting protocols were, therefore, designed to extract the maximum amount of information about aluminum and calcium. The IVNAA facility at McMaster Accelerator Laboratory (MAL) has been developed for *in vivo* measurement of major, minor, and trace elements in the hand bone and previously utilized for measurements of aluminum [18], manganese [19], fluorine [20], and Mg [2]. ^{26}Mg has a cross-section of 38.2 mb for thermal neutron activation through the $^{26}Mg(n,\gamma)^{27}Mg$ reaction. The reaction product ^{27}Mg has a half-life of 9.46 min and decays via beta emission, de-exciting to stable ^{27}Al following emission of two gamma rays with energies of 0.844 MeV (71.8%) and 1.014 MeV (28%), respectively. The accelerator and detection system have been described in detail in previous publications [21, 22]. Briefly, the Tandetron accelerator is a double stage or tandem machine designed to accelerate protons to a maximum energy of 2.5 MeV. Neutrons are produced via the $^{7}Li(p,n)^{7}Be$ reaction in the lithium target and undergo further thermalization and shielding within the irradiation cavity, which has an opening for inserting the hand or phantoms. The counting system consists of an array of 9

NaI(Tl) detectors arranged in 4π geometry to detect the maximum number of radiation events.

As mentioned before, the skeleton contains 50-60% of the 24 g body burden of Mg, which translates into approximately 180-220 mg of Mg in the hand bone [1, 23]. Hand bone is mostly comprised of cortical bone which contains less Mg compared to trabecular bone. The choice of hand as the preferred site of measurement was mainly due to radiation protection considerations and secondarily for convenience of positioning for irradiation and counting. Any *in vivo* measurement technique developed for humans should pose no or minimum risk to the subject. As such, the radiation dose to the subject should be kept as low as reasonably achievable (ALARA). Human extremities have a relatively high regulatory dose limit due to their lower radiosensitivity [23]. Providing shielding to confine the radiation dose to the extremities is also less challenging as they can be extended far from the body and more radiosensitive organs.

2.2. Hand phantoms

Hand phantoms were made based on the composition of the human hand with varying amounts of Mg. Of the elements composing the human hand, only those with significant cross-sections for neutron activation together with appreciable abundances, namely calcium (Ca), sodium (Na), and chlorine (Cl) with reactions $^{48}Ca(n,\gamma)^{49}Ca$, $^{23}Na(n,\ \gamma)^{24}Na$, $^{37}Cl(n,\ \gamma)^{38}Cl$ were considered. Phantoms were irradiated for 45 sec at the proton energy of 2.3 MeV and proton beam current of

400 μA, a protocol which had been optimized for *in vivo* aluminum measurement. Following irradiation, the phantoms were transferred to the counting room located at some distance away from the irradiation facility to avoid activating the detectors and as well as reducing the background radiation. The average transfer time was 20 sec. Each phantom was counted for 10 cycles of 60 sec, allowing for approximately one half-life of ^{27}Mg to be measured.

Multi-element activation is one of the important characteristics of IVNAA allowing for simultaneous assessment of multiple elements in the sample. This, however, presents challenges with respect to interferences. In the case of Mg, interference is caused by the thermal neutron activation of manganese (Mn) through the reaction ^{55}Mn(n,γ)^{56}Mn with a considerable cross-section of 13.3 b. ^{56}Mn de-excites through gamma emission at 0.847 MeV (99%) with a half-life of 2.58 hours. This gamma-ray cannot be resolved from the adjacent photo-peak of Mg at 0.844 MeV due to the relatively poor resolution of NaI(Tl) detectors. Although the neutron activation cross-section for Mn reaction is significantly larger than that of Mg, there is far less Mn present in the human bone than there is Mg. Furthermore, due to the longer half-life of ^{56}Mn, its relative contribution to counts in counting intervals of 60 sec is fairly small. As a result, the overall impact of the ^{56}Mn interference is considered as negligible. To confirm this, the previously reported Mn content in human hand bone (1.6 μg Mn/g Ca) was used to calculate the impact of Mn on Mg content of human bone measured in the current study [19]. This resulted in a relative contribution of about 2%. It is noted that the

reported value of 1.6 µg Mn/g Ca is amongst the highest reported in the literature [19,24].

2.3. Human measurements

Following approval by the research ethics boards at McMaster University and Ryerson University, 15 AD and 15 control subjects (of which 16 were females and 14 were males), residing in Hamilton, Ontario were recruited. All subjects provided informed consent prior to entering the study or a legal proxy provided consent if it was felt that the subject was incapable of doing so. All AD subjects were diagnosed according to DSM 4 criteria and were categorized as mild or moderate, based on the Clinical Dementia Ranking Scale (CDR) and the standardized Mini-Mental State Examination (MMSE), shown in Tables 4.1 and 4.2. The minimum age criterion for recruitment was 60 years of age as the focus of the study was measuring aluminum in late-onset of AD. The subjects' age ranged from 63 to 89 years with a mean of 77.6 years. Orientation to the facility was provided upon arrival at the MAL. In order to provide convenient, safe, and fast transfer between irradiation and counting facilities, the subjects were seated in a wheelchair. Subjects were accompanied by their physician at all times. As keeping the dose as low as reasonably achievable is of utmost importance, the subject's arm was fitted with a water sleeve to fill the gap between subject's arm and the cavity wall, thus confining radiation exposure to the hand. Water was chosen because of the neutron-moderating properties of hydrogen which

significantly absorbs neutrons, reducing the dose to the subject and accompanying caretaker. The effective dose to the subjects was 0.21 mSv, based on the previous dose simulations and measurements [25], which is in the same order of magnitude as a chest x-ray (0.1 mSv)[26]. At the end of the irradiation the water sleeve was removed and the subject was transferred to the counting room for acquisition of the activity in the hand using the 4π detection system. In order to eliminate possible contamination, the subjects were asked to remove any jewelry and nail polish from the irradiated hand, although an extensive neutron activation analysis of different nail polish brands has shown no Mg contamination [27].

The National Institute of Standards and Technology's (NIST) standard reference material 1400 which consists of bone ash with certified Ca and Mg concentrations was also measured in order to validate the system performance.

Table 4.1. CDR scores of AD subjects.

Score	Stage	Number of subjects
CDR-0	Normal	0
CDR-0.5	Questionable	0
CDR-1	Mild	4
CDR-2	Moderate	11
CDR-3	Severe	0
Total		15

Table 4.2. MMSE scores of AD subjects recruited for this study (*one subject was categorized as aphasic with no MMSE score).

Score	Stage	Number of subjects
26 - 30	Normal	1
20 - 25	Mild	5
10 - 19	Moderate	8
0 - 9	Severe	0
Total		14*

2.4. Analysis of the spectra

There are two major factors that influence the activity detected in the sample. These are neutron fluence and counting irradiation geometry. While the irradiation protocol is followed for each measurement, there are variations in neutron production due to steering of the beam and condition of the target. Irradiation geometry is also subject to variation, as the size of the hand and positioning in the irradiation cavity varies among different patients. This is accounted for by taking the ratio of Mg to Ca as an indicator of bone mass. The analysis of the spectra should, therefore, include both Mg and Ca. In order to extract the area under Ca and Mg peaks, the Levenberg-Marquardt algorithm for non-linear least squares fitting was used for each of the well-isolated peaks, fitting each with a Gaussian function and a linear function to account for the continuum present throughout the spectrum. For Mg this includes the energy region from 0.75 MeV to 0.94 MeV and for Ca the energy range of interest is

2.85-3.32 MeV. The inverse-variance weighted mean of the 10 individually analysed spectra was taken as the estimate of Mg and Ca counts.

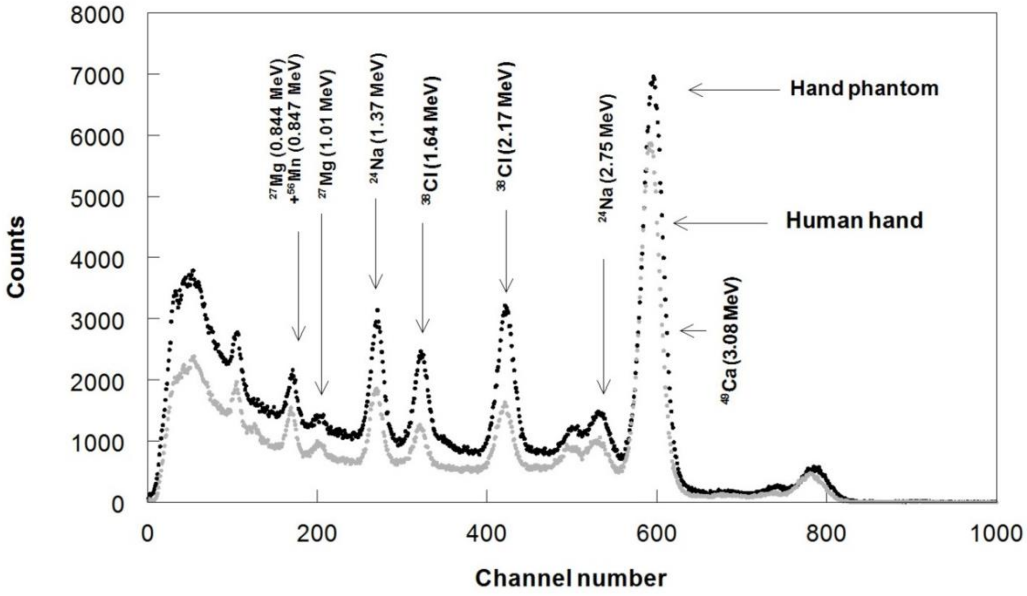

Figure 4.1. Gamma spectra of a 150 mg Mg phantom and and AD subject's hand.

3. Results

Figure 4.1 compares the spectrum of a phantom containing 150 mg Mg with the spectrum collected from one of study subjects. The two spectra agree closely in that all the major radioisotopes in a human hand are accounted for in the phantom. The difference in the total number of counts is due to the possible variations in the neutron fluence and the differences in the positioning of the phantom and the subject inside the irradiation cavity, as well as differences in the total irradiated mass, and therefore the content of different radionuclides.

The calibration line generated based on phantoms is shown in Figure 4.2. The slope of the calibration line was used to convert from counts to mass. The minimum detectable limit (MDL) of the system can also be determined using the calibration line. Traditionally defined as twice the uncertainty in the measured Mg in the zero concentration phantom divided by the slope of the calibration line, the phantom MDL in this study was 0.2 mg Mg/g Ca or 3.3 mg Mg. When *in vivo* measurements are involved, MDL can also be defined as twice the median uncertainty of all study subjects or 0.9 mg Mg/g Ca in this case.

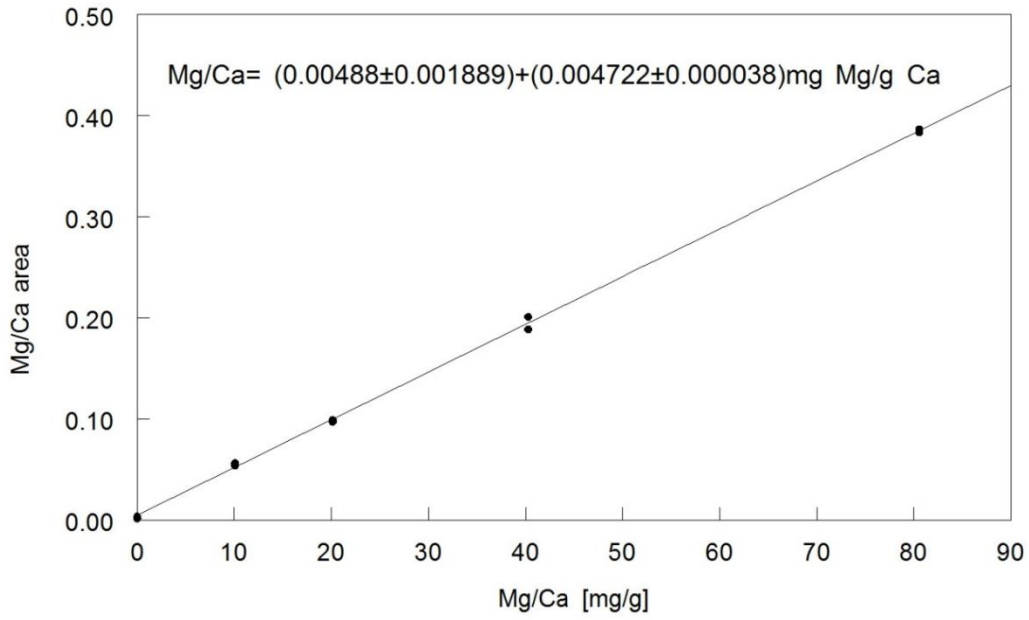

Figure 4.2. Calibration line constructed based on hand phantoms with varying concentrations of Mg, resulting in an MDL of 0.23 mg Mg/g Ca or 3.33 mg Mg (r = 0.9997).

Table 4.3 shows the results of measurements performed on the NIST 1400 bone ash sample with certified Ca and Mg concentrations. As discussed before, the

contribution of ^{55}Mn counts to the Mg content of hand bone is negligible. The concentration of Mn in the NIST 1400 sample, however, is about an order of magnitude higher than the Mn found in human hand bone, and thus, cannot be ignored. It should be noted the Mn concentration in NIST 1400 sample is not certified. The calculated contribution was 32% for the NIST 1400 sample, the corrected values based on subtracting this Mn interference are reflected in Table 4.3.

Table 4.3. NIST 1400 bone ash measurements of Mg, Mn, and Ca (Ca and Mg are certified, Mn is uncertified).

Measurement	μg Mg/g Ca ±σ before correction for ^{56}Mn	μg Mg/g Ca ±σ after correction for ^{56}Mn
1	24.17 ± 0.43	16.36 ± 0.29
2	25.27 ± 0.55	17.11 ± 0.37
3	24.30 ± 0.67	16.45 ± 0.45
4	24.64 ± 0.51	16.67 ± 0.35
5	24.77 ± 0.44	16.77 ± 0.30
Inverse-variance weighted mean	24.61 ± 0.22	16.66 ± 0.15
NIST 1400 (uncertified)	17.92 ± 0.35	

Figure 4.3-a and –b illustrate the Mg/Ca content of the hand bone in AD and control subjects, with the error bars representing the uncertainty of one sigma (68% confidence level). The mean concentration in AD subjects was 13.3 ± 1.1 mg Mg/g Ca with a range of 11.9 ± 0.6 to 14.6 ± 0.3 mg Mg/g Ca. For the control

group, the mean concentration and range were 12.8 ± 1.4 mg Mg/g Ca and 9.2 ± 0.5 to 15.4 ± 0.8 mg Mg/g Ca, respectively. The difference in the mean concentrations between AD and control subjects was 0.5 ± 0.5 mg Mg/g Ca which failed to reach significance with a p-value of 0.3. There was also no difference observed in Mg/Ca between female and male participants ($p = 0.6$).

Another area of interest was the possible trend in Mg content of the bone with respect to age, depicted in Figure 4.4. No statistically significant correlation in the Mg content of the bone with age was observed ($r=0.09$). No significant correlation with age was found in either the AD or control groups.

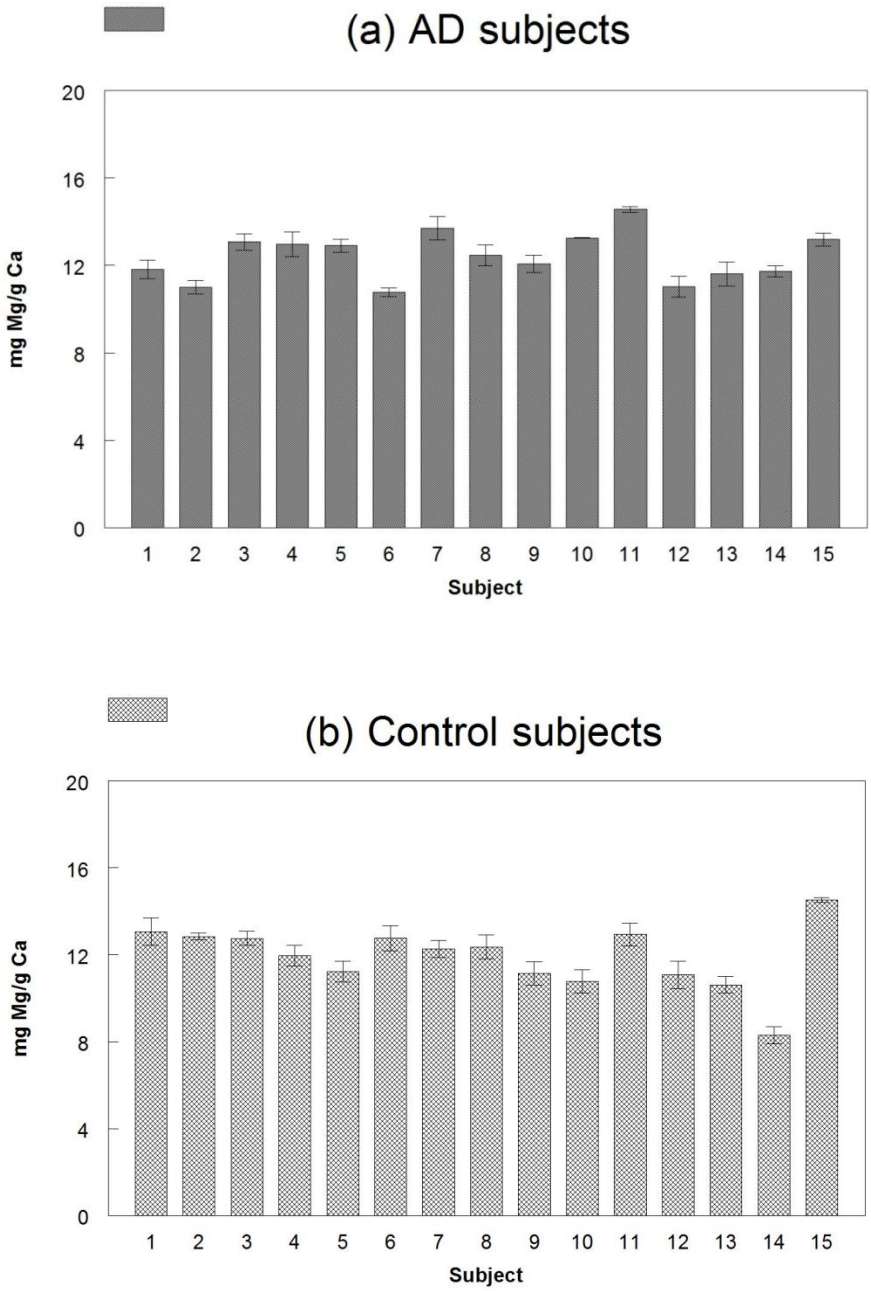

Figure 4.3. Mg concentrations in (a) AD subjects and (b) control subjects expressed in μg Mg/g Ca.

4. Discussion

The MDLs achieved in this study, both for phantoms and *in vivo* are significantly lower than the average content of Mg in the hand bone found in the control group**,** which confirms that the developed IVNAA system is sensitive enough to measure very low levels of Mg in the bone in human subjects.

Certified reference materials are an important means of validating the experimental setup. The results of repeated measurements of the NIST 1400 bone ash confirmed that the IVNAA system is capable of both accurate and precise measurement of Mg/Ca concentrations. Moreover, since the amount of Mn in the bone ash was known (albeit uncertified), the method of accounting for the interference of Mn and the accuracy with which it estimated the contribution from activation of Mn was confirmed by the close agreement of the certified and measured Mg/Ca ratio.

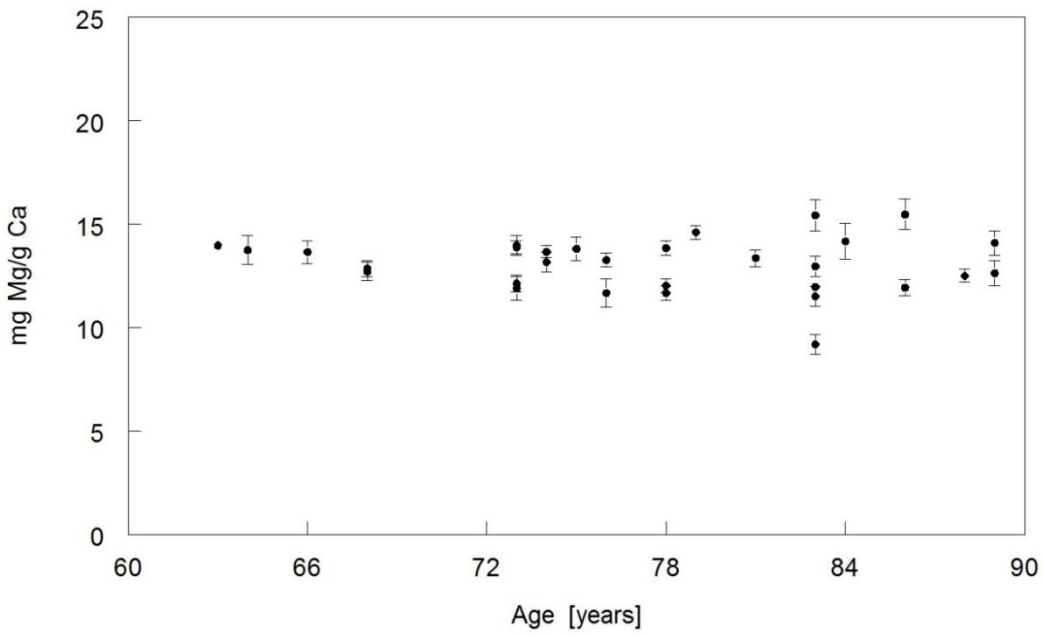

Figure 4.4. Distribution of Mg/Ca ratio of all subjects as a function of age, expressed in mg Mg/g Ca.

To the best of the authors' knowledge, there are no published studies involving *in vivo* measurement of Mg content of the bone in AD subjects, and therefore, no comparison can be made. However, Mg/Ca ratio has been previously measured using IVNAA in healthy subjects, where a mean ratio of 11.0 ± 1.3 (1 SD) was reported in 17 male subjects [2]. The mean Mg/Ca ratio found in control subjects in the present study is higher than the above value and other reported concentrations in various bones using *in vitro* techniques [2].

The absence of a significant difference in Mg/Ca ratio between AD and control subjects, given the high sensitivity of the technique is indeed an interesting finding. These results may be explained through the understanding that although

skeleton is the main storage unit for Mg, its relatively low bioavailability of 30% indicates that bone may not be responsive enough to reflect the changes in the Mg status of the body, such as the Mg depletion observed in the brain of AD patients. Another, less likely explanation is the relatively lower content of Mg in the mostly cortical hand bone. In this context, it would be beneficial to conduct an *in vivo* measurement of Mg concentration in the trabecular bone in AD subjects, a favourable site for which would be the calcaneus bone in the foot due to radiation protection considerations discussed earlier.

No significant correlation was found between the Mg content of the hand bone and age of the subjects, although Mg in bone has been shown to decrease with age in animals [26]. One possible reason for lack of correlation is the relatively small age range of the participants in the current study. Also, in this study the Mg content was normalized to the Ca content of the hand. In these circumstances, an age-related decline in Ca would mask any similar age-related decline in Mg.

The current study was limited to AD participants ranging from mild to moderate in the severity and progression of the disease, omitting severe cases due to the difficulties in recruitment arising from mental and emotional inconvenience to the patients and their caretakers. Where possible, it would be interesting to measure Mg in the bone in AD subjects in advanced stages of the disease to provide a wider image of bone Mg status in these subjects.

5. Conclusions

The present work puts forth the results of the first non-invasive and non-destructive *in vivo* measurement of Mg concentration in the hand bone in patients suffering from AD, as well as control subjects. The main objectives of this study were to investigate the feasibility of using bone as a proxy system for measuring Mg content in the brain of AD patients and also to determine whether IVNAA can be used as a tool for monitoring the Mg content of the bone as biomarker for the progression of AD.

IVNAA has proven to be a reliable tool for measuring and monitoring Mg content of the bone, given the low MDLs achieved in this study relative to lowest normal concentrations reported in the literature. While the results of the current study do not support a role for bone Mg as a biomarker for AD, IVNAA, as a non-invasive method, can be used to monitor the Mg content of the bone in individuals with AD to follow any changes in bone Mg levels with the progression of the disease.

Acknowledgements

The authors would like to extend their gratitude to Justin Bennett, the accelerator operator at the MAL for assisting in conducting experiments and patient irradiation. They also thank Dr. Farshad Mostafaei for his assistance in patient data collection and Michael Inskip for valuable advice and access to his laboratory. This work was made available through the funding provided by the

Canadian Nuclear Laboratories (CNL) and Natural Sciences and Engineering Research Council of Canada (NSERC).

References

[1] Jahnen-Dechent W, Ketteler M (2012) Magnesium basics. *Clin Kidney J* **5**, i3-i14.

[2] Aslam, Pejovic-milic A, McNeill FE, Byun SH, Prestwich WV, Chettle DR (2008) *In vivo* assessment of magnesium status in human body using accelerator-based neutron activation measurement of hands: A pilot study. *Med Phys* **35**, 608-616.

[3] Prince M, Wimo A, Guerchet M, Ali G, Wu Y, Prina M (2015) World Alzheimer Report, http://www.alz.co.uk/research/world-report-2015, Accessed 8 December 2015.

[4] Mirra SS, Heyman A, McKeel D, Sumi SM, Crain BJ, Brownlee LM, Vogel FS, Hughes JP, van Belle G, Berg L, participating CERAD neuropathologist (1991) The consortium to Establish a Registry for Alzheimer's Disease (CERAD) Part II. Standardization of the neuropathological assessment of Alzheimer's disease. *Neurology* **41**, 479-486.

[5] Glick JL (1990) Dementias: The role of magnesium deficiency and an hypothesis concerning the pathogenesis of Alzheimer's disease. *Med Hypotheses* **31**, 212-225.

[6] Perl DP, Broady AR (1980) Alzheimer's disease X-ray spectrometric evidence of aluminum accumulation in the neuro fibrillary tangle-bearing neurons. *Science* **208**, 297-299.

[7] Durlach J (1990) Magnesium depletion and pathogenesis of Alzheimer's disease. *Magnesium Res* **3**, 217-218.

[8] Andrasi E, Iqaz S, Molnar Z, Mako S (2000) Disturbances of magnesium concentrations in various brain areas in Alzheimer's disease*. Magnes Res* **13**, 189-196.

[9] Veronese N, Zurlo A, Solmi M, Luchini C, Trevisan C, Bano G, Manzato E, Sergi G, Rylander R (2015) Magnesium Status in Alzheimer's Disease: A Systematic Review. Am J Alzheimers Dis Other Demen, doi 10.1177/1533317515602674.

[10] Cilliler AE, Ozturk S, Ozbakir S (2007) Serum magnesium level and clinical deterioration in Alzheimer's disease. *Gerontology* **53**, 419-422.

[11] Barbagallo M, Belvedere M, Di Bella G, Dominiquez LJ (2011) Altered ionized magnesium levels in mild-to-moderate Alzheimer's disease. *Magnes Res* **24**, 115-121.

[12] Xu ZP, Li L, Bao J, Wang ZH, Zeng J, Liu EJ, Li XG, Huang RX, Gao D, Li MZ, Zhang Y, Liu GP, Wang JZ (2014) Magnesium protects cognitive

functions and synaptic plasticity in streptozotocin-induced sporadic Alzheimer's model. *PLoS One* **9**, doi: 10.1371/journal.pone.0108645.

[13] Ozturk S, Cillier AE (2006) Magnesium supplementation in the treatment of dementia patients. *Med Hypotheses* **67**, 1223-1225.

[14] Ozawa M, Ninomiya T, Ohara T, Hirakawa Y, Doi Y, Hata J, Uchida K, Shirota T, Kitazono T, Kiyohara Y (2012) Self-reported dietary intake of potassium, calcium, and magnesium and risk of dementia in the Japanese: the Hisayama Study. *J Am Geriatr Soc* **60**, 1515-1520.

[15] Zhang RQ, Ellis KJ (1989) In vivo measurement of total body magnesium and manganese in rats. *Am J Physiol* **257**, 1136-1140.

[16] Zaichick V (2006) INAA of Ca, Cl, K, Mg, Mn, Na, P, and Sr contents in the human cortical and trabecular bone. *J Radioanal Nucl Chem* **269**, 653–659.

[17] Takata MK, Saiki M, Sumita NM, Saldiva PHN, Pasqualucci CA (2005) Trace element determinations in human cortical and trabecular bones. *J Radioanal Nucl Chem* **264**, 5–8.

[18] Aslam, Davis K, Pejović-Milić A, Chettle DR (2009) Noninvasive measurement of aluminium in human bone: preliminary human study and improved system performance. *J Inorg Biochem* **103**, 1585–90.

[19] Aslam, Pejovic-Milic A, Chettle DR, McNeill FE (2008) Quantification of manganese in human hand bones: A feasibility study. *Phys Med Biol* **53**, 4081-4092.

[20] Mostafaei F, McNeill FE, Chettle DR, Wainman BC, Pidruczny AE, Prestwich WV (2015) Measurements of fluorine in contemporary urban Canadians: A comparison of the levels found in human bone using *in vivo* and *ex vivo* neutron activation analysis. *Physiol Meas* **36**, 465-487.

[21] Pejović-Milić A, Byun SH, Comsa DC, McNeill FE, Prestwich WV, Chettle DR (2005) *In vivo* measurement of bone aluminium: recent developments. *J Inorg Biochem* **99**, 1899–903.

[22] Byun SH, Prestwich WV, Chin K, McNeill FE, Chettle DR (2006) 4-pi NaI(Tl) detector array for *in vivo* neutron activation analysis. *IEEE Trans Nucl Sci* **53**, 2944–2947.

[23] ICRP (1974) *Report of the task group on reference man*, Publication 23. Pergamon, Oxford.

[24] Benes B, Jakubec K, Smid J, Spevackova V (2000) Determination of thirty-two elements in human autopsy tissue. *Biol Trace Elem Res* **75** 195–203.

[25] Favaro PC, Bode P, De Nadai Fernandes EA (2005) Trace elements in nail polish as a source of contamination when used in epidemiological studies. *J Radioanal Nucl Chem* **264**, 61-65.

[25] Darvish-Molla S, Prestwich WV, Byun SH (2015) Comprehensive radiation dose measurements and Monte Carlo simulation for the 7Li(p,n) accelerator neutron field. *Radiat Prot Dosimetry*, doi:10.1093/rpd/ncv428.

[26] NCRP (2009) Ionizing Radiation Exposure of the Population of the United States, Report No. 160.

[27] Mcguire ME, Cowan JA (2002) Magnesium chemistry and biochemistry. *Biometals* **15**, 203-210.

Chapter 5

In Vivo Neutron Activation Study of the Short-term Kinetic Behaviour of Sodium and Chlorine in the Human Hand

Introduction to Article V

Article V is an investigation of the biological half-lives of sodium and chlorine in the human body. Both sodium and chlorine are essential for the human body and are known to have exchangeable and non-exchangeable compartments. Moreover, total exchangeable pools of sodium have been linked to several diseases. The change in the biokinetic behaviour of sodium and chlorine with age was also explored.

The experimental work and analyses presented in the following article were performed by the author of this thesis under the supervision of Dr. David Chettle, and with guidance of Dr. Bill Prestwich, Dr. David Cowan, Dr. Soo Hyun Byun, Dr. Nicholas Priest, and Dr. Jovica Atanackovic.

Contents of Article V

The following article has been submitted for publication in Physiological Measurement (manuscript ID: PMEA-101331).

In vivo neutron activation study of the short-term kinetic behaviour of sodium and chlorine in the human hand

H. K. Mohseni[1], D. Cowan[2], D.R. Chettle[1], N.D. Priest[3], J. Atanackovic[4], S.H. Byun[1], W.V. Prestwich[1]

[1]Medical Physics & Applied Radiation Sciences, McMaster University, Hamilton, Canada
[2]Department of Medicine, McMaster University, Hamilton, Canada
[3]Canadian Nuclear Laboratories, Chalk River, Canada
[4]Ontario Power Generation, Whitby, Ontario, Canada

Abstract

The time-dependent behaviour of sodium and chlorine was studied as a spinoff from a study of aluminum in the hand of subjects suffering from Alzheimer's disease and a control group, involving 15 Alzheimer's and 16 control subjects with an age range of 63 - 89 years. This was achieved using the *in vivo* neutron activation analysis system developed at McMaster University for the non-invasive measurement of aluminum, where a subject's hand is placed in a beam of accelerator-based thermalized neutrons, which activates elements by neutron capture. Following irradiation, the subject's hand is placed in a detection system comprising 9 NaI(Tl) detectors arranged in a 4π geometry to measure activated elements.

The removal rates of the activation products ^{24}Na and ^{38}Cl were determined after correction for the physical half-life, by sequential analysis of the residual activity in the hand. The removal rates of sodium and chlorine were best characterized by an exponential function corresponding to the rapidly exchangeable pool. The mean removal rates for sodium and chlorine in the control subjects were 40.5 ± 17.4 min and 24.2 ± 8.5 min, respectively. For Alzheimer's disease subjects the mean removal rates were 58.2 ± 36.1 min for sodium and 33.6 ± 16.7 min for chlorine. A linear increase with age was observed in the retention of sodium and chlorine, indicating a possible reduction in their rate of exchange with age. There was no significant difference in chlorine and sodium clearance between the Alzheimer's disease and control group subjects. These results are promising, given that the irradiation and counting protocol were optimized for the aluminum study, rendering them suboptimal for analyzing other elements and their rate of change with time. Further improvements include optimizing the irradiation protocol, longer counting times, and measuring the activity in the un-irradiated hand in various time intervals following irradiation.

Keywords- Biokinetic behaviour, sodium, chlorine, *in vivo* neutron activation analysis, Alzheimer's disease.

1. Introduction

Sodium (Na) is an essential element and the main cation in the extracellular fluid. It is also present in soft tissue and the skeleton. Na is known to exist in

exchangeable and non-exchangeable pools in the body. Studies done in the 1960s and 70s identified two pools of rapidly and slowly exchanging sodium in the body, with the former being associated with soft tissue and maintaining the homeostasis and the latter being stored in the skeleton [1-3]. Sodium has been mostly investigated in the context of total body concentration. There are only a few studies on the metabolic activity of Na *in vivo*, the majority of which focus on the exchangeability of Na as it relates to conditions such as hypertension and bone disease [2-7]. Differences in the clearance half-life of Na have been reported in subjects suffering from different types of bone ailments [7]. The total exchangeable Na has also been linked to high blood pressure [8].

The total body content of chlorine (Cl) has been previously investigated; however, there is a lack of research on the exchangeable behaviour of chlorine [9, 10]. It has been shown that the amount of chlorine undergoes changes in certain diseases associated with the endocrine system [1]. Most of the total body chlorine can be found in the extracellular pool and is readily available for exchange.

Neutron activation analysis has been mostly utilized to measure the content of different elements both *in vivo* and *in vitro*. *In vivo* neutron activation analysis (IVNAA) has the advantage of enabling repeated measurements over time, while exposing the subjects only to low doses of ionizing radiation, in order to follow the kinetic behaviour of activated elements regardless of whether it is stored in

bone or soft tissue. Moreover, neutron activation is an effective tool for investigating the turnover of different elements, as all the atoms in the sample are activated simultaneously, with the same probability, and independent of the possible compartments and their turnover times.

This study aims to identify the rapidly exchangeable pools of Na and Cl and their removal rates in the human hand with the available data and to investigate the possible differences in the removal rates of these essential elements between subjects suffering from Alzheimer's disease (AD) and healthy individuals. Furthermore, the investigation of age and gender dependent correlations is of interest.

2. Materials and methods

The current work is a spinoff of a study measuring aluminum in human hand bone in AD and control subjects using IVNAA. The neutron activation analysis facility at McMaster University has been optimized and previously utilized for *in vivo* measurement of several major and minor elements in the human hand bone [11-13]. A tandem accelerator is used to produce thermal neutrons via the $^{7}Li(p,n)^{7}Be$ reaction. The irradiation cavity which has an opening for inserting the hand is designed to thermalize the neutrons further and provide shielding against stray neutrons and prompt gamma-rays produced within the target and moderating material. Irradiating biological tissues activates the isotopes of several elements with significant thermal neutron capture cross-section within the

tissues, which subsequently de-excite by emitting gamma-rays. For the hand as the biological system under investigation, these major isotopes are ^{23}Na, ^{37}Cl, ^{26}Mg, and ^{48}Ca. More than 99% of total body calcium is found in the skeleton with very little bioavailability [14]. Sodium and chlorine are found both in the skeleton and soft tissue and are more readily available for exchange within the two compartments, and were therefore, investigated further.

2.1. The study subjects

Upon receiving approval by the research ethics boards of McMaster and Ryerson Universities in southern Ontario, 15 AD and 16 control subjects (16 females and 15 males) were recruited from the Hamilton, Ontario region. Where it was felt that AD subjects were incapable of providing consent, consent was obtained from their legal proxies. The minimum age requirement for participation was 60 years and age range of the subjects was 63 to 89 years with a mean of 77.6 years. All AD subjects had mild or moderate diagnoses. All subjects were seated in a wheelchair for ease and safety of transport between the irradiation and counting facilities which are located at some distance from each other to avoid the activation of the detector crystals. Measures were taken to keep the radiation dose to the subjects as low as achievable by fitting the subjects arm with a water sleeve to shield the rest of the body from exposure to ionizing radiation.

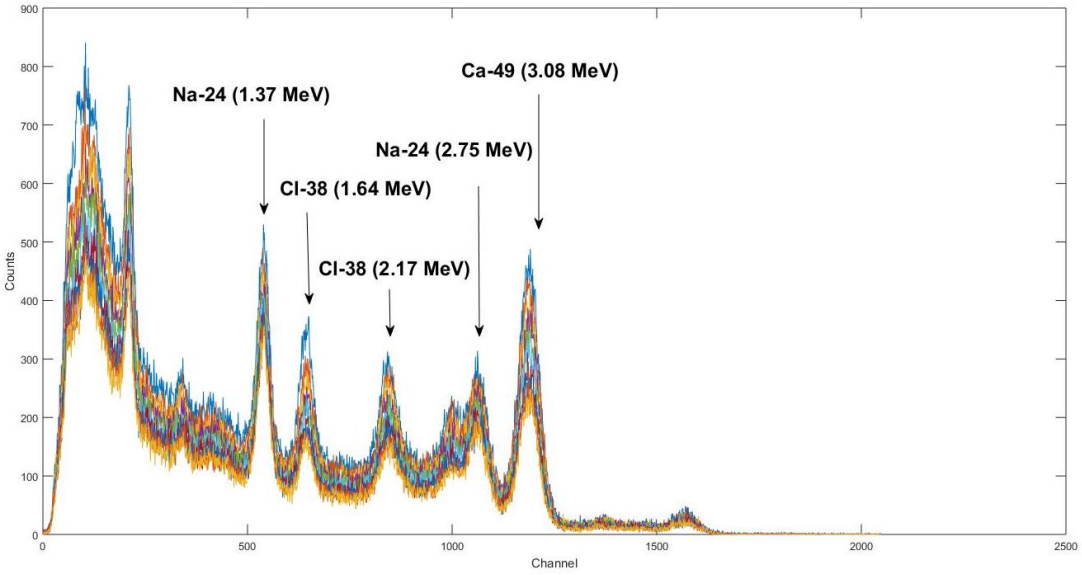

Figure 5.1. Gamma-ray spectra for a human subject showing 10 cycles of data acquisition

The subjects were irradiated at the proton energy of 2.3 MeV and proton beam current of 400 μA for 45 sec. The irradiation and counting protocols were optimized based on the 2.24 min half-life of aluminum and its cross-section. The counting time of 10 cycles of 60 sec was chosen to include multiple half-lives of aluminum while being reasonably short to avoid causing inconvenience to the subjects. The irradiation time was optimized to allow sufficient activation for aluminum and minimize decay during irradiation. It is noted that given the half-lives of ^{38}Cl and ^{24}Na, the aforementioned protocols are suboptimal for studying the kinetic behavior of sodium and chlorine *in vivo*. Nonetheless, the cyclic data acquisition can provide valuable information about the metabolic behavior of Na and Cl.

2.2. Data acquisition and analysis

The detection system consists of 9 NaI(Tl) detectors arranged in a near 4π geometry with an opening for inserting the hand [15]. The spectra from all 9 detectors for each of the 10 cycles were summed and used for analysis. Figure 5.1 shows a typical set of spectra consisting of 10 cycles of data acquisition. ^{24}Na decays to the stable ^{24}Mg via beta decay followed by the emission of two cascade gamma-rays with energies of 2.75 MeV and 1.37 MeV with a half-life of 15 hours. ^{38}Cl decays with a half-life of 37.24 min to ^{38}Ar via beta decays and emission of 2.17 MeV (42.4%) and 1.64 MeV (31.9%) gamma-rays. The analysis was limited to the stronger and more isolated peaks of 2.17 MeV for Cl and 1.37 MeV for Na. The peaks were fitted with a model consisting of a Gaussian function together with a linear background. Following the fitting, corrections were made to account for the physical half-lives of the radioisotopes and the transfer time from the irradiation to counting room. Furthermore, the delay between data acquisition cycles, while small relative to the half-lives of Na and Cl, was corrected for. To determine the biological half-life of the elements, a single exponential function (Equation 1) was fitted to the corrected data.

$$A(t) = a_0 \exp(-a_1 t) \qquad \text{Equation (1)}$$

where $\ln 2 / a_1$ represents the biological half-life.

Figure 5.2 illustrates the exponential fits to Na and Cl data for a control subject.

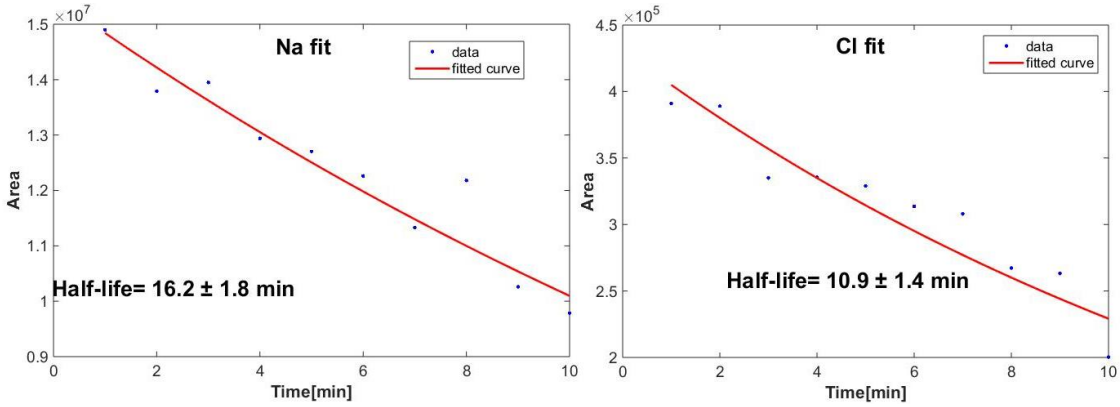

Figure 5.2. Exponential fits for Na and Cl with half-lives

3. Results

The bar graphs in Figure 5.3-a and –b illustrate the half-life of Na in AD and control subjects. The error bars represent 1σ uncertainty (68% confidence interval). The mean half-life of Na in the AD subjects was 58.2 ± 36.1 min with a range of 18.6 ± 2.7 to 161.6 ± 309.1 min. Control subjects had a mean Na half-life of 40.5 ± 17.4 min, ranging from 16.2 ± 1.8 to 82.1 ± 28.4. In analyzing the results for the presence of a significant difference, Student's t-test, a standard test of the means of the distributions, and χ^2, a variance-based test, were applied. The p-value for the Student's t-test was 0.1 and χ^2 value was 4.7 ($p < 0.001$). The same tests were applied to the results of Cl half-life in control and AD subjects. The Cl half-life distributions are shown in Figure 5.4-a and 4-b. For the AD subjects, Cl half-lives ranged from 10.5 ± 3.4 to 78.8 ± 97.1 min with a mean of 33.6 ± 16.7 min and for control subjects the mean was 24.2 ± 8.5 min, with a range of 10.9 ± 1.4 to 47.0 ± 40.9 min. The χ^2 test with a value of 4.3 revealed a

significant difference in the Cl content between the two groups ($p < 0.001$), while a p-value of 0.1 showed no significant difference.

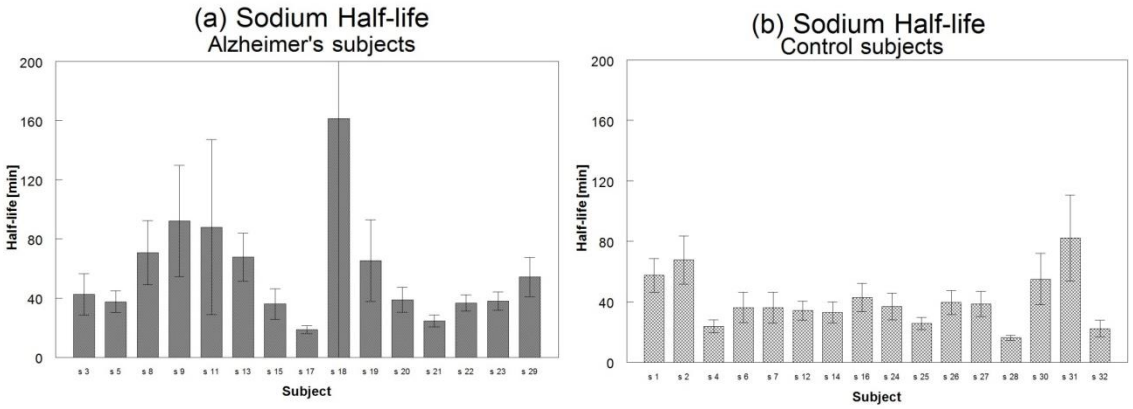

Figure 5.3. Sodium biological half-lives for (a) AD and (b) control subjects.

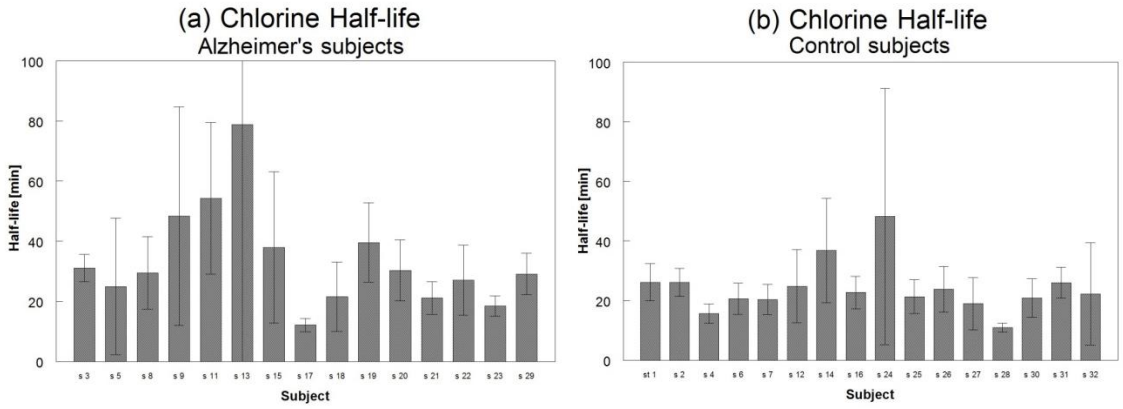

Figure 5.4. Chlorine biological half-lives for (a) AD and (b) control subjects.

The age distributions for Na and Cl in all subjects are shown in Figure 5.5 and Figure 5.6. Significant linear correlations ($p < 0.001$) were found for both Na ($r = 0.82$) and Cl ($r = 0.69$) distributions.

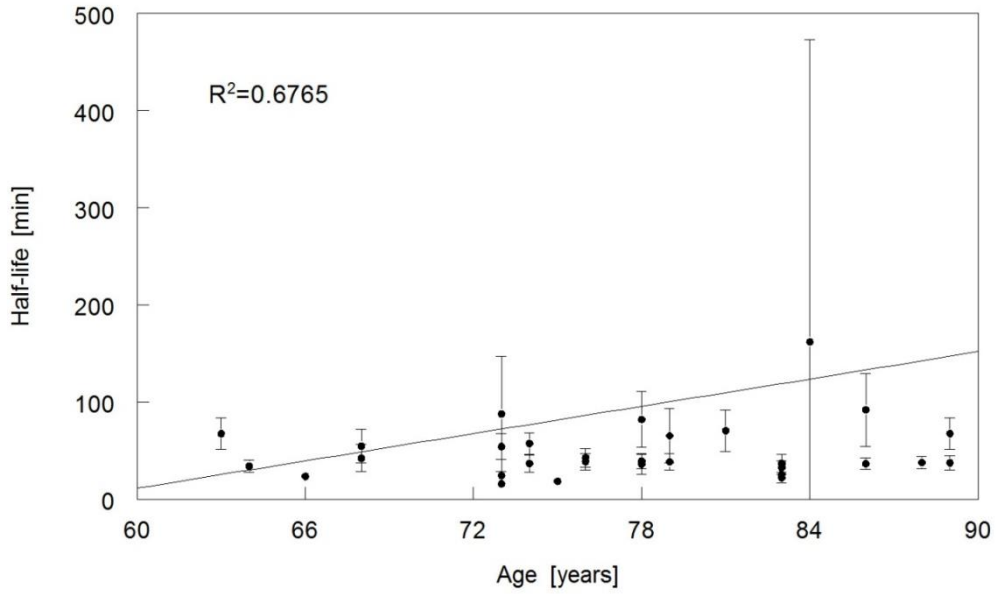

Figure 5.5. Sodium biological half-life of all subjects as a function of age.

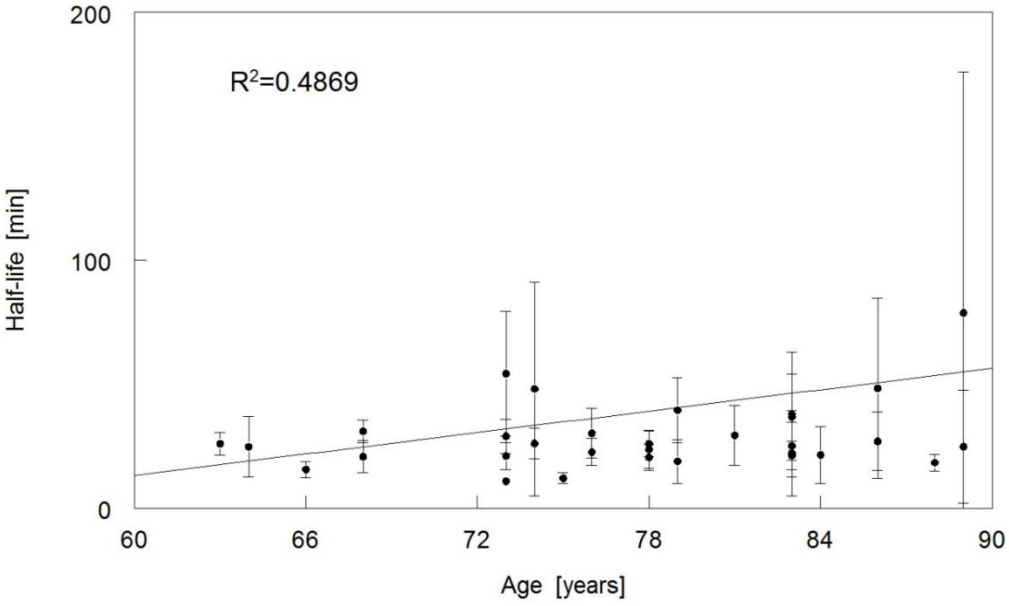

Figure 5.6. Chlorine biological half-life of all subjects as a function of age.

There was no significant difference in the biological half-life of Na (p = 0.4) and Cl (p = 0.5) between male and female subjects.

The relationship between the metabolic behaviour of Cl and Na with respect to each other is shown in Figure 5.7-a for AD and Figure 5.7-b for control subject by taking the ratio of Cl to Na for the two study cohorts. No significant difference was found between AD and control groups using the Student's t-test (p = 1) and χ^2 test (χ2 = 0.9 and p > 0.6).

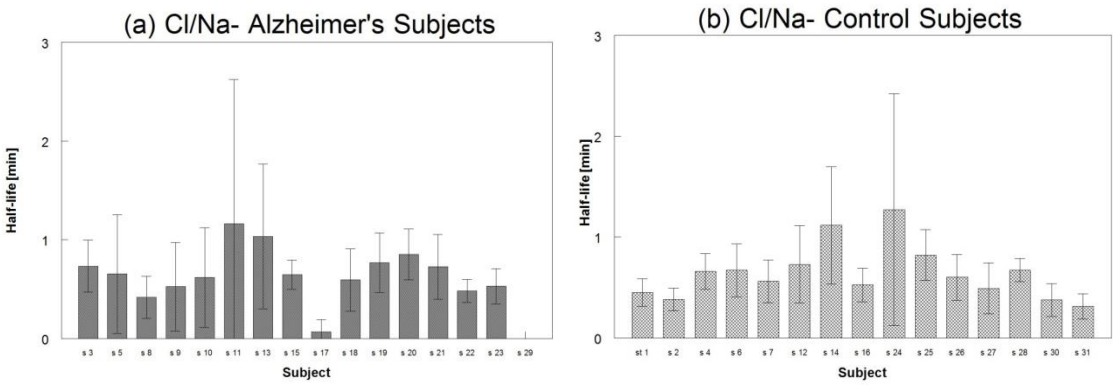

Figure 5.7. Chlorine and sodium biological half-life ratios for (a) AD and (b) control subjects.

4. Discussion

The mean Na removal rate of 40.5 ± 9.4 min for the rapidly exchangeable pool in control subjects agrees with the reported values in the literature. Cohen et al. reported a removal rate of one hour in the healthy subjects [2]. Spinks et al. found a range of 26 ± 5 to 119 ± 27 min with a mean half-life of 46 ± 7 min for faster clearance for a total of 5 control subjects [6]. Our current results are in close agreement with the mean and range reported by Spinks et al. and within 3σ

of the half-life reported by Cohen et al [2,6]. The standard test of the mean half-life values of AD and control subject shows no significant difference with a p-value of 0.1, However, as shown in Figures 3 and 4, the biological half-life of Na and Cl in AD subjects exhibit a more erratic pattern compared to the control group stemming from the significantly more variable half-lives observed in AD subjects ($p < 0.001$). While the standard test of the mean remains the standard method of investigating the difference between two groups, presence of significant variability might warrant further investigation of the biological half-life of these elements in the AD subjects.

The steady increase in the half-lives of Na and Cl with age, governed by the linear function shown in Figures 5 and 6 indicate an age-dependent reduction in the body's capacity to exchange Cl and Na between the extracellular tissue and bone crystal. This is an interesting finding, especially in the case of Na, as it may be related to medical conditions such as hypertension which is known to be related to the variations in the slow and fast exchanging compartments of Na [8].

Changes in the exchangeable pool of Na are generally linked to the changes in the total body content of Na. If changes in the biological half-life of Na are an indication of changes in the exchangeable pool, then it can be concluded that an increase in the biological half-life of Na with age is an indicator for reduced total body sodium [1].

Based on a literature search and to the best of the authors' knowledge, there are no existing data on the metabolic behaviour of Cl in humans. There have been few studies measuring the total body Cl in healthy individuals [1,5,9,10]. The differences in the removal rates of Na and Cl between AD and control subjects is removed when taking the ratio of Na/Cl. This could imply that there is a possible electrolyte balance in the metabolic behaviour and exchangeability of Na and Cl in the body.

Two of the subjects (subject 1 and 2) were available for longer measurements for whom multiple sequential measurements were made up to 45 hours following irradiation. A two exponential function was used to fit the data. Two separate removal rates were observed for both subjects corresponding to rapidly and slowly exchangeable compartments of Na within the body. The fast and slow removal rates for subject 1 were 52 min and 40 hours, respectively, and 52 min and 79 hours for subject 2. These results agree with the rapid and slow turnover half-lives of 1 hour and 79 hours for healthy subjects reported by Cohen et al [2].

5. Conclusions

The aim of the present study was to investigate the kinetic behaviour of Cl and Na via IVNAA as a spinoff study using the available data from a study examining the bone Aluminum content in subjects with AD and normal controls. The rapid removal rate in control subjects was compared to the previously reported values in the literature and was found to be in close agreement. The biological half-lives

of Na and Cl, while not significantly different in the mean values, showed considerably greater variation in AD subjects compared to the controls, warranting possible further investigation. These results are encouraging given the fact that the experiments were not optimized for activation or detection of Na or Cl resulting in large uncertainties. The kinetic behaviour of Cl and the slowing down of the exchange rate in the soft tissue compartment for both Na and Cl were demonstrated for the first time in this work.

Acknowledgements

The authors would like to extend their gratitude to Justin Bennett, the accelerator operator at the MAL for assisting in conducting experiments and patient irradiation. They also thank Dr. Farshad Mostafaei for his assistance in patient data collection and Michael Inskip for valuable advice and access to his laboratory. This work was made available through the funding provided by the Canadian Nuclear Laboratories (CNL) and Natural Sciences and Engineering Research Council of Canada (NSERC).

References

[1] Ellis KJ, Vaswani A, Zanzi I, Cohn SH (1976) Total body sodium and chlorine in normal adults, *metabolism* **25**, 645-654.

[2] Cohen-Boulakia F, Maziere B, Comar D (1981) Application of in vivo activation analysis to the study compartmental sodium in the hand. *Phys Med Biol* **26**, 857-865.

[3] Rakovic M, Pilecka N (1992) Two compartments of slowly exchangeable sodium in bone. *Phys Med Biol* **37**, 1399-1402.

[4] Davies RE, Kornberg HL (1952) Non-exchangeable sodium in the body. *Short communications* **9**, 703-704.

[5] Williams ED, Boddy K, Brown JJ, Cumming AMM, Daviest DL, Harvey IR, Haywood JK, Lever AF, Robertson IS (1984) Bone elemental composition, with particular reference to total and exchangeable sodium and potassium and total chlorine, in untreated and treated primary in hyperaldosteronism. *J Hypertension* **2**, 171-176.

[6] Spinks TJ, Bewley DK, Joplin GF, Ranicar ASO (1976) Neutron-activation measurement of metabolic activity of sodium in the human hand. *J Nucl Med* **17**, 724-729.

[7] Spinks TJ, Bewley DK, Paolillo M, Vlotides J, Joplin GF, Ranicar ASO (1980) Metabolic activity of sodium measured by neutron activation in the

hands of patients suffering from bone diseases: concise communication. *J Nucl Med* **21**, 41-46.

[8] Williams ED, Boddy K, Brown JJ, Cumming AMM, Daviest DL, Harvey IR, Haywood JK, Lever AF, Robertson IS (1982) Whole body elemental composition in patients with essential hypertension. *Eur J Clin Invest* **12**, 321-325.

[9] Kennedy NSJ, Eastell R, Smith MA, Tothill P (1983) Normal levels of total body sodium and chlorine by neutron activation analysis. Phys Med Biol 28, 2115-221.

[10] Mitra S, Plank LD, Knight GS, Hill GL (1993) *In vivo* measurement of total body chlorine using the 8.57 MeV prompt de-excitation following thermal neutron capture. *Phys Med Biol* **38**, 161-172.

[11] Aslam, Davis K, Pejović-Milić A, Chettle DR (2009) Noninvasive measurement of aluminium in human bone: preliminary human study and improved system performance. *J Inorg Biochem* **103**, 1585–90.

[12] Aslam, Pejovic-Milic A, Chettle DR, McNeill FE (2008) Quantification of manganese in human hand bones: A feasibility study. *Phys Med Biol* **53**, 4081-4092.

[13] Mostafaei F, McNeill FE, Chettle DR, Wainman BC, Pidruczny AE, Prestwich WV (2015) Measurements of fluorine in contemporary urban

Canadians: A comparison of the levels found in human bone using *in vivo* and *ex vivo* neutron activation analysis. *Physiol Meas* **36**, 465-487.

[14] ICRP (1974) *Report of the task group on reference man*, Publication 23. Pergamon, Oxford.

[15] Byun SH, Prestwich WV, Chin K, McNeill FE, Chettle DR (2006) 4-pi NaI(Tl) detector array for *in vivo* neutron activation analysis. *IEEE Trans Nucl Sci* **53**, 2944–2947.

Chapter 6

6. Conclusions and Future Work

6.1. Thesis Conclusions

The present thesis included five original contributions, four of which were presented in the form of articles. The conclusions and significant contributions to the field for each of the chapters are presented in this section.

6.1.1. Optimization of Data Analysis

Over the past four decades, attempts have been made to improve the performance of IVNAA, both in terms of instrumentation and data analysis. The work presented in chapter 2 focused on improving the methods of data analysis for detecting Al in human hand bone. This was achieved by producing new high purity phantoms to reduce Al contamination and advancing the data analysis and manipulations methods. Two main approaches to data analysis were investigated, namely, spectral decomposition and Gaussian fitting. The Gaussian fit was further complemented by time-dependent, inverse-variance weighted mean, and 3 minute summation analyses to find the lowest MDL achievable. The lowest MDL found on the basis of these analyses was 5 μg Al/g Ca using the spectral decomposition method, an improvement by a factor of 1.7 compared the lowest MDL reported in the literature. It is noted that while these analyses were

optimized for bone Al measurements, they can be applied to other gamma-ray measurements.

6.1.2. IVNAA Measurement of Bone Al in Alzheimer's Disease and Control Subjects

Given the high prevalence of AD, there is an ongoing effort in the scientific community to identify the factors involved in its causality. Environmental toxins, among which Al has the highest abundance, have been of great interest in this regard. Measuring Al is particularly challenging due to its ubiquitous nature, rendering most *in vitro* measurements prone to Al contamination. The work shown in this thesis presents, for the first time, the results on the *in vivo* measurement of Al in the hand bone of patients suffering from AD and also control subjects. It was shown that the Al/Ca ratio in bone in AD subjects was significantly higher than the control group ($p = 0.02$). A linear increase in the bone Al levels with age was also identified in the study subjects. While these results are encouraging, it is important to note that most of the measurements were close to or lower than the MDL of the system, and therefore, the results should be interpreted with caution. The results of the present study suggest an association between bone Al and AD. It can also be concluded that bone may be considered suitable as a proxy for brain Al measurements.

6.1.3. IVNAA Measurement of Magnesium in Bone

Mg as one of elements of interest in the etiology of AD has been measured in different organs and media, such as serum, hair, and brain tissues. There is a lack of data on bone Mg levels in patients with AD, although a significant amount of Mg is stored in bone. Mg is also one of the elements with a significant cross-section for neutron activation. As result, it was possible to measure Mg in the AD and control subjects as a spinoff of the Al study. The objectives of the study were to investigate the possibility of using bone as a substitute for post-mortem brain sample measurement and compare the Mg levels in AD subject against control subjects. While there was no significant difference between the Mg levels in AD and control subjects, the MDL achieved was far lower than the values in subjects' hands, indicating the feasibility of using IVNAA for monitoring Mg in the bone.

6.1.4. Short-term Kinetic Behaviour of Na and Cl

In addition to measuring the content of certain elements in the biological tissues, IVNAA has the capability of providing valuable information about the turnover of elements with known exchangeable pools. These include, but are not limited to, Na and Cl. The current measurement protocol, due to the short counting period, only allowed for the short-term kinetic behaviour of Na and Cl to be investigated. The results indicated that there was no significant difference in the biological half-lives of Na and Cl between the AD and control groups, although a more erratic pattern was observed in AD subjects. An age-dependent linear decline in the

exchangeability of both Na and Cl was observed for the first time in this work. The biological half-life of Cl was also reported for the first time in this article.

6.2. Future Work- System Upgrade

The focus of the suggested future directions is on improving the detection limit of the system with the goal of performing measurements on more AD subjects to solidify the results of the present clinical study as well extending the measurements to include other groups of individuals with occupational or medical exposure to Al. A significant improvement in the detection limit is necessary in order to justify a large-scale study, as the current measurements are very close to the detection limit of the system, forcing a conservative interpretation of the achieved results.

6.2.1. Improving the Detection System

The detection system currently used for the IVNAA consists of an array of 9 NaI(Tl) detectors. NaI(Tl) detectors have a high efficiency, but a poor resolution, which proves to present a challenge when resolving the interfering gamma peaks, such as those of Al and Cl. Some of the detectors in the current setup, more specifically, detectors 7, 8, and 9, have a lower resolution compared to the rest of the detectors. Replacing these detectors with newer ones could lead to an improved detection and stronger counting statistics. Furthermore, It is possible to explore the use of hyperpure germanium (HPGe) detectors, which have higher resolution, but lower efficiency compared to NaI(Tl) detectors. Using a setup of 2

or 4 HPGe detectors to improve the efficiency, can lower the detection limit of the system. This may be achieved in collaboration with other groups such as the IVNAA research group at Purdue University that is currently using a D-D set together with a HPGe detector for measuring manganese and fluorine (Mostafaei et al, 2015, Liu et al., 2015).

6.2.2. Optimization of the Irradiation Parameters

A relatively limited study of the optimization of the irradiation protocol was performed and is described in detail in Appendix A. There is a need for further investigation of the irradiation parameters. In particular, protocols involving higher proton currents need to be tested. The only high-current test performed so far is protocol 2 in Table A.1 with E_P = 2.1 MeV, t_{irr} = 45 sec, and a current of 600 μA, leading to a dose equivalent of 56.5 mSv. Although the low uncertainty and FOM associated with this set of parameters is encouraging, it is noted that drawing a current of 600 μA for an irradiation time of 45 sec for repeated measurements is beyond the capabilities of the Tandetron accelerator. Therefore, the same set of parameters, but with a lower current of 500 μA could be tested. Additionally, given the low FOM values in the lower proton energies, it would be interesting to investigate different parameters for proton energies of 2.05 MeV and 2.15 MeV, provided that the dose calculations or simulation for these energies are available.

6.2.3. Spectral Decomposition

As mentioned in Chapter 2, the method of spectral decomposition showed a marginally superior performance compared to the Gaussian model. The performance of any method can be improved upon by further reducing the statistical uncertainty of the measurements. For the specific case of the spectral decomposition, this can be achieved by making library standards or elemental phantoms with high concentrations of each element and thus reducing the counting uncertainty in the library measurements. The library standard phantoms used for the spectral decomposition were made of physiologically relevant concentrations of the elements found in the IVNAA analysis of the human hand bone. The only exception is the Al phantom where a concentration of 5 mg was used. Producing high-concentration library phantoms is a step that can be simply achieved which could potentially improve the results of the analysis for the bone Al and Mg studies.

6.2.4. Possible Alternatives to Ca as a Means of Normalizing Al Counts

The method of IVNAA requires the normalization of the measurements in order to cancel the variations in activation due to the changes in the thermal neutron fluence and the positioning of the samples in irradiation cavity. Furthermore, measuring human subjects introduces variations due to the size and shape of the individuals' hands. Historically, Ca has been used for normalization of the measurements, as it is known to be present in the bone crystal and non-

exchangeable. However, the variation in Ca with age, especially in elderly subjects, puts forth the question of alternative means of normalization. The neutron count and the integrated current are the only two beam parameters available for normalization. However, long-term examination of these values has shown that neither neutron count, nor the integrated current is reliable for the purpose of normalization, and they generate noise that obliterates the signal. Of the elements activated in the hand by thermal neutrons only Na can be considered for normalization. Although Na is known to be present in exchangeable and non-exchangeable pools within the body, it can be assumed to be more or less constant during the 10 min counting period due to its 15 hour half-life. Following the analysis for the Na peak in the subjects, the content of both Ca and Na were estimated in grams by comparing to the known concentrations in the phantoms measured before or after each subject. Normalization was made based on both neutron count and integrated current, the results of which are shown in Tables 7.1 and 7.2, respectively. Unfortunately, the neutron count and integrated current data were not available for all phantom measurements and as a result, the comparison was not available for all patients. The coefficients of variation for Ca and Na show more variation for Na than Ca regardless of the normalization. The fact that the coefficient of variation did not get smaller when taking the ratio of Na to Ca indicates that at least for the present dataset Na/Ca cannot be assumed to be near constant. It can be

concluded, based on these analyses, that normalization to Na is not deemed a suitable replacement for normalization to Ca.

A possible normalization approach in the context of the future work would be using an indium (^{115}In) strip taped to the subject's hand during irradiation to monitor for the neutron fluence. ^{115}In has a neutron cross-section of 194 b and emits a gamma with a half-life of 54.3 min. Following the irradiation the activated ^{116m}In would be counted in a separate detector to provide a more accurate estimate of the neutron fluence in the irradiation cavity.

Table 6.1. Estimates of Na and Ca in the study subjects in grams based on the neutron counts.

	Subjects' Ca (g)	Uncertainty	Subjects' Na (g)	Uncertainty	Na/Ca	Uncertainty
Subject 1	1.23E+01	6.56E-02	6.58E-01	1.58E-02	5.33E-02	1.31E-03
Subject 2	1.92E+01	1.03E-01	1.35E+00	2.45E-02	7.03E-02	1.33E-03
Subject 3	7.44E+00	6.64E-02	4.06E-01	9.35E-03	5.46E-02	1.35E-03
Subject 4	3.92E+00	3.67E-02	2.08E-01	6.09E-03	5.30E-02	1.63E-03
Subject 5	2.09E+00	1.89E-02	1.25E-01	5.04E-03	5.99E-02	2.48E-03
Subject 6	1.25E+01	6.80E-02	7.42E-01	1.46E-02	5.92E-02	1.21E-03
Subject 7	6.85E+00	4.27E-02	3.82E-01	8.60E-03	5.57E-02	1.30E-03
Subject 8	6.72E+00	3.60E-02	1.47E+00	2.24E-02	2.18E-01	3.53E-03
Subject 9	2.31E+00	1.99E-02	1.53E-01	5.33E-03	6.65E-02	2.38E-03
Subject 11	7.43E+00	5.40E-02	4.73E-01	1.07E-02	6.37E-02	1.52E-03
Subject 12	5.75E+00	4.34E-02	3.59E-01	8.97E-03	6.23E-02	1.63E-03
Subject 13	4.11E+00	3.12E-02	2.34E-01	6.44E-03	5.70E-02	1.63E-03
Subject 15	4.11E+00	2.80E-02	2.60E-01	7.47E-03	6.33E-02	1.87E-03
Subject 16	9.32E+00	4.82E-02	5.74E-01	1.19E-02	6.16E-02	1.32E-03
Subject 17	2.86E+00	2.24E-02	2.10E-01	6.43E-03	7.35E-02	2.32E-03
Subject 20	3.36E+00	2.56E-02	3.45E-01	9.04E-03	1.03E-01	2.80E-03
Subject 21	4.53E+00	2.93E-02	3.66E-01	9.10E-03	8.08E-02	2.07E-03
Subject 23	8.67E+00	4.13E-02	5.30E-01	1.19E-02	6.12E-02	1.40E-03
Subject 24	5.21E+00	3.46E-02	2.40E-01	7.93E-03	4.60E-02	1.55E-03
Subject 27	6.40E+00	5.17E-02	2.12E+00	3.72E-02	3.32E-01	6.40E-03
Subject 28	5.59E+00	3.90E-02	2.74E-01	8.80E-03	4.89E-02	1.61E-03
Subject 29	1.56E+01	7.34E-02	9.80E-01	2.00E-02	6.28E-02	1.31E-03
Subject 30	5.94E+00	3.34E-02	3.31E-01	7.79E-03	5.58E-02	1.35E-03
Subject 31	7.46E+00	4.00E-02	4.46E-01	9.68E-03	5.98E-02	1.34E-03
Subject 32	4.05E+00	6.11E-02	1.84E-01	6.58E-03	4.54E-02	1.76E-03
Mean	6.95E+00		5.37E-01		7.87E-02	
SD	4.17E+00		4.78E-01		6.24E-02	
CV%	6.00E+01		8.90E+01		7.93E+01	

Table 6.2. Estimates of Na and Ca in the study subjects in grams based on the integrated current.

	Subjects' Ca (g)	Uncertainty	Subjects' Na (g)	Uncertainty	Na/Ca	Uncertainty
Subject 3	8.65E+00	7.72E-02	4.73E-01	1.09E-02	5.46E-02	1.35E-03
Subject 4	4.58E+00	4.28E-02	2.43E-01	7.10E-03	5.30E-02	1.63E-03
Subject 7	7.85E+00	4.89E-02	4.38E-01	9.86E-03	5.57E-02	1.30E-03
Subject 8	7.61E+00	4.07E-02	1.66E+00	2.54E-02	2.18E-01	3.53E-03
Subject 9	2.59E+00	2.24E-02	1.72E-01	5.98E-03	6.65E-02	2.38E-03
Subject 13	4.68E+00	3.56E-02	2.66E-01	7.34E-03	5.70E-02	1.63E-03
Subject 15	4.59E+00	3.13E-02	2.90E-01	8.35E-03	6.33E-02	1.87E-03
Subject 16	1.03E+01	5.32E-02	6.33E-01	1.32E-02	6.16E-02	1.32E-03
Subject 17	3.13E+00	2.45E-02	2.30E-01	7.03E-03	7.35E-02	2.32E-03
Subject 20	3.83E+00	2.91E-02	3.93E-01	1.03E-02	1.03E-01	2.80E-03
Subject 21	5.03E+00	3.25E-02	4.06E-01	1.01E-02	8.08E-02	2.07E-03
Subject 23	1.00E+01	4.77E-02	6.13E-01	1.37E-02	6.12E-02	1.40E-03
Subject 24	6.02E+00	4.00E-02	2.77E-01	9.15E-03	4.60E-02	1.55E-03
Subject 27	7.03E+00	5.68E-02	2.33E+00	4.09E-02	3.32E-01	6.40E-03
Subject 28	6.30E+00	4.39E-02	3.08E-01	9.91E-03	4.89E-02	1.61E-03
Subject 29	1.68E+01	7.92E-02	1.06E+00	2.15E-02	6.28E-02	1.31E-03
Subject 30	7.01E+00	3.94E-02	3.91E-01	9.19E-03	5.58E-02	1.35E-03
Subject 31	8.75E+00	4.70E-02	5.24E-01	1.14E-02	5.98E-02	1.34E-03
Subject 32	4.22E+00	6.36E-02	1.91E-01	6.85E-03	4.54E-02	1.76E-03
Mean	6.79E+00		5.74E-01		8.41E-02	
SD	3.31E+00		5.53E-01		7.11E-02	
CV%	4.87E+01		9.65E+01		8.45E+01	

6.3. Future Work- Human Studies

6.3.1. Recruiting Subjects with Severe AD

As discussed in Chapter 3, one limitation of the current study was that the recruitment of the AD subjects was limited to patients with mild and moderate diagnoses. This decision was made based upon the practical considerations in the recruitment process. It would be interesting to measure the bone Al levels in subjects in the severe stage of the disease to investigate the pattern of bone Al concentration with the severity of AD. Furthermore, including urine aluminum measurements to determine the intake could be considered. Bone density measurements, if possible, can also provide more information about the Ca content in subjects' bones.

6.3.2. Bone Al Measurements in Occupationally Exposed Individuals

As mentioned in the introduction, measuring Al in the context of occupational exposures was of interest from the 1980s (Sjogren et al., 1983, Exley, Vickers, 2014). While measuring subjects' bone Al for the Alzheimer's study, a significantly high concentration of bone Al was found in one of the control subjects (subject 26), compared to both control and AD subjects. The subject's bone Al/Ca level was 56.2 ± 3.5 μg Al/g, a concentration which is greater than the mean control and AD concentrations by factors of 21.2 and 4.5, respectively. The serum Al level for subject 26 was 70 nmol/L, which is about 3 times lower than the mean serum level for the control subjects. The subject was

accompanied by his spouse, also a control subject, whose bone Al level was 1.5 ± 4.5 µg Al/g Ca, well within the normal range for control subjects, and thus reducing the possibility of exposure to Al due to lifestyle or diet.

This prompted further investigation into the medical and occupational history of the subject in question. The list of medications taken by the subject was provided by his geriatrician, Dr. Cowan, some of which are known to contain Al coating. It was also revealed that the subject had worked as an electrician on construction sites, with the last 15-20 years in a supervisory capacity. His job entailed welding and a fair amount of soldering. It is noted that subject 26 was removed from the study as the individual's Al/Ca ratio satisfied the criteria for removal as an outlier based on Peirce's criterion and Chauvenet's criterion.

Such high concentration of bone Al in a case of possible occupational exposure merited further investigation of individuals with occupational exposure to Al. An amendment was made to the AD study's ethics approval to allow for measurement of additional subjects with self-reported occupational exposure. Although arrangements were made for at least 2 subjects, no measurements have been made to this date. This is an interesting area with potential for further investigation. If indeed higher Al levels are found in a small group of individuals envisioned for the preliminary study, it could pave the way for larger occupational investigations.

6.3.3. *In vivo* Bone Al Measurement in Parenteral Nutrition Patients

Patients receiving PN are in risk of Al toxicity due to Al contamination in the ingredients and the process of preparing the PN solutions and need to be monitored for their Al levels on a regular basis. Kruger et al (Kruger, 2013) have previously demonstrated elevated Al concentrations in the PN bone samples acquired post-mortem. The measurements performed and reported in Chapter 6 can be considered as an exploratory investigation of the feasibility of using (IV)NAA for monitoring PN patients for long-term toxicity. As mentioned in Appendix E, the results of the (IV)NAA measurements are yet to be confirmed by the collaborators in Albany, NY. Assuming agreement between the results of the IVNAA measurements and those performed at the New York State Department of Health, recruiting PN patients for a small clinical study could be envisioned as the next step in utilizing the IVNAA in measurement of bone Al in PN patients. Given the significantly higher concentrations of Al found in PN bone samples compared to controls, reported by Kruger et al (Kruger, 2013), and the high levels of Al/Ca measured by our group, it is reasonable to assume that the current IVNAA setup is capable of successfully detecting the Al levels in PN patients with acceptable uncertainty, as the measured concentrations are much higher than the MDL of the system.

References

Aslam, Pejovic-milic A, McNeill FE, Byun SH, Prestwich WV, Chettle DR (2008) *In vivo* assessment of magnesium status in human body using accelerator-based neutron activation measurement of hands: A pilot study. *Med Phys* **35**, 608-616.

Darvish-Molla S, Prestwich WV, Byun SH (2015) Comprehensive radiation dose measurements and Monte Carlo simulation for the ^{7}Li(p,n) accelerator neutron field. *Radiat Prot Dosimetry*, doi:10.1093/rpd/ncv428.

Fewtrell MS, Bishop NJ, Edmonds CJ, Isaacs EB LA (2009) Aluminum exposure from parenteral nutrition in preterm infants: bone health at 15-year follow-up. *Pediatrics* **124**, 1372–9.

Klein GL, Targoff CM, Ament ME, Sherrard DJ, Bluestone R, Young JH, Norman AW, Coburn JW (1980) Bone-disease associated with total parenteral nutrition. *Lancet* **2**, 1041–1044.

Kruger PC, Parsons PJ, Galusha AL, Morrissette M, Recker RR, Howard LJ (2013) Excessive aluminum accumulation in the bones of patients on long-term parenteral nutrition: postmortem analysis by electrothermal atomic absorption spectrometry. *JPEN. J Parenter Enteral Nut.* **38**, 728-735.

Liu Y, Koltick D, Byrne P, Wang H, Zheng W, Nie LH (2013) Development of a transportable neutron activation analysis system to quantify manganese in bone in vivo: feasibility and methodology. *Physiol Meas* **34**, 1593-609.

Mostafaei F, Blake SP, Liu Y, Sowers DA, Nie LH (2015) Compact DD generator-based neutron activation analysis (NAA) system to determine fluorine in human bone in vivo: a feasibility study. *Physiol Meas* **36** 2056-67.

Appendix A

A.1. Optimization Study of the Irradiation Protocol

The goal of neutron activation analysis is to achieve the highest activation with the lowest measurement uncertainty. The optimization of the irradiation parameters is a crucial step in realizing this goal. The importance of the optimization process is even more highlighted when it involves *in vivo* measurements on humans, where the dose to the subjects becomes a major limiting factor. The irradiation parameters in question here include the proton energy (E_P), the proton current, and the irradiation time (t_{irr}). The present irradiation protocol (protocol 8 with E_P = 2.3 MeV, I_P= 400 μA, and t_{irr} =45 sec) applied throughout this study was adopted from the previous studies and aims to increase the sensitivity of the measurements. A preliminary investigation into the different combinations of these parameters, within the capabilities of the equipment, was conducted with the goal of exploring alternative irradiation protocols with stronger performance. The approach taken in choosing the parameters was to investigate the effect of the irradiation time and proton current for the proton energies for which the dose equivalent data were available. It is noted that both the current and t_{irr} are directly proportional to dose. These measurements are shown in Table A.1.

All the doses quoted here are based on the measurements and the simulation performed by Darvish-Molla et al. (Darvish-Molla et al., 2015), at the centre of the irradiation cavity and include both neutron and gamma doses.

A figure of merit (FOM) was defined as the product of the square root of dose equivalent and the uncertainty in the measurement, in order to assess the performance of each set of parameters. A lower FOM signifies a higher performance, as both lower uncertainty and dose are favorable. The measurements tabulated in Table A.1 are ranked according to their FOMs. Figure A.1 illustrates the ratio of Al to Ca counts with proton energy for t_{irr} = 20 sec and t_{irr} =45 sec. It can be seen that the Al/Ca ratio for all energies agree within the uncertainties. For all proton energies, the shorter irradiation time of 20 sec yields higher number of counts. Another consideration when assessing the performance of each protocol is the uncertainty in the measurements. Bone aluminum concentrations in healthy individuals are generally very low and often close to or lower than the detection limit of the system. Therefore, where possible, it is important to keep the measurement uncertainties as low as achievable. The Al/Ca uncertainties with proton energy for t_{irr} = 20 sec and t_{irr} =45 sec are shown in Figure A.2, showing a sharp decrease from 2.1 MeV to 2.2 MeV, followed by a slowly decreasing pattern from 2.2 MeV onward.

Neutron energy and its yield increases with proton energy. Higher neutron energies result in higher dose per neutron capture event as the high-energy

neutrons are not absorbed within the phantom or the body. At lower energies, the low neutron yield leads to fewer activation events. The shorter irradiation time offers the benefit of less decay during irradiation, as shown in Figures A.1 and A.2, which is important when short-lived radionuclides, such as Al, are of interest.

As shown in Table A.1, the lowest FOMs were achieved at the lowest energy tested which is E_P = 2.1 MeV, and for the irradiation times of 20 and 45 sec, respectively. However, as mentioned before, the measurement uncertainties for these protocols, shown in Figure A.2 and Table A.1 were considerably higher than the current protocol (by factors of 2 and 1.5, respectively), while Al/Ca ratio was lower.

Protocol 11 produced the lowest uncertainty amongst the protocols tested; however, this came at the cost of delivering an unfavorably high dose of 637.1 mSv. It is noted that protocol 2 offers a low FOM and uncertainty; however, the accelerator at its current state is not capable of delivering a proton current of 600 μA for 45 sec on repeated measurements.

Based on the current data and considering the FOM, activation, uncertainty, and the dose, protocol 4 with E_P = 2.2 MeV delivers a low FOM, with a reasonable activity and measurement uncertainty at a lower dose than the current protocol. There is a need for more thorough investigation of the different parameters to further confirm the most suitable combination of parameters for the *in vivo* activation of Al.

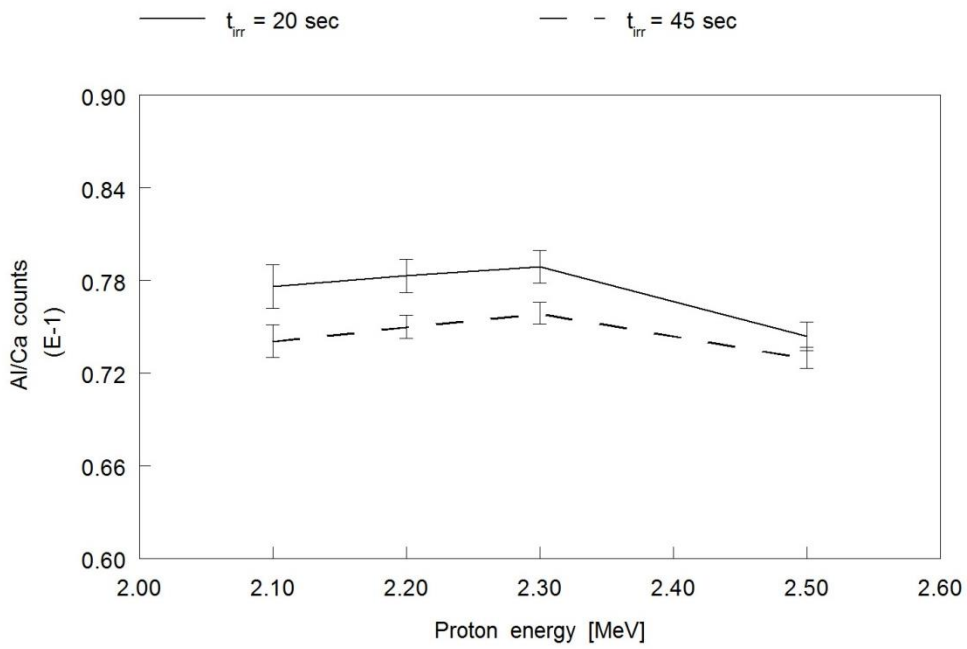

Figure A.1. Al/Ca area with proton energy for irradiation times of 20 and 45 sec.

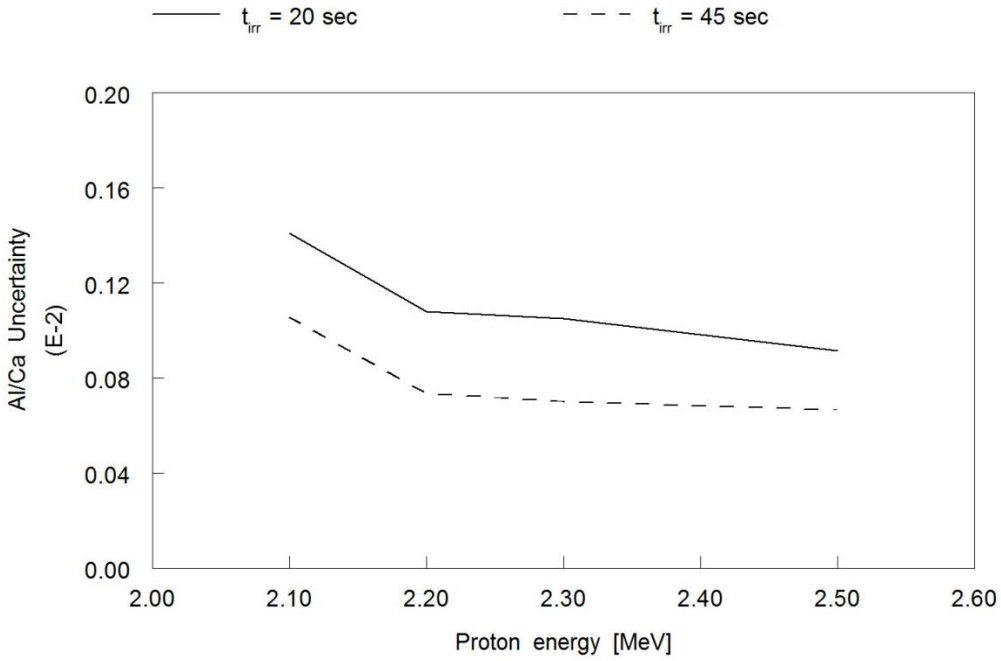

Figure A.2. Al/Ca area uncertainty with proton energy for irradiation times of 20 and 45 sec.

Table A.1. Tested irradiation protocols ranked by the FOM.

Protocol	E_P (MeV)	t_{irr} (sec)	Current (μA)	Dose equivalent (mSv)	Al/Ca counts	Al/Ca uncertainty	FOM	sensitivity (count/mSv)
1	2.1	20	400	16.8	7.76E-02	1.41E-03	5.79E-03	4.62E-03
2	2.1	45	600	56.5	7.33E-02	8.14E-04	6.12E-03	1.96E-03
3	2.1	45	400	37.7	7.41E-02	1.06E-03	6.50E-03	1.30E-03
4	2.2	20	400	49.7	7.83E-02	1.08E-03	7.63E-03	1.58E-03
5	2.2	45	400	111.8	7.50E-02	7.39E-04	7.82E-03	1.35E-03
6	2.3	45	80	57.5	7.77E-02	1.44E-03	1.09E-02	6.70E-04
7	2.3	20	400	126.6	7.89E-02	1.05E-03	1.18E-02	1.33E-03
8	2.3	45	400	287.8	7.59E-02	7.03E-04	1.19E-02	6.23E-04
9	2.5	45	36	57.3	7.63E-02	1.78E-03	1.35E-02	2.64E-04
10	2.5	20	400	280.3	7.44E-02	9.15E-04	1.53E-02	2.65E-04
11	2.5	45	400	637.1	7.30E-02	6.69E-04	1.69E-02	1.15E-04

A.2. Tables

Tables A.2 to A.6 show the results of different methods of analysis performed on the calibration phantoms discussed in chapter 2. The detailed results of the reproducibility study involving 17 measurements of the 33.6 µg Al/g Ca phantom are tabulated in Table A.7.

Table A.2. Results of the Gaussian fitting with the time-dependent analysis.

Phantom (µg Al/g Ca)	Al/Ca	Uncertainty	µg Al/g Ca	Uncertainty	Mean	SD	Mean Uncertainty
0	3.40E-14	1.07E-03	1.21E-10	3.80E+00	2.90E-07	4.32E-07	3.90E+00
0	2.21E-10	8.08E-04	7.87E-07	2.87E+00			
0	2.36E-11	1.41E-03	8.41E-08	5.02E+00			
16.8	5.91E-03	1.01E-03	2.10E+01	3.59E+00	1.97E+01	2.03E+00	3.54E+00
16.8	4.88E-03	1.03E-03	1.74E+01	3.66E+00			
16.8	5.82E-03	9.49E-04	2.07E+01	3.38E+00			
33.6	8.72E-03	1.24E-03	3.10E+01	4.40E+00	3.49E+01	4.89E+00	3.13E+00
33.6	9.36E-03	6.18E-04	3.33E+01	2.20E+00			
33.6	1.14E-02	7.82E-04	4.04E+01	2.78E+00			
50.3	1.36E-02	6.71E-04	4.86E+01	2.39E+00	5.11E+01	2.74E+00	3.18E+00
50.3	1.52E-02	1.07E-03	5.40E+01	3.81E+00			
50.3	1.43E-02	9.42E-04	5.07E+01	3.35E+00			
67.1	1.85E-02	1.03E-03	6.60E+01	3.66E+00	6.60E+01	4.03E-01	3.65E+00
67.1	1.87E-02	9.88E-04	6.64E+01	3.52E+00			
67.1	1.84E-02	1.06E-03	6.56E+01	3.76E+00			
134.2	4.28E-02	1.62E-03	1.52E+02	5.75E+00	1.43E+02	1.27E+01	5.81E+00
134.2	3.77E-02	1.65E-03	1.34E+02	5.86E+00			
335.6	9.31E-02	2.11E-03	3.31E+02	7.50E+00	3.36E+02	7.43E+00	7.39E+00
335.6	9.33E-02	1.90E-03	3.32E+02	6.76E+00			
335.6	9.68E-02	2.23E-03	3.45E+02	7.92E+00			

Table A.3. Results of phantom analysis using the Gaussian fitting with the inverse-variance weighted mean.

Phantom (µg Al/g Ca)	Al/Ca	Uncertainty	µg Al/g Ca	Uncertainty	Mean	SD	Mean Uncertainty
0	1.36E-03	5.64E-04	6.13E+00	2.53E+00	5.07E+00	1.62E+00	2.58E+00
0	7.16E-04	5.82E-04	3.21E+00	2.61E+00			
0	1.31E-03	5.81E-04	5.87E+00	2.60E+00			
16.8	4.70E-03	5.76E-04	2.11E+01	2.59E+00	2.33E+01	1.93E+00	2.59E+00
16.8	5.40E-03	5.69E-04	2.42E+01	2.55E+00			
16.8	5.53E-03	5.93E-04	2.47E+01	2.65E+00			
33.6	7.58E-03	5.29E-04	3.42E+01	2.38E+00	3.67E+01	3.10E+00	2.51E+00
33.6	7.97E-03	5.65E-04	3.58E+01	2.53E+00			
33.6	8.99E-03	5.84E-04	4.02E+01	2.61E+00			
50.3	1.13E-02	5.23E-04	5.09E+01	2.36E+00	5.60E+01	4.41E+00	2.59E+00
50.3	1.30E-02	5.63E-04	5.82E+01	2.52E+00			
50.3	1.32E-02	6.51E-04	5.88E+01	2.90E+00			
67.1	1.56E-02	5.49E-04	7.06E+01	2.47E+00	7.04E+01	1.15E+00	2.64E+00
67.1	1.59E-02	5.50E-04	7.15E+01	2.46E+00			
67.1	1.54E-02	6.63E-04	6.92E+01	2.98E+00			
134.2	3.47E-02	6.31E-04	1.54E+02	2.78E+00	1.47E+02	1.09E+01	2.82E+00
134.2	3.09E-02	6.39E-04	1.39E+02	2.86E+00			
335.6	7.63E-02	7.38E-04	3.40E+02	3.19E+00	3.40E+02	3.02E+00	3.29E+00
335.6	7.49E-02	8.06E-04	3.37E+02	3.54E+00			
335.6	7.69E-02	7.26E-04	3.43E+02	3.14E+00			

Table A.4. Results of phantom analysis using spectral decomposition.

Phantom (µg Al/g Ca)	µg Al/g Ca	Uncertainty	Mean	SD	Mean Uncertainty
0	7.09E-01	2.59E+00	3.54E+00	3.11E+00	2.47E+00
0	3.04E+00	2.37E+00			
0	6.86E+00	2.47E+00			
16.8	1.67E+01	2.51E+00	2.03E+01	3.25E+00	2.50E+00
16.8	2.10E+01	2.19E+00			
16.8	2.31E+01	2.79E+00			
33.6	2.65E+01	2.68E+00	3.22E+01	5.48E+00	2.61E+00
33.6	3.25E+01	2.44E+00			
33.6	3.75E+01	2.70E+00			
50.3	4.24E+01	2.65E+00	5.05E+01	7.04E+00	2.51E+00
50.3	5.47E+01	2.22E+00			
50.3	5.44E+01	2.65E+00			
67.1	6.06E+01	2.60E+00	6.56E+01	5.22E+00	2.54E+00
67.1	7.10E+01	2.26E+00			
67.1	6.53E+01	2.75E+00			
134.2	1.50E+02	3.01E+00	1.41E+02	1.30E+01	2.64E+00
134.2	1.32E+02	2.26E+00			
335.6	3.25E+02	3.06E+00	3.28E+02	3.83E+00	2.87E+00
335.6	3.28E+02	2.73E+00			
335.6	3.32E+02	2.83E+00			

Table A.5. Results of phantom analysis using the Gaussian fit to the sum of the first 3 cycles.

Phantom (µg Al/g Ca)	Al/Ca	Uncertainty	µg Al/g Ca	Uncertainty	Mean	SD	Mean Uncertainty
0	8.22E-04	7.48E-04	3.73E+00	3.40E+00	2.96E+00	6.82E-01	3.19E+00
0	5.42E-04	7.50E-04	2.46E+00	3.41E+00			
0	5.87E-04	6.09E-04	2.67E+00	2.77E+00			
16.8	4.59E-03	8.32E-04	2.08E+01	3.78E+00	2.34E+01	2.29E+00	3.37E+00
16.8	5.27E-03	7.07E-04	2.39E+01	3.21E+00			
16.8	5.57E-03	6.88E-04	2.53E+01	3.13E+00			
33.6	7.29E-03	6.44E-04	3.32E+01	2.93E+00	3.73E+01	4.21E+00	3.37E+00
33.6	8.20E-03	7.87E-04	3.73E+01	3.58E+00			
33.6	9.15E-03	7.96E-04	4.16E+01	3.62E+00			
50.3	1.20E-02	7.40E-04	5.45E+01	3.36E+00	6.22E+01	8.75E+00	3.31E+00
50.3	1.33E-02	6.78E-04	6.05E+01	3.08E+00			
50.3	1.58E-02	7.66E-04	7.17E+01	3.48E+00			
67.1	1.58E-02	7.66E-04	7.17E+01	3.48E+00	7.04E+01	1.22E+00	3.29E+00
67.1	1.54E-02	5.71E-04	7.02E+01	2.59E+00			
67.1	1.52E-02	8.36E-04	6.93E+01	3.80E+00			
134.2	3.59E-02	9.42E-04	1.63E+02	4.28E+00	1.50E+02	1.86E+01	3.69E+00
134.2	3.01E-02	6.83E-04	1.37E+02	3.11E+00			
335.6	7.75E-02	1.08E-03	3.52E+02	4.93E+00	3.57E+02	5.17E+00	5.07E+00
335.6	7.83E-02	1.21E-03	3.56E+02	5.48E+00			
335.6	7.97E-02	1.06E-03	3.62E+02	4.82E+00			

Table A.6. Results of phantom analysis using the Gaussian fitting and the inverse-variance weighted mean for the first 3 cycles.

Phantom (µg Al/g Ca)	Al/Ca	Uncertainty	µg Al/g Ca	Uncertainty	Mean	SD	Mean Uncertainty
0	5.85E-04	6.07E-04	2.66E+00	2.76E+00	2.53E+00	2.35E-01	2.83E+00
0	4.97E-04	6.40E-04	2.26E+00	2.91E+00			
0	5.88E-04	6.23E-04	2.67E+00	2.83E+00			
16.8	4.62E-03	6.33E-04	2.10E+01	2.88E+00	2.26E+01	1.73E+00	2.89E+00
16.8	4.90E-03	6.27E-04	2.23E+01	2.85E+00			
16.8	5.38E-03	6.47E-04	2.44E+01	2.94E+00			
33.6	7.42E-03	5.80E-04	3.37E+01	2.64E+00	3.63E+01	3.06E+00	2.77E+00
33.6	7.84E-03	6.13E-04	3.56E+01	2.79E+00			
33.6	8.73E-03	6.32E-04	3.97E+01	2.87E+00			
50.3	1.12E-02	5.79E-04	5.07E+01	2.63E+00	5.51E+01	3.84E+00	2.91E+00
50.3	1.25E-02	6.17E-04	5.68E+01	2.81E+00			
50.3	1.27E-02	7.25E-04	5.79E+01	3.30E+00			
67.1	1.51E-02	6.18E-04	6.84E+01	2.81E+00	6.91E+01	9.99E-01	2.96E+00
67.1	1.54E-02	5.97E-04	7.02E+01	2.71E+00			
67.1	1.51E-02	7.37E-04	6.85E+01	3.35E+00			
134.2	3.38E-02	7.01E-04	1.54E+02	3.19E+00	1.45E+02	1.15E+01	3.21E+00
134.2	3.02E-02	7.10E-04	1.37E+02	3.23E+00			
335.6	7.39E-02	8.48E-04	3.36E+02	3.85E+00	3.39E+02	6.12E+00	3.96E+00
335.6	7.37E-02	9.33E-04	3.35E+02	4.24E+00			
335.6	7.61E-02	8.34E-04	3.46E+02	3.79E+00			

Table A.7. The results of 17 measurements of the 33.6 µg Al/g Ca phantom for testing the reproducibility of measurements, using the inverse-variance weighted mean of the Gaussian fitting.

Measurement date	Al/Ca	Uncertainty	µg Al/g Ca	Uncertainty
04/02/2014	9.04E-03	5.92E-04	4.09E+01	2.68E+00
10/02/2014	8.49E-03	5.83E-04	3.84E+01	2.64E+00
21/02/2014	8.77E-03	5.78E-04	3.97E+01	2.61E+00
03/03/2014	8.02E-03	5.68E-04	3.63E+01	2.57E+00
14/03/2014	8.10E-03	5.50E-04	3.66E+01	2.49E+00
28/03/2014	9.04E-03	5.97E-04	4.09E+01	2.70E+00
05/09/2014	7.79E-03	6.15E-04	3.52E+01	2.78E+00
17/11/2014	8.99E-03	7.29E-04	4.07E+01	3.30E+00
16/01/2015	7.57E-03	7.59E-04	3.43E+01	3.44E+00
10/02/2015	8.87E-03	5.91E-04	4.01E+01	2.68E+00
17/02/2015	9.10E-03	6.23E-04	4.12E+01	2.82E+00
20/03/2015	8.90E-03	5.85E-04	4.03E+01	2.65E+00
10/04/2015	9.77E-03	5.51E-04	4.42E+01	2.49E+00
17/04/2015	8.70E-03	6.25E-04	3.94E+01	2.83E+00
15/05/2015	7.36E-03	6.35E-04	3.33E+01	2.88E+00
20/05/2015	7.98E-03	5.22E-04	3.61E+01	2.36E+00
29/05/2015	8.24E-03	5.39E-04	3.73E+01	2.44E+00
Mean			3.85E+01	2.73E+00
SD			2.91E+00	
IVWM*			3.86E+01	
IVWM uncertainty			6.53E-01	
CV(%)**			7.32E+00	

* Inverse-variance weighted mean
** Coefficient of variation

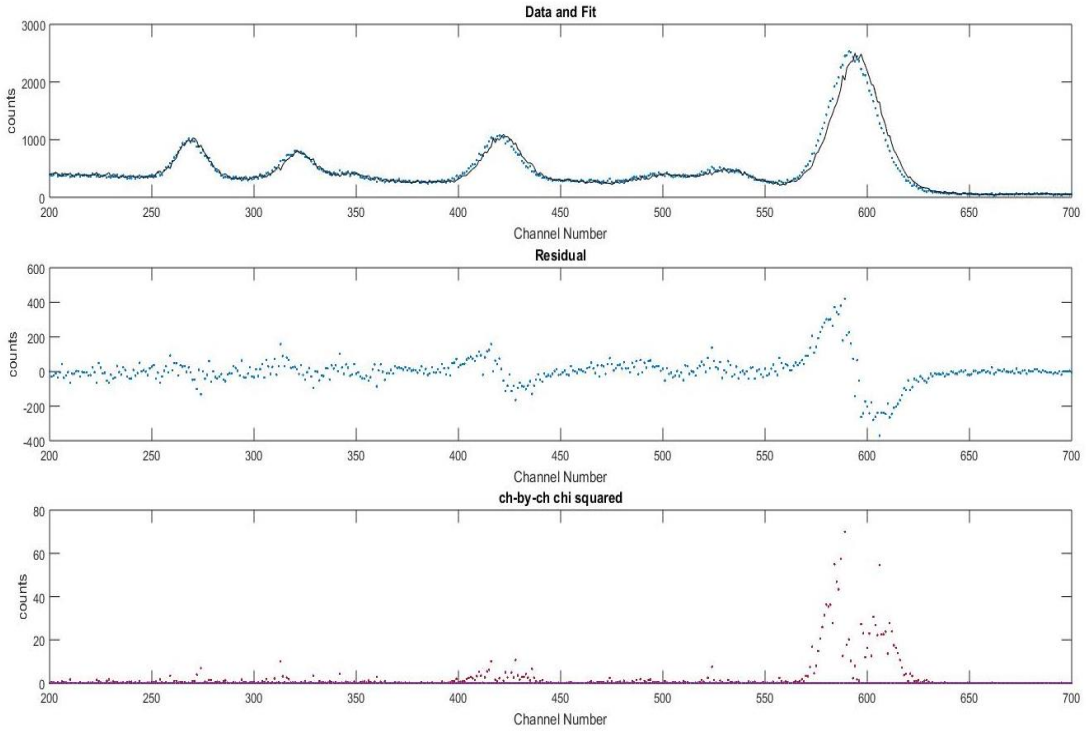

Figure A.3. Spectral decomposition fitting of the 1st minute of the 50.3 µg Al/g Ca phantom with χ^2= 7.9 without gain alignment.

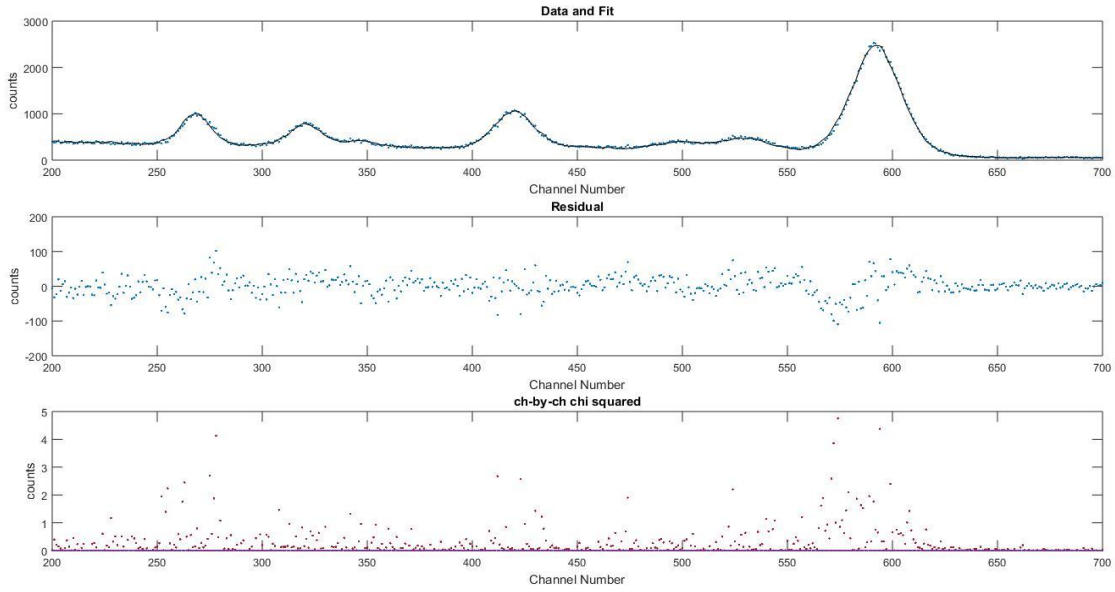

Figure A.4. Spectral decomposition fitting of the 1st minute of the 50.3 µg Al/g Ca phantom with gain alignment, reducing the χ^2 to 1.7.

Table A.8. Fit weights for different radioisotopes in the spectra using spectral decomposition and the χ2 for a 50.3 µg Al/g Ca phantom with (right) and without (left) gain alignment tabulated for each cycle. The counter shows the number of times the gain alignment was executed.

Cycle	Background	Uncertainty	Cl weight	Uncertainty	Al weight	Uncertainty	Na weight	Uncertainty	Ca weight	Uncertainty	χ^2
1	-2.34E-01	7.53E-01	1.00E+00	2.12E-02	1.37E-01	2.76E-02	9.84E-01	3.79E-02	9.10E-01	6.78E-03	7.79E+00
2	-1.59E-01	6.77E-01	1.01E+00	1.99E-02	1.52E-01	3.55E-02	9.67E-01	3.39E-02	9.07E-01	6.71E-03	7.59E+00
3	-2.01E-02	6.52E-01	9.89E-01	1.85E-02	1.68E-01	4.43E-02	9.68E-01	3.20E-02	9.12E-01	6.67E-03	7.09E+00
4	6.18E-01	5.84E-01	9.84E-01	1.74E-02	1.65E-01	5.64E-02	9.41E-01	3.04E-02	9.11E-01	6.67E-03	6.28E+00
5	-5.11E-02	5.49E-01	9.85E-01	1.67E-02	1.52E-01	7.30E-02	9.43E-01	2.78E-02	9.19E-01	6.96E-03	6.32E+00
6	4.05E-01	4.91E-01	9.86E-01	1.50E-02	1.25E-01	8.76E-02	9.32E-01	2.42E-02	9.23E-01	6.58E-03	5.20E+00
7	1.33E-01	4.62E-01	9.84E-01	1.45E-02	1.22E-01	1.07E-01	9.24E-01	2.30E-02	9.18E-01	6.65E-03	5.12E+00
8	3.69E-01	4.49E-01	9.71E-01	1.41E-02	5.34E-02	1.37E-01	9.23E-01	2.19E-02	9.14E-01	6.89E-03	5.05E+00
9	-5.05E-02	4.05E-01	9.90E-01	1.29E-02	-8.64E-02	1.61E-01	9.40E-01	1.94E-02	9.18E-01	6.70E-03	4.92E+00
10	3.47E-01	4.07E-01	9.64E-01	1.31E-02	4.21E-02	1.99E-01	9.09E-01	1.97E-02	9.23E-01	7.33E-03	4.82E+00

Cycle	Background	Uncertainty	Cl weight	Uncertainty	Al weight	Uncertainty	Na weight	Uncertainty	Ca weight	Uncertainty	χ^2	Counter
1	-8.47E-01	2.78E-01	1.00E+00	7.25E-03	1.46E-01	9.44E-03	9.92E-01	1.34E-02	9.24E-01	2.30E-03	1.65E+00	5
2	-1.01E+00	2.69E-01	1.00E+00	7.40E-03	1.67E-01	1.32E-02	9.82E-01	1.29E-02	9.22E-01	2.48E-03	1.76E+00	5
3	-7.94E-01	2.50E-01	9.90E-01	6.65E-03	1.84E-01	1.60E-02	9.84E-01	1.18E-02	9.25E-01	2.38E-03	1.52E+00	4
4	-1.51E-01	2.78E-01	9.87E-01	7.65E-03	1.93E-01	2.48E-02	9.62E-01	1.38E-02	9.23E-01	2.90E-03	1.81E+00	5
5	-5.24E-01	2.45E-01	9.83E-01	6.98E-03	1.76E-01	3.07E-02	9.54E-01	1.19E-02	9.32E-01	2.88E-03	1.75E+00	5
6	-7.49E-02	2.30E-01	9.86E-01	6.60E-03	1.47E-01	3.90E-02	9.45E-01	1.09E-02	9.34E-01	2.87E-03	1.58E+00	4
7	-5.08E-01	2.45E-01	9.87E-01	7.07E-03	1.88E-01	5.36E-02	9.42E-01	1.16E-02	9.30E-01	3.24E-03	1.64E+00	3
8	-3.85E-01	2.51E-01	9.80E-01	7.19E-03	1.07E-01	7.26E-02	9.46E-01	1.15E-02	9.24E-01	3.49E-03	1.71E+00	3
9	-4.14E-01	3.35E-01	9.94E-01	1.01E-02	-3.86E-02	1.30E-01	9.50E-01	1.54E-02	9.23E-01	5.22E-03	3.25E+00	1
10	-1.31E-01	2.48E-01	9.72E-01	7.26E-03	7.73E-02	1.19E-01	9.22E-01	1.12E-02	9.34E-01	4.03E-03	1.88E+00	3

Appendix B

B.1. Bone Al and Ca Data of the Study Subjects

Tables B.1 and B.2 contain the data pertaining to the bone Al measurements for the AD and control subjects, respectively, which were presented in Chapter 3. As mentioned earlier, the method of analysis was based on taking the inverse-variance weighted mean of the counts in the Al and Ca peaks, calculated using Gaussian fittings of these peaks. It is expected that after correcting for the physical half-lives to the end of the irradiation time, the calculated counts for each cycle will be similar with the uncertainties increasing as the cycles progress. A z-score test was performed to confirm the consistency of each set of measurements. The z-score is a measure of the number of standard deviations an observation is from the mean. A mean of zero and a standard deviation of one are expected for a data set converted to z-scores. As such, for the Al and Ca counts corrected to the same point in time i.e. the end of the irradiation time, the z-score for each measurement is expected to be close to zero, and the standard deviation of the of the set of 10 measurements is expected to be close to one. For all the subjects measured in this study, the z-scores ranged from -0.97 $\pm$ 0.53 to 0.32 $\pm$ 0.40 and the standard deviation range was 0.55 – 2.25 . The z-scores in the 30 subjects, although variable, did not achieve the 5% probability of being different from zero.

Table B.1. Al and Ca analysis results for the AD subjects.

	Al counts	Uncertainty	Ca counts	Uncertainty	µg Al/g Ca	Uncertainty	Age (years)	Serum Al (nmol/L)	Sex
Subject 3	7.79E+02	4.12E+02	4.28E+05	3.03E+03	8.24E+00	4.35E+00	68	323	M
Subject 5	7.13E+02	2.06E+02	1.38E+05	1.11E+03	2.34E+01	6.75E+00	89	93	F
Subject 8	2.03E+02	2.66E+02	4.30E+05	1.43E+03	2.13E+00	2.80E+00	81	203	M
Subject 9	9.65E+02	1.86E+02	1.45E+05	1.11E+03	3.01E+01	5.81E+00	86	235	F
Subject 11	7.07E+01	3.47E+02	2.55E+05	1.33E+03	1.26E+00	6.16E+00	73	191	M
Subject 13	1.94E+03	2.76E+02	2.35E+05	1.47E+03	3.74E+01	5.33E+00	89	391	F
Subject 15	9.42E+01	2.56E+02	2.62E+05	1.55E+03	1.63E+00	4.41E+00	83	89	F
Subject 17	-6.04E+00	1.89E+02	1.71E+05	1.22E+03	-1.59E-01	-4.97E+00	75	189	F
Subject 18	4.89E+02	2.18E+02	1.28E+05	9.88E+02	1.72E+01	7.68E+00	84	R	F
Subject 19	1.86E+03	4.43E+02	8.22E+05	2.95E+03	1.02E+01	2.44E+00	79	51	M
Subject 20	1.49E+03	2.87E+02	2.13E+05	1.46E+03	3.16E+01	6.11E+00	76	140	M
Subject 21	1.25E+03	2.75E+02	3.11E+05	1.71E+03	1.81E+01	4.01E+00	73	87	F
Subject 22	3.74E+02	3.16E+02	4.61E+05	2.11E+03	3.68E+00	3.10E+00	86	99	M
Subject 23	7.90E+02	3.61E+02	5.91E+05	2.07E+03	6.05E+00	2.76E+00	88	403	M
Subject 29	-7.67E+02	4.80E+02	8.90E+05	2.90E+03	-3.90E+00	-2.44E+00	73	R	M

Table B.2. Al and Ca analysis results for the control subjects.

	Al counts	Uncertainty	Ca counts	Uncertainty	µg Al/g Ca	Uncertainty	Age (years)	Serum Al (nmol/L)	Sex
Subject 1	2.07E+03	3.99E+02	7.17E+05	2.34E+03	1.31E+01	2.52E+00	74	NA	M
Subject 2	-5.97E+02	5.77E+02	1.09E+06	3.32E+03	-2.48E+00	-2.41E+00	63	NA	M
Subject 4	9.73E+01	2.42E+02	2.41E+05	1.96E+03	1.82E+00	4.55E+00	66	297	F
Subject 6	2.25E+02	4.17E+02	7.76E+05	2.69E+03	1.31E+00	2.43E+00	83	46	M
Subject 7	2.54E+02	3.07E+02	4.54E+05	2.09E+03	2.53E+00	3.06E+00	78	308	F
Subject 12	-9.74E+02	3.37E+02	2.01E+05	1.12E+03	-2.19E+01	-7.58E+00	64	356	F
Subject 14	1.97E+02	2.42E+02	2.46E+05	1.54E+03	3.63E+00	4.44E+00	83	43	F
Subject 16	8.35E+02	3.85E+02	5.68E+05	2.29E+03	6.65E+00	3.06E+00	76	311	M
Subject 24	4.65E+02	2.53E+02	2.98E+05	1.69E+03	7.05E+00	3.83E+00	74	323	M
Subject 25	7.58E+02	2.35E+02	2.28E+05	1.30E+03	1.50E+01	4.66E+00	83	225	F
Subject 27	3.62E+02	2.75E+02	3.35E+05	2.34E+03	4.90E+00	3.71E+00	79	79	F
Subject 28	1.61E+02	2.55E+02	3.30E+05	2.01E+03	2.21E+00	3.50E+00	73	R	F
Subject 30	3.67E+02	3.16E+02	4.35E+05	2.02E+03	3.81E+00	3.29E+00	68	37	F
Subject 31	-3.29E+01	3.30E+02	5.37E+05	2.33E+03	-2.77E-01	-2.78E+00	78	202	M
Subject 32	1.33E+02	2.05E+02	2.46E+05	3.82E+03	2.45E+00	3.77E+00	83	R	F

B.2. Bone Al Results for Male and Female Subjects

The difference in the Al/Ca between the female and male subjects was studied to investigate possible gender-specific patterns in the accumulation of Al in the bone. No significant difference was observed upon comparing Al/Ca ratios between the two groups; although women (mean= 8.89 $\pm$ 14.13 µg Al/g Ca) on average had a numerically higher Al/Ca ratio than men (mean= 6.04 $\pm$ 8.79 µg Al/g Ca). The bar graphs representing the ratios can be seen in Figure B.1 (-a and -b).

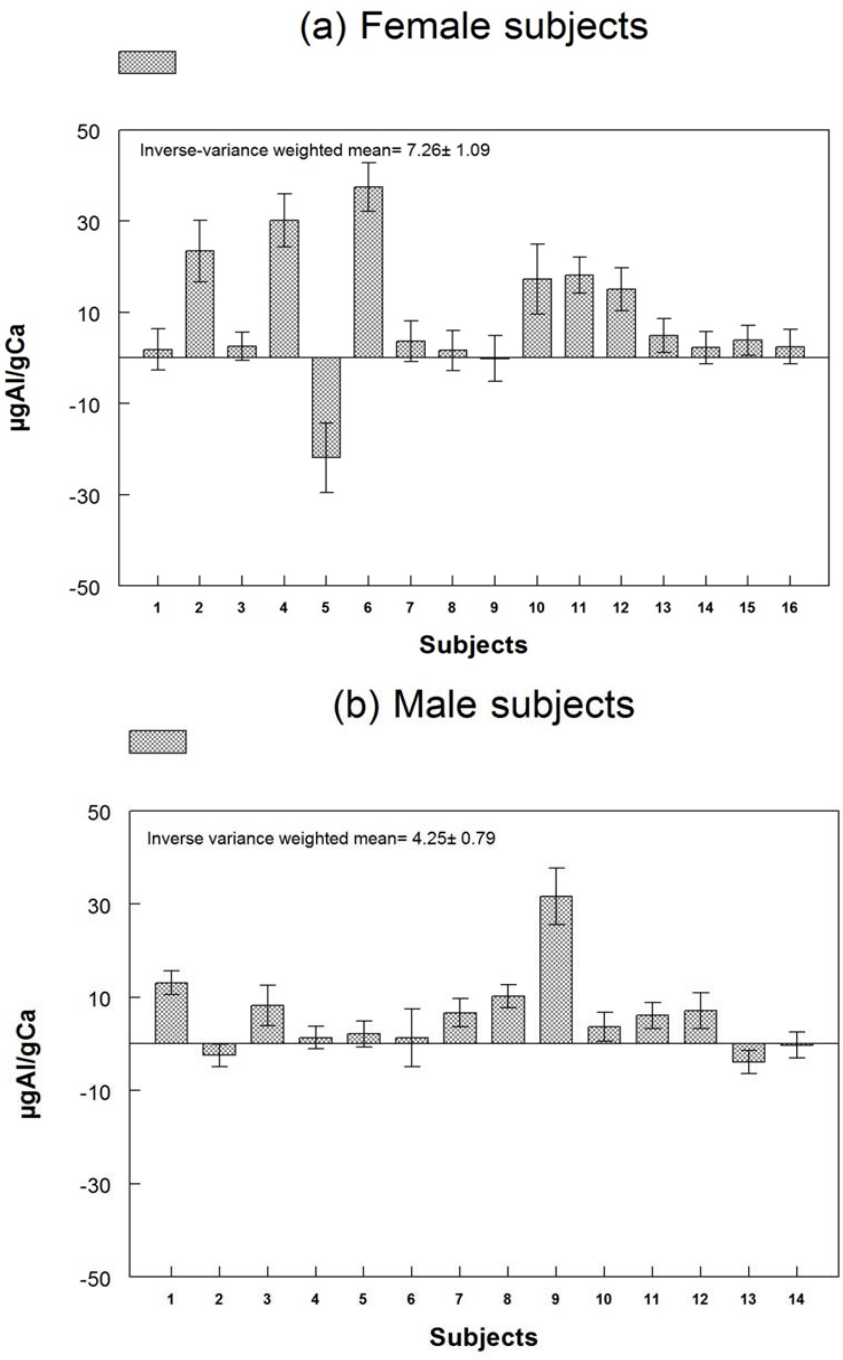

Figure B.1. Aluminum concentration expressed in µg Al/g Ca in (a) female subjects and (b) male subjects.

Appendix C

C. 1. Magnesium Phantom Data

Table C.1. Results of phantom analysis using the Gaussian fitting with the inverse-variance weighted mean.

Concentration (mg Mg/g Ca)	Mg/Ca	Uncertainty	mg Mg/g Ca	Uncertainty	Mean	Mean uncertainty
0	2.49E-03	6.03E-04	5.25E-01	1.27E-01	4.27E-01	1.15E-01
0	3.26E-03	6.58E-04	6.89E-01	1.39E-01		
0	3.18E-04	3.76E-04	6.72E-02	7.95E-02		
10.1	5.41E-02	1.57E-03	1.14E+01	3.31E-01	1.17E+01	3.28E-01
10.1	5.65E-02	1.54E-03	1.19E+01	3.25E-01		
20.1	9.73E-02	1.46E-03	2.06E+01	3.09E-01	2.07E+01	3.16E-01
20.1	9.91E-02	1.53E-03	2.09E+01	3.23E-01		
40.3	2.01E-01	1.93E-03	4.25E+01	4.08E-01	4.12E+01	4.03E-01
40.3	1.89E-01	1.88E-03	3.99E+01	3.97E-01		
80.5	3.87E-01	2.69E-03	8.16E+01	5.69E-01	8.14E+01	5.49E-01
80.5	3.84E-01	2.51E-03	8.11E+01	5.30E-01		

C. 2. Magnesium Subject Data

Table C.2. Mg and Ca analysis results for the AD subjects.

	Mg counts	Uncertainty	Ca counts	Uncertainty	mg Mg/g Ca	Uncertainty	Age
Subject 3	2.57E+04	8.94E+02	4.28E+05	3.03E+03	1.27E+01	4.51E-01	68
Subject 5	8.23E+03	3.94E+02	1.38E+05	1.11E+03	1.26E+01	6.14E-01	89
Subject 8	2.71E+04	8.07E+02	4.30E+05	1.43E+03	1.34E+01	4.00E-01	81
Subject 9	1.06E+04	5.01E+02	1.45E+05	1.11E+03	1.55E+01	7.40E-01	86
Subject 11	1.43E+04	6.75E+02	2.55E+05	1.33E+03	1.19E+01	5.65E-01	73
Subject 13	1.56E+04	6.36E+02	2.35E+05	1.47E+03	1.41E+01	5.81E-01	89
Subject 15	1.61E+04	5.85E+02	2.62E+05	1.55E+03	1.30E+01	4.78E-01	83
Subject 17	1.12E+04	4.62E+02	1.71E+05	1.22E+03	1.38E+01	5.78E-01	75
Subject 18	8.59E+03	5.24E+02	1.28E+05	9.88E+02	1.42E+01	8.72E-01	84
Subject 19	5.67E+04	1.28E+03	8.22E+05	2.95E+03	1.46E+01	3.34E-01	79
Subject 20	1.17E+04	6.82E+02	2.13E+05	1.46E+03	1.17E+01	6.84E-01	76
Subject 21	2.05E+04	7.09E+02	3.11E+05	1.71E+03	1.40E+01	4.89E-01	73
Subject 22	2.60E+04	8.57E+02	4.61E+05	2.11E+03	1.19E+01	3.98E-01	86
Subject 23	3.49E+04	8.64E+02	5.91E+05	2.07E+03	1.25E+01	3.13E-01	88
Subject 29	5.83E+04	1.29E+03	8.90E+05	2.90E+03	1.39E+01	3.10E-01	73

Table C.3. Mg and Ca analysis results for the control subjects.

	Mg counts	Uncertainty	Ca counts	Uncertainty	mg Mg/g Ca	Uncertainty	Age
Subject 1	4.63E+04	9.85E+02	7.17E+05	2.34E+03	1.37E+01	2.94E-01	74
Subject 2	6.98E+04	1.14E+03	1.06E+06	3.23E+03	1.40E+01	2.32E-01	63
Subject 4	1.56E+04	6.18E+02	2.41E+05	1.96E+03	1.37E+01	5.54E-01	66
Subject 6	4.39E+04	8.99E+02	7.76E+05	2.69E+03	1.20E+01	2.49E-01	83
Subject 7	2.58E+04	7.15E+02	4.54E+05	2.09E+03	1.20E+01	3.38E-01	78
Subject 12	1.31E+04	6.70E+02	2.01E+05	1.12E+03	1.38E+01	7.10E-01	64
Subject 14	1.34E+04	5.61E+02	2.46E+05	1.54E+03	1.15E+01	4.88E-01	83
Subject 16	3.56E+04	8.88E+02	5.68E+05	2.29E+03	1.33E+01	3.35E-01	76
Subject 24	1.85E+04	6.63E+02	2.98E+05	1.69E+03	1.32E+01	4.77E-01	74
Subject 25	9.91E+03	5.17E+02	2.28E+05	1.30E+03	9.20E+00	4.83E-01	83
Subject 26	3.69E+04	1.08E+03	6.69E+05	2.26E+03	1.17E+01	3.45E-01	78
Subject 28	1.89E+04	6.09E+02	3.30E+05	2.01E+03	1.21E+01	3.98E-01	73
Subject 30	2.64E+04	8.04E+02	4.35E+05	2.02E+03	1.29E+01	3.96E-01	68
Subject 31	3.51E+04	8.82E+02	5.37E+05	2.33E+03	1.38E+01	3.53E-01	78
Subject 32	1.14E+04	5.14E+02	1.57E+05	3.32E+03	1.54E+01	7.68E-01	83

C. 3. Manganese Interference Calculations

As mentioned previously, the multi-element activation property of NAA can lead to interferences when measuring certain elements such as Mg and Mn. The NaI(Tl) detector's poor energy resolution does not allow for adjacent peaks to be resolved, which in the case of Mn and Mg is a 3 keV difference. It has been previously shown by Aslam et al. that the interference from Mn does not present a problem when measuring Mg in the human hand primarily because of the small amount of Mn found in the human skeleton compared to Mg (Aslam et al., 2008). Additionally, the 2.58 hour half-life of Mn results in fewer decay events during the 10 min counting period, as compared to the 9.46 min half-life of Mg. However, since the NIST 1400 bone sample has a considerable concentration of Mn, this interference cannot be ruled out as insignificant and needs to be accounted for.

$$A = N\sigma\varphi\gamma(1 - exp(-\lambda t_{irr}))$$

$$N = \frac{m\theta}{A_m} 6.02 \times 10^{23}$$

Where A is the activity of the radioisotope, σ is the neutron activation cross-section, φ is the neutron fluence, γ is the branching ratio of gamma-rays, m is the mass of the element (mg), θ is the abundance of the isotope of the element before irradiation, and A_m is atomic mass of the element (mg/mol). The contents of Mn and Mg in the NIST 1400 bone ash sample are 0.684% $\pm$ 0.013% and 17 µg/g, respectively. After substituting the relevant values, the ratio of the activities of Mn and Mg is as follows:

$$\frac{A_{Mn}}{A_{Mg}} = \frac{1.38 \times 10^{-32}}{4.27 \times 10^{-32}} = 0.32$$

Given that the inverse-variance weighted mean of the NIST 1400 measurements is 24.61 $\pm$ 0.22 mg Mg/g Ca for Mg and Mn combined, the real contribution from Mg to the NIST 1400 measured concentration will be 16.66 $\pm$ 0.15.

The certified NIST 1400 Mg/Ca is 17.92 $\pm$ 0.35 (Ca concentration is 38.8% $\pm$ 0.03%). The certified value and the corrected measurement agree within less than 3σ.

Appendix D

D. 1. Biological Half-life Data

Table D.1. Biological half-life data for AD subjects.

	Na half-life	Uncertainty	Cl half-life	Uncertainty	Cl/Na	Uncertainty
subject 3	4.25E+01	1.40E+01	3.11E+01	4.57E+00	7.33E-01	2.64E-01
subject 5	3.76E+01	7.41E+00	2.49E+01	2.28E+01	6.63E-01	6.19E-01
subject 8	7.07E+01	2.17E+01	2.95E+01	1.21E+01	4.17E-01	2.13E-01
subject 9	9.22E+01	3.76E+01	4.84E+01	3.64E+01	5.25E-01	4.49E-01
subject 11	8.81E+01	5.92E+01	5.44E+01	2.52E+01	6.17E-01	5.04E-01
subject 13	6.78E+01	1.62E+01	7.88E+01	9.71E+01	1.16E+00	1.46E+00
subject 15	3.61E+01	1.03E+01	3.80E+01	2.52E+01	1.05E+00	7.60E-01
subject 17	1.86E+01	2.67E+00	1.21E+01	2.24E+00	6.50E-01	1.52E-01
subject 18	1.62E+02	3.11E+02	2.16E+01	1.15E+01	1.33E-01	2.65E-01
subject 19	6.55E+01	2.78E+01	3.96E+01	1.32E+01	6.04E-01	3.26E-01
subject 20	3.89E+01	8.50E+00	3.03E+01	1.01E+01	7.79E-01	3.11E-01
subject 21	2.45E+01	3.98E+00	2.11E+01	5.42E+00	8.62E-01	2.61E-01
subject 22	3.68E+01	5.57E+00	2.71E+01	1.17E+01	7.35E-01	3.36E-01
subject 23	3.81E+01	6.17E+00	1.85E+01	3.36E+00	4.85E-01	1.18E-01
subject 29	5.44E+01	1.34E+01	2.91E+01	6.88E+00	5.36E-01	1.83E-01
Mean	5.83E+01		3.36E+01		6.64E-01	
Variance	1.30E+03		2.61E+02		5.86E-02	
SD	3.61E+01		1.67E+01		2.51E-01	

Table D.2. Biological half-life data for control subjects.

	Na half-life	Uncertainty	Cl half-life	Uncertainty	Cl/Na	Uncertainty
subject 1	5.75E+01	1.12E+01	2.62E+01	6.21E+00	4.55E-01	1.40E-01
subject2	6.77E+01	1.60E+01	2.61E+01	4.65E+00	3.86E-01	1.14E-01
subject 4	2.38E+01	4.18E+00	1.56E+01	3.17E+00	6.59E-01	1.77E-01
subject 6	3.63E+01	1.02E+01	2.06E+01	5.24E+00	5.67E-01	2.15E-01
subject 7	3.62E+01	1.02E+01	2.03E+01	5.12E+00	5.61E-01	2.12E-01
subject 12	3.41E+01	6.38E+00	2.48E+01	1.23E+01	7.28E-01	3.85E-01
subject 14	3.29E+01	7.02E+00	3.68E+01	1.75E+01	1.12E+00	5.81E-01
subject 16	4.28E+01	9.33E+00	2.27E+01	5.44E+00	5.30E-01	1.72E-01
subject 24	3.69E+01	8.98E+00	4.82E+01	4.31E+01	1.31E+00	1.21E+00
subject 25	2.57E+01	3.92E+00	2.13E+01	5.70E+00	8.30E-01	2.56E-01
subject 26	3.96E+01	7.93E+00	2.38E+01	7.64E+00	6.01E-01	2.28E-01
subject 27	3.86E+01	8.33E+00	1.90E+01	8.80E+00	4.91E-01	2.51E-01
subject 28	1.62E+01	1.79E+00	1.10E+01	1.44E+00	6.76E-01	1.16E-01
subject 30	5.50E+01	1.70E+01	2.09E+01	6.48E+00	3.80E-01	1.67E-01
subject 31	8.23E+01	2.85E+01	2.60E+01	5.13E+00	3.16E-01	1.26E-01
subject 32	2.22E+01	5.47E+00	2.22E+01	1.72E+01	1.00E+00	8.13E-01
Mean	4.05E+01		2.41E+01		6.40E-01	
Variance	2.85E+02		7.14E+01		6.89E-02	
SD	1.74E+01		8.47E+00		2.78E-01	

Appendix E

Neutron Activation Analysis of Parenteral Nutrition Bones

E. 1. Introduction

As mentioned in the introduction, one of the conditions associated with elevated bone aluminum levels is parenteral nutrition (PN) (Klein et al., 1980, Fewtrell et al., 2009). This is mostly due to the aluminum (Al) contamination in the ingredients of the PN solutions and also the handling processes involved in preparing these solutions (Kruger et al., 2013). Patients receiving PN are at the risk of accumulating high concentrations of Al and need to be monitored to avoid Al toxicity. The purpose of this study was to compare the NAA Al bone measurements to those of the Electro-thermal atomic absorption spectrometry (ETAAS) to benchmark the IVNAA system at McMaster University and explore the possibility of employing the current system for monitoring of PN patients.

E. 2. Material and Methods

Twenty two bone samples were provided by the collaborating research group from the New York State Department of Health in Albany, New York. All samples were pre-processed in preparation for the ETAAS measurements, the details of sample processing are discussed in detail by Kruger et al. (Kruger et al., 2013). No diagnosis was provided for the samples to avoid possible biases in analysis. The sample masses varied from 20 mg up to 10 g. the neutron fluence of the

accelerator beam poses a limitation on the minimum sample mass that can be measured with acceptable counting statistics. For this reason, only 4 samples with the largest masses, all weighing more than 1 g were chosen for measurements, which are listed in Table E.1. Two smaller samples of 0.67 ± 0.005 g and 0.51 ± 0.005 g were also measured to confirm that the smaller samples in fact suffer from poor statistics. The results of these measurements can be found in Table E.7.

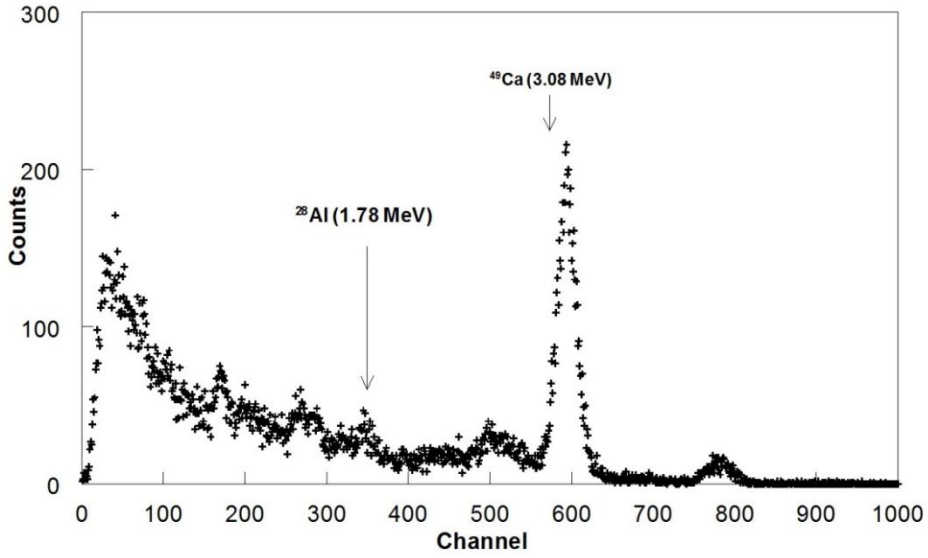

Figure E.1. The spectrum from the first cycle of P8 bone sample.

The bone samples were irradiated at the proton energy of 2.3 MeV and proton current of 400 μA for 45 sec and were subsequently counted for 10 cycles of 60 sec, consistent with all other Al measurements discussed in the previous chapters. The acquired spectrum from the first cycle of P8 bone sample is shown Figure E.1.

All samples were irradiated in their original containers due to concerns about environmental Al contamination. These containers were standard laboratory containers of different sizes and origins, which were previously acid-washed and rinsed at the New York State Department of Health laboratories. While washing the containers with diluted nitric acid removes Al from the surface of the material, there is still a considerable source of contamination due to the presence of Al in the material used in manufacturing of the containers. Figure E.2 shows the sum of the first 3 cycles acquired from a blank sample vial. It can be seen that Al is one of the main features in these spectra. To prevent this activation contamination from interfering with the Al counts from the bone samples, all samples were transferred to un-irradiated acid-washed containers immediately after irradiation and prior to the start of counting.

The analysis of the results was performed by fitting a Gaussian and a linear function to account for the peak and the background in the regions of the spectra containing Al and Ca peaks. Corrections were made to account for the radioactive decay during the transfer and each counting cycle, as well as the delay in the data acquisition program. The inverse-variance weighted mean of the 10 spectra was reported as the estimate of Al and Ca. The results were reported as the ratio of μg Al/g Ca to cancel the effect of variations in the thermal neutron fluence and the positioning of the sample in the irradiation cavity.

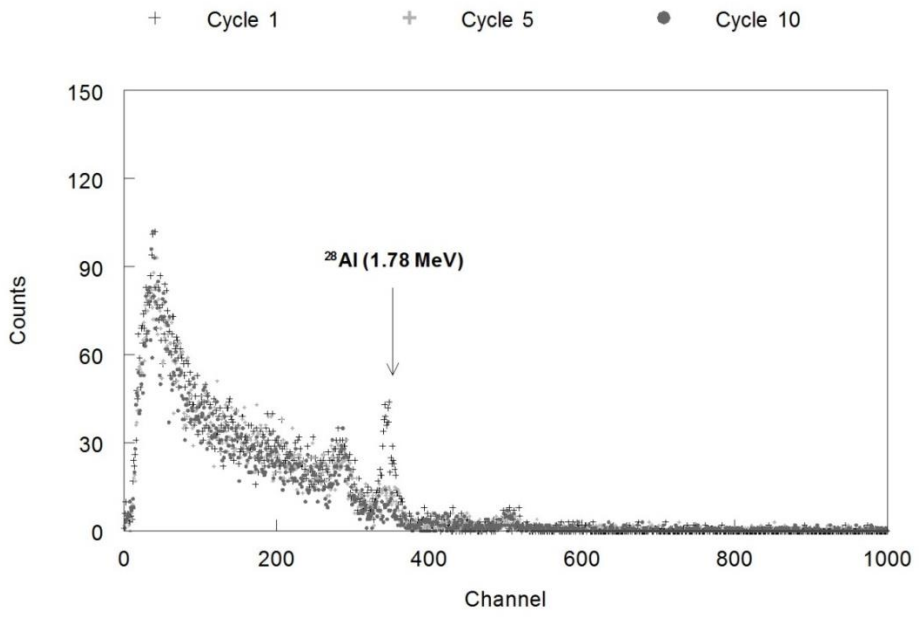

Figure E.2. The spectra acquired from a blank vial showing the Al peak and its decay through the cycles.

E. 3. Results and Discussion

The results for measured samples are shown in Table E.1. The details of all measurements are listed in Tables E.3 to E.7. The fact that the standard deviation is close to the mean uncertainty in the measurements suggests that there are limited sources of variation beyond what is accounted for in the counting statistics.

The results for the smaller samples are shown in Table E.2. The fractional uncertainty (ratio of uncertainty to the measurement) for P07-0003 and P07-0034 are 72% and 55%, respectively. Although these uncertainties are not far from

those observed in human subjects, they may not be suitable for the purpose of benchmarking NAA against ICP-MS, which typically shows smaller uncertainties.

Table E.1. Results of the Al PN bone measurements for the largest samples expressed in µg Al/g Ca.

Sample	Weight (g)	Mean ± SD	Inverse-variance weighted mean	Mean uncertainty	Number of measurements
P8	8.86 ± 0.005	89.79 ± 9.84	89.72 ± 2.68	7.24	7
P6	10.03 ± 0.005	53.19 ± 6.15	53.73 ± 2.94	8.39	8
P4	0.67 ± 0.005	196.35 ± 62.42	187.80 ± 29.12	59.60	4
P3	0.89 ± 0.005	219.79 ± 75.29	219.48 ± 20.15	51.25	5

* Coefficient of variation

Table E. 2. Results of the Al PN bone measurements for the small samples expressed in µg Al/g Ca.

Sample	Weight (g)	µg Al/g Ca ± uncertainty
P07-0003	0.67 ± 0.005	41.40 ± 29.83
P07-0034	0.51 ± 0.005	95.51 ± 52.82

E. 4. Conclusions

These results are yet to be validated by the research group at the New York State Department of Health. Although the results of the ETAAS measurements have been published (Kruger et al., 2013), it is not possible to compare and validate the results. This is due to the blind nature of the current measurements

and the fact that the published Al contents are reported in µg/g of dry weight which cannot be accurately converted to µg Al/g Ca.

Table E.3. Results of multiple measurement of bone P8 with a mass of 8.86 ± 0.005 g.

Measurement date	Al counts	Uncertainty	Ca counts	Uncertainty	µg Al/g Ca	Uncertainty
05/02/2014	1.22E+03	9.58E+01	5.94E+04	7.18E+02	9.28E+01	7.38E+00
14/03/2014	1.30E+03	9.65E+01	6.98E+04	8.41E+02	8.46E+01	6.34E+00
15/08/2014	1.36E+03	1.15E+02	6.21E+04	7.47E+02	9.93E+01	8.45E+00
24/04/2015	7.91E+02	9.13E+01	4.89E+04	6.75E+02	7.33E+01	8.52E+00
15/05/2015	1.47E+03	1.06E+02	7.37E+04	8.63E+02	9.04E+01	6.62E+00
20/05/2915	1.32E+03	9.52E+01	7.00E+04	8.44E+02	8.55E+01	6.24E+00
27/05/2015	1.50E+03	1.03E+02	6.62E+04	7.47E+02	1.03E+02	7.11E+00

Table E.4. Results of multiple measurement of bone P6 with a mass of 10.03 ± 0.005 g.

Measurement date	Al counts	Uncertainty	Ca counts	Uncertainty	µg Al/g Ca	Uncertainty
05/02/2014	5.95E+02	1.05E+02	5.62E+04	6.53E+02	4.79E+01	8.50E+00
03/03/2014	6.19E+02	8.87E+01	5.08E+04	6.39E+02	5.51E+01	7.93E+00
14/03/2014	5.76E+02	9.58E+01	4.85E+04	6.58E+02	5.38E+01	8.98E+00
15/08/2014	5.38E+02	1.01E+02	4.84E+04	6.37E+02	5.03E+01	9.49E+00
24/04/2015	4.23E+02	8.17E+01	4.10E+04	6.15E+02	4.67E+01	9.04E+00
15/05/2015	7.70E+02	9.37E+01	5.65E+04	7.10E+02	6.16E+01	7.54E+00
20/05/2915	6.35E+02	1.04E+02	6.00E+04	7.03E+02	4.79E+01	7.82E+00
27/05/2015	7.45E+02	9.28E+01	5.41E+04	6.74E+02	6.22E+01	7.80E+00

Table E.5. Results of multiple measurement of bone P4 with a mass of 0.67 ± 0.005 g.

Measurement date	Al counts	Uncertainty	Ca counts	Uncertainty	µg Al/g Ca	Uncertainty
24/04/2015	3.34E+02	6.07E+01	3.99E+03	2.09E+02	2.33E+02	7.18E+01
15/05/2015	3.51E+02	5.96E+01	4.72E+03	1.95E+02	1.70E+02	5.88E+01
20/05/2915	2.48E+02	5.48E+01	4.98E+03	2.08E+02	1.22E+02	5.06E+01
27/05/2015	3.93E+02	6.12E+01	5.01E+03	2.13E+02	2.60E+02	5.72E+01

Table E.6. Results of multiple measurement of bone P3 with a mass of 0.89 ± 0.005 g.

Measurement date	Al counts	Uncertainty	Ca counts	Uncertainty	µg Al/g Ca	Uncertainty
05/02/2014	4.22E+02	6.76E+01	8.18E+03	2.48E+02	2.33E+02	3.81E+01
03/03/2014	3.26E+02	6.35E+01	8.68E+03	2.75E+02	1.70E+02	3.36E+01
24/04/2015	1.00E+02	6.56E+01	3.73E+03	1.92E+02	1.22E+02	7.99E+01
20/05/2915	3.11E+02	6.20E+01	5.41E+03	2.13E+02	2.60E+02	5.28E+01
27/05/2015	3.97E+02	6.40E+01	5.72E+03	2.13E+02	3.14E+02	5.19E+01

Table E.7. Results of measurements of the smaller bone samples P07-0003 (0.67 ± 0.005 g) and P07-0034 (0.51 ± 0.005).

Sample	Al counts	Uncertainty	Ca counts	Uncertainty	µg Al/g Ca	Uncertainty
P07-0003	9.66E+01	6.95E+01	3.19E+02	1.07E+04	4.14E+01	2.98E+01
P07-0034	1.23E+02	6.78E+01	5.82E+03	2.18E+02	9.55E+01	5.28E+01